Predictive Control of Buildings for Demand Response and Ancillary Services Provision

THÈSE N^{O} 7897 (2017)

PRÉSENTÉE LE 17 NOVEMBRE 2017
À LA FACULTÉ DES SCIENCES ET TECHNIQUES DE L'INGÉNIEUR
LABORATOIRE D'AUTOMATIQUE 3
PROGRAMME DOCTORAL EN GÉNIE ÉLECTRIQUE

ÉCOLE POLYTECHNIQUE FÉDÉRALE DE LAUSANNE

POUR L'OBTENTION DU GRADE DE DOCTEUR ÈS SCIENCES

PAR

Faran Ahmed QURESHI

acceptée sur proposition du jury:

Dr A. Karimi, président du jury
Prof. C. N. Jones, directeur de thèse
Prof. J. B. Jørgensen, rapporteur
Prof. L. Glielmo, rapporteur
Prof. D. Bonvin, rapporteur

ÉCOLE POLYTECHNIQUE
FÉDÉRALE DE LAUSANNE
Suisse
2017

بسم الله الرحمن الرحيم

To my parents, sister, and family

Acknowledgements

This thesis would not have been possible without the support of a number of people. I wish to express my gratitude to all those who directly or indirectly contributed towards the completion of this thesis.

I'll like to thank my supervisor, Colin Jones for his invaluable advice and guidance over the years. I especially appreciate Colin's positive and friendly attitude, which has always been a source of motivation for me. I have learned a lot, not only from Colin's creative way of thinking about research problems, but also from his elegant way of presenting and communicating results.

I feel lucky to have the opportunity to collaborate with an amazing bunch of people. I'll like to especially thank my PhD buddy, Tomasz for the work that we've achieved together and the long scientific discussions we've had over the years. It has been a real pleasure to collaborate and work with him on various projects. I'll particularly like to thank Luca, Tomasz, and Altug for the joint work we did to develop the LADR experimental platform. I'll like to thank Ioannis for his guidance and the fruitful discussions we've had over the years.

I'll like to thank my lab mates, Milan, Jean-Hubert, Andrea, Ye, Francisco, Tomasz, Altug, Georgios, Luca, Sanket, Harsh, Ivan, Petr, Martand, Ehsan, Kristoph, Tafarel, Predrag, Diogo, Zlatko, Rene, Ioannis, Truong, Ali, Philippe, Sean, Sriniketh, Mahdieh, Timm, Michele, Pulkit, and all others who've been a part of LA and have contributed in making it an exceptional place. I've enjoyed a lot, spending time with my lab mates, and traveling with some of them.

I'll like to thank all the professors, Colin, Roland, Dominique, Ali, and Giancarlo for maintaining a friendly, open, and collaborative working environment in the lab. I'll like to thank the secretaries, Ruth, Francine, Eva, and Margot for helping with the administrative matters. I'll like to thank Christophe for patiently helping me on numerous occasions.

My deepest gratitude goes to my family, especially my parents and sister who have been a constant source of motivation and support for me. I would not have achieved any of this without them.

Lausanne, 2017 F. Q.

Abstract

This thesis develops optimization based techniques for the control of building heating, ventilation, and air-conditioning (HVAC) systems for the provision of demand response and ancillary services to the electric grid.

The first part of the thesis focuses on the development of the open source MATLAB toolbox OpenBuild, developed for modeling of buildings for control applications. The toolbox constructs a first-principles based model of the building thermodynamics using EnergyPlus model data. It also generates the disturbance data affecting the models and allows one to simulate various usage scenarios and building types. It enables co-simulation between MATLAB and EnergyPlus, facilitating model validation and controller testing. OpenBuild streamlines the design and deployment of predictive controllers for control applications.

The second part of the thesis introduces the concept of buildings acting as virtual storages in the electric grid and providing ancillary services. The control problem (for the bidding phase) to characterize the flexibility of a building, while also participating in the intraday energy market, is formulated as a multi-stage uncertain optimization problem. An approximate solution method based on a novel intraday control policy and two-stage stochastic programming is developed to solve the bidding problem. A closed loop control algorithm based on a stochastic MPC controller is developed for the online operation phase. The proposed control method is used to carry out an extensive simulation study using real data to investigate the financial benefits of office buildings providing secondary frequency control services to the grid in Switzerland. The technical feasibility of buildings providing a secondary frequency control service to the grid is also demonstrated in experiments using the experimental platform (LADR) developed in the Automatic Control Laboratory of EPFL. The experimental results validate the effectiveness of the proposed control method.

The third part of the thesis develops a hierarchical method for the control of building HVAC systems for providing ancillary services to the grid. Three control layers are proposed: The local building controllers at the lowest level track the temperature set points received from the thermal flexibility controller that maximizes the flexibility of a building's thermal consumption. At the highest level, the electrical flexibility controller controls the HVAC system while maximizing the flexibility provided to the grid. The two flexibility control layers are based on robust optimization methods. A control-oriented model of a typical air-based HVAC system with a thermal storage tank is developed and the efficacy of the proposed control scheme is demonstrated in simulations.

Abstract

Key words: demand response, ancillary services, building control, building thermodynamic modeling, HVAC modeling and control, secondary frequency control, smart grids, stochastic optimization, robust optimization, MPC.

Résumé

Cette thèse développe des méthodes basées sur l'optimisation pour la commande du chauffage, de l'air conditionné des bâtiments (HVAC) pour la provision de services de réponse et services auxiliaires pour le réseau électrique.

La première partie de la thèse se concentre sur le développement de la toolbox open source Openbuild, développée pour la modélisation des bâtiments pour des applications de commandes. La toolbox construit un modèle du bâtiment basé sur la thermodynamique en utilisant les données d'un modèle EnergyPlus. Elle génère également les données de perturbations affectant le modèle et permet de simuler le bâtiments dans divers scénarios. Elle permet la co-simulation entre Matlab et EnergyPlus, facilitant la validation des modèles créés et le test de contrôleurs. Openbuild améliore la conception et le déploiement de contrôleurs prédictifspour les applications de commande.

La deuxième partie de la thèse introduit le concept de bâtiments agissant comme des unités de stockage virtuelles sur le réseau électrique et offrant des services auxiliaires. Le problème (pour la phase d'offre) de formuler le problème de flexibilité, tout en participant au marché d'énergie intra-jour, est formulé comme un problème d'optimisation incertain multi-périodes. Une méthode de solution approchée basée sur une nouvelle loi de commande intra-jour et l'optimisation stochastique deux-périodes a été développée pour résoudre le problème d'offre. Un algorithme de commande en boucle fermée basé sur un algorithme MPC stochastique a été développé pour la phase opérationnelle en temps réel. La méthode proposée est utilisée pour une études extensive en simulation utilisant des données réelles pour explorer le potentiel financier de bâtiments participant à la provision de services auxiliaires en Suisse. La faisabilité technique de la provision de contrôle de fréquence secondaire au réseau est également démontré dans des expériences avec la plateforme LADR développée au laboratoire d'automatique de l'EPFL. Les résultats expérimentaux valident l'efficacité de la méthode de commande proposée.

La troisième partie de la thèse développe une méthode hiérarchique pour la commande des systèmes de chauffage et air conditionné des bâtiments pour la provision de services auxiliaires au réseau. Trois niveaux de commandes sont proposés : le contrôleur local du batiment au niveau le plus bas poursuit la consigne de température reçue du contrôleur de flexibilité thermique qui maximise la flexibilité dans la consommation thermique du batiment. Au plus haut niveau, le contrôleur de flexibilité électrique contrôle le systeme HVAC tout en maximisant la flexibilité offerte au réseau. Les deux contrôleurs de flexibilité sont basés sur des méthodes d'optimisation robuste. Un modèle adapté à la commande d'un système

Résumé

HVAC aveccirculation d'air typique avec un stockage thermique est développé et l'efficacité du schéma de commande proposé est démontrée en simulations.

Mots clés : Demande Réponse, services auxiliaires, commande des bâtiments, modélisation de la thermodynamique des bâtiments, modélisation et commande des systèmes HVAC, optimisation stochastique, optimisation robuste, smart grids, contrôle de fréquence secondaire, MPC.

Contents

List of Figures

List of Tables

List of abbreviations

AGC	Area Generation Control
AHU	Air Handling Unit
ALD	ASHRAE Likelihood of Dissatisfied
AS	Ancillary Services
ASP	Ancillary Services Provider
COP	Coefficient Of Performance
DR	Demand Response
EMS	Energy Management System
HVAC	Heating Ventilation and Air-conditioning
LADR	Laboratoire d'Automatique Demand Response
LPD	Long-term Percentage of Dissatisfied
MPC	Model Predictive Control
PMV	Predicted Mean Vote
PPD	Predicted Percentage of Dissatisfied
RBC	Rule Based Control
RC	Resistor Capacitor
TSO	Transmission System Operator
VAV	Variable Air Volume

1 Introduction

The generation of electricity from clean renewable sources (wind and solar) is increasing around the world, and this trend is expected to continue. The European Union 2030 Energy Strategy has set a target of at least 27% share of renewables in the total energy consumption by the year 2030 [1]. Although renewable energy has many benefits, including a reduction in greenhouse gas emissions, the intermittent nature of renewable sources (wind and solar) create new challenges for grid operators [2]. Critically, an increasing amount of balancing reserves are required by the grid to maintain smooth operation [3]. This has compelled grid operators to look beyond traditional providers (power generators) of balancing reserves to demand-side resources [4], i.e., loads providing ancillary services (AS). Loads have the potential to facilitate the integration of renewable energy by providing AS at reduced financial and carbon costs.

While providing AS, the loads are required to achieve their primary objectives, therefore only flexible loads have the potential of providing AS. Various different types of loads have been identified in literature for providing AS [5], [6], [7], and commercial buildings are considered to be particularly suitable for various reasons.

In the European Union, 37% of the total energy consumption is by buildings, of which approximately one third is consumed by commercial buildings. It is estimated that approximately 50% of the energy in buildings is consumed by heating ventilation and air-conditioning (HVAC) systems. The primary objective of a building HVAC system is to maintain occupant comfort, while minimizing the operational costs. The comfort requirements are usually defined by a temperature range, and since the building thermodynamics are slow, this allows the buildings to have a flexible consumption. Moreover, most commercial buildings are also equipped with the sensors and building management systems needed to run advanced control. All these factors make buildings an excellent target for providing flexibility to the grid.

The model predictive control (MPC) framework has been identified to be ideally suited for

building control because of its ability to handle constraints and to incorporate predictions of future weather, electricity prices, and disturbances impacting building operation. This optimization based control framework is perfectly suited to design novel controllers that enable buildings to act as virtual storages, providing flexibility in the modern electric grid. This has the potential to not only help the grid, but to also result in a financial benefit for the buildings.

Several research questions must be examined to enable buildings to provide flexibility to the grid:

- How to model the building thermodynamics efficiently for optimization based control?
- How to characterize the flexibility in electricity consumption of a building?
- What is the financial value of buildings providing ancillary services?
- Can a demand response / ancillary services provision solution be practically deployed in buildings?
- How to control the different components of a complex HVAC system (in commercial buildings) to interact with the different markets involved in the provision of flexibility (ancillary service) to the grid?

This thesis is based on an MPC framework and addresses all the above research questions. The thesis is structured in three parts, and the main contributions of all the following chapters are summarized below.

Part I - OpenBuild

Chapter 2 - Literature review
This chapter reviews the existing literature relevant for this part, and presents the necessary background material. The objectives of a traditional building controller are presented, and the components and control of a typical HVAC system are discussed. The advantages and challenges of using model predictive control for the control of buildings are discussed. The existing building energy simulation tools (particularly EnergyPlus) are introduced followed by a discussion on the existing methods for building modeling and their drawbacks. The components of a typical MPC problem for building control are introduced, and it is highlighted that obtaining a control-oriented model of the building is one of the major challenges in using MPC for buildings.

Chapter 3 - The OpenBuild Toolbox
Many high performance building energy modeling and simulation tools exist, but they are too complicated to use as prediction models in optimization based control design. Efficient control-oriented modeling of building thermodynamics remains one of the major difficulties

in deploying MPC controllers in practice. This chapter presents the MATLAB toolbox OpenBuild, developed together with another PhD student Tomasz T. Gorecki, to facilitate modeling, controller design, and simulations for buildings. The toolbox works in combination with the simulation software EnergyPlus, and enables automatic generation of linear state-space building thermodynamic models using EnergyPlus building models. The modeling procedure in OpenBuild is based on a first principles RC modeling approach. The physical phenomena modeled include heat transfer through conduction, convection, long-wave, and short-wave radiation. The impact of external weather conditions (outside temperature, solar gains, etc.), and internal gains (heat transfer due to occupants, electrical equipment, and lights) is added to the model as a disturbance input. The disturbance data affecting the model is also extracted from EnergyPlus simulation data. The quality of the generated models is validated against the original EnergyPlus models and an example illustrating the use of the toolbox is presented.

The main contributions of the OpenBuild toolbox are:

- The toolbox enables control-oriented modeling of building thermodynamics, and streamlines the design and deployment of predictive controllers.
- The toolbox gives access to a large number of validated realistic building models and disturbance data (from EnergyPlus model databases) to simulate various usage scenarios and building types.
- The toolbox facilitates co-simulation between MATLAB and EnergyPlus which allows one to do realistic simulations with a controller implemented in MATLAB, and simulation model in EnergyPlus for model validation and controller testing.

Chapter 3 is based on the following paper, and most of the text and content in Sections 3.2, 3.3, and 3.5 has appeared in this paper.

- T. Gorecki, F. Qureshi, and C. Jones, "Openbuild : an integrated simulation environment for building control", in *Control Applications (CCA), 2015 IEEE Conference on*, 2015, pp. 1522–1527. DOI: 10.1109/CCA.2015.7320826

Chapter 4 - Use of the OpenBuild toolbox
OpenBuild is developed on open-source principles and is freely available for use. Chapter 4 lists the teaching and research projects conducted in our lab, and in other institutes that use OpenBuild.

Part II - Ancillary Services

Chapter 5 - Ancillary Services Provision: Theory
This chapter introduces the concept of buildings acting as virtual storages in the electric

grid and providing ancillary services. The objective is to characterize the flexibility in the electric consumption of a building, and to use this flexibility for grid support. It is shown that participating in the intraday energy market may increase the virtual storage capacity of a building. The two phases - online and offline of secondary frequency control provision are introduced. The control problem of a building providing a secondary frequency control service to the grid, while also participating in the intraday energy market is formulated, and solved using a novel approximation method. The efficacy of the proposed control solution is demonstrated in simulations.

The key novelties of this chapter are:

- To formulate the problem of characterizing the flexibility of a building, while also participating in the intraday energy market, as a multi-stage uncertain optimization problem.
- To develop an approximate solution method for the flexibility characterization problem using a novel intraday control policy and two-stage stochastic programming.
- To develop a closed loop control algorithm based on a stochastic MPC controller for the online phase of operation.

This chapter is based on the following paper, and most of the text and content in Sections 5.3, 5.4, and 5.5 has appeared in this paper.

- F. A. Qureshi, I. Lymperopoulos, A. A. Khatir, and C. N. Jones, "Economic advantages of office buildings providing ancillary services with intraday participation", *IEEE Transactions on Smart Grid*, vol. PP, no. 99, pp. 1–1, 2016, ISSN: 1949-3053. DOI: 10.1109/TSG.2016.2632239

Chapter 6 - Ancillary Services Provision: Economics
Sufficient financial benefits are required for large commercial buildings to invest in deploying advanced control methods for providing flexibility to the grid. This chapter investigates the economic benefit for a typical office building providing a secondary frequency control service to Swissgrid, the Swiss Transmission System Operator (TSO). The control methodology presented in Chapter 5 is adapted for the particular building, HVAC, and the Swiss market remuneration structure and is used to carry out a detailed simulation study. The operation of the Swiss ancillary services, electricity spot, and intraday markets is summarized, and all the costs and rewards associated with the provision of ancillary services in Switzerland are considered. Extensive simulations are carried out with real data for energy prices, ancillary service bids, meteorological records and the frequency control signals for the year 2014.

The key outcomes of the study are:

- Significant savings are achieved, on average, for the building providing secondary frequency control service to the grid, and these savings are further increased by participating in the intraday energy market.

- The occupant comfort is increased as a by-product of providing flexibility to the grid which is counter-intuitive.

- The economic benefit is sensitive to the price of electricity. Since, electricity prices are slightly different (due to different distribution charges) at different locations in Switzerland, the financial benefit varies with the physical location of the building within Switzerland.

This chapter is based on the following paper, and most of the text and content in Chapter 6 has appeared in this paper.

- F. A. Qureshi, I. Lymperopoulos, A. A. Khatir, and C. N. Jones, "Economic advantages of office buildings providing ancillary services with intraday participation", *IEEE Transactions on Smart Grid*, vol. PP, no. 99, pp. 1–1, 2016, ISSN: 1949-3053. DOI: 10.1109/TSG.2016.2632239

Chapter 7 - Ancillary Services Provision: Experiments
This chapter demonstrates the technical feasibility of office buildings providing regulation services using a laboratory-scale experimental setup. Specifically, the case of a building providing secondary frequency control service in Switzerland is considered. The experimental platform LADR (Laboratoire d'Automatique Demand Response), developed with three other PhD students (Tomasz Gorecki, Luca Fabietti, and Altug Bitlislioglu), for the validation of control algorithms is introduced. The control method described in Chapter 5 for the provision of ancillary services is used to characterize the flexibility of the building and closed loop experiments are carried out, over an extended period of time (10 to 24 hours), to control the heating in occupied offices in the lab, for the provision of ancillary services, while maintaining occupant comfort and operational constraints.

The main novelties of this chapter are:

- To demonstrate the technical feasibility of buildings providing a secondary frequency control service.

- To experimentally validate the flexibility characterization method and the closed loop control algorithm presented in Chapter 5. The success of the experiments despite uncertainties in weather prediction and occupancy demonstrate the robustness of the proposed control approach.

- To compare (in simulations and experiments) the control methodology proposed in Chapter 5 to an alternative robust optimization based control method developed in the lab. The results showed that the proposed control method is less conservative compared to the alternative approach.

Most of the text and content in Section 7.3, and 7.4 has appeared in the following paper.

- L. Fabietti, T. Gorecki, F. Qureshi, A. Bitlislioglu, I. Lymperopoulos, and C. Jones, "Experimental implementation of frequency regulation services using commercial buildings", *IEEE Transactions on Smart Grid*, vol. PP, no. 99, pp. 1–1, 2016, ISSN: 1949-3053. DOI: 10.1109/TSG.2016.2597002

Part III - Hierarchical Control

Chapter 8 - Hierarchical Control of Building HVAC System for Ancillary Services Provision

Most large commercial buildings have complicated HVAC systems, while the existing methods to characterize a building's flexibility assume simplistic HVAC systems, restricting their applicability to controlled (laboratory) environments. This chapter presents a hierarchical scheme for the control of a typical building HVAC system for providing secondary frequency control service to the grid. The proposed scheme separates the control of the building zones and the HVAC system. The problem is decoupled into three layers - local zone controllers, thermal flexibility controller, and electrical flexibility controller. The local building controllers are at the lowest level and track the temperature setpoints received from the thermal flexibility controller. The thermal flexibility controller maximizes the flexibility in the thermal consumption of the building zones, and abstracts out all the information required at the higher control layer. At the highest level, the electrical flexibility controller uses the thermal flexibility and controls the HVAC system to provide flexibility to the grid. The two flexibility control layers are based on robust optimization methods. The thermal flexibility problem is formulated as a convex robust optimization problem and is approximated using linear decision rule policy, while the electrical flexibility problem is formulated as a non-convex robust optimization problem and is approximated using two-stage robust programming. A control-oriented model of a typical HVAC system is developed, and simulations are carried out to demonstrate the efficacy of the proposed approach. The results show that exploiting the variable COP of the HVAC system might add extra flexibility on top of the flexibility from the building thermodynamics and thermal storage.

The key contributions of this chapter are:

- To develop a control-oriented model of a typical air-based HVAC system and thermal storage.

- To develop a hierarchical method for the control of a typical HVAC system for ancillary services provision. The developed method separates the thermal and electrical flexibility of the building and scales better for large buildings due to its hierarchical structure.

This chapter is based on the following technical report and most of the text and content in this chapter has appeared in this report.

- Faran A. Qureshi, and Colin N. Jones. "Hierarchical Control of Building HVAC System for Ancillary Services Provision". Technical Report, 2017.

Additional Publications
The following papers were published during the Ph.D. study, and are not included in this thesis.

- F. Qureshi, T. Gorecki, and C. N. Jones, "Model Predictive Control for Market-Based Demand Response Participation", in *Proceedings of the 19th IFAC World congress*, vol. 47, Cape Town, South Africa, 2014, pp. 11 153–11 158
- I. Lymperopoulos, F. A. Qureshi, T. Nghiem, A. A. Khatir, and C. N. Jones, "Providing Ancillary Service with Commercial Buildings: The Swiss Perspective", in *9th IFAC International Symposium on Advanced Control of Chemical Processes (ADCHEM)*, Whistler, BC, Canada, 2015
- X. T. Nghiem, A. Bitlislioglu, T. T. Gorecki, F. A. Qureshi, and C. Jones, "OpenBuildNet Framework for Distributed Co-Simulation of Smart Energy Systems", in *Proceedings of the 14th International Conference on Control, Automation, Robotics and Vision*, 2016
- T. T. Gorecki, L. Fabietti, F. A. Qureshi, and C. N. Jones, "Experimental Demonstration of Buildings Providing Frequency Regulation Services in the Swiss Market", *Energy and Buildings*, pp. –, 2017, ISSN: 0378-7788. DOI: http://dx.doi.org/10.1016/j.enbuild.2017.02.050

OpenBuild Part I

This part of the thesis focuses on the development of the toolbox OpenBuild for modeling of buildings for control applications. We start by introducing the problem of building control in Chapter 2 and we examine the shortcomings of the current practice of optimal control of buildings. In Chapter 3, we introduce the OpenBuild toolbox and demonstrate how it helps alleviating some of these shortcomings and give examples of its use. Finally, we review where the OpenBuild toolbox was used in Chapter 4 before providing a detailed description of the modeling procedure in Appendix A.

The OpenBuild toolbox has been developed as a joint work between Faran A. Qureshi, and Tomasz T. Gorecki within the Green Energy Management of Structure (GEMS) project. As a consequence, this part of the thesis is co-authored and appears for the most part identically in both theses.

2 Literature review

2.1 Building Control

2.1.1 The main objectives of building control

The objectives of building control and the most important aspects of room automation are discussed here. Building control aims to fulfill the following objectives, by order of importance:

- Maintain occupant comfort in the building, for example keeping the temperature in occupied spaces at an appropriate level.
- Maintain the equipment in a safe operating mode, for example avoiding excessive cycling of compressors in heat pumps.
- Optimize the cost of operation of the building, for example by minimizing the energy consumption, using storage systems efficiently, and operating the equipment at its optimal coefficient of performance.

For the temperature management of the building, regulation and stability are not the primary control issues. The main issue is rather related to the economically efficient use of the heating, ventilation, and air-conditioning (HVAC) system to maintain optimal comfort conditions.

Comfort in buildings

Americans spend 87% of their time indoors [15], and since comfort conditions directly influence the productivity and well-being of building occupants [16], comfort is a crucial objective in the design and operation of building spaces and equipment. Comfort in indoor

spaces depends on multiple factors, including temperature, humidity, air quality and lighting. It is important to note that comfort depends both on the design of the indoor space, for example the materials used for construction and on the proper operation and active control of the HVAC system and other elements such as blinds. Thermal comfort has been studied extensively and multiple models have been devised to measure it quantitatively, such as the predicted mean vote (PMV) and the predicted percentage of dissatisfied (PPD) [17], [18], relating temperature, humidity but also season to comfort. Some of these are discussed in more detail in Appendix B.

Energy cost

Buildings are responsible for 37% of the total energy consumed in the European Union [19], one third of which concerns commercial buildings and the rest residential buildings. It is estimated that about 50% of the energy in buildings is consumed by the HVAC system. That represents a very large share of the total energy consumed worldwide and a great target for potential savings [20]. Policies have recently focused on setting new standards for building energy efficiency, such as the recent European Energy Performance of Buildings Directive [21], reflecting a global concern for improving energy efficiency of buildings. Accordingly, academic research has also focused more and more on energy efficiency of buildings, including the control sytems of buildings [22], [23].

2.1.2 A traditional HVAC system and its control

There exists a very large range of HVAC systems, but structural similarities exist, in particular in their overall organization. Large HVAC systems include a supply loop and a distribution loop. The heat or cold is generated in the supply loop in a boiler/chiller/heat pump. It is then transported to heating/cooling coils through a fluid loop (generally water). The heating/cooling coils transfer the heat/cold to the fluid (air or water) circulating in the distribution loop. The fluid of the distribution loop is in turn circulated to the zones and the heat/cold is delivered to the room through air exchangers or a radiant system. Figures 2.1 and 2.2 illustrate standard heating and cooling system architectures.

The control systems also have typical configurations as reported in [24]:

HVAC systems are typically controlled using a two-level control structure. Lower-level local-loop control of a single set point is provided by an actuator. For example, the supply air temperature from a cooling coil is controlled by adjusting the opening of a valve that provides chilled water to the coil. The upper control level, also called supervisory control, specifies set points and other time-dependent modes of operation.

Control of a variable air volume (VAV) cooling system (Figure 2.1) responds to changes

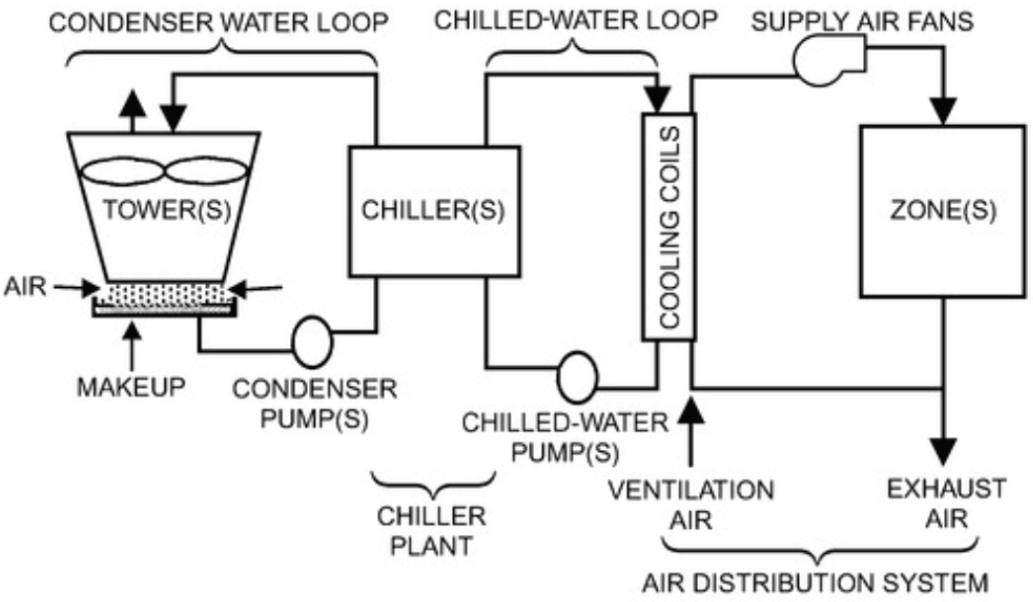

Figure 2.1 – Prototypical cooling system. From [24]

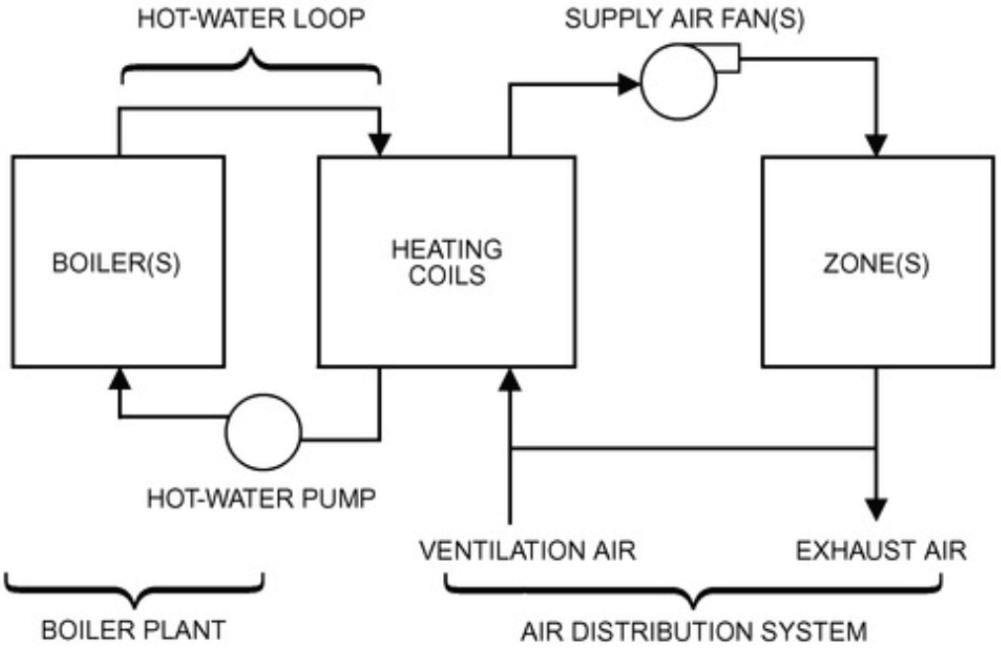

Figure 2.2 – Prototypical heating system. From [24]

in building cooling requirements. As the cooling demand increases, the zone temperature rises as energy gains to the zone air increase. The zone controller responds to higher temperatures by increasing local flow of cool air by opening a damper. Opening a damper reduces static pressure in the primary supply duct, which causes the fan controller to create additional airflow. With greater airflow, the supply air temperature of the cooling coils increases, which causes the air handler feedback controller to increase the water flow by opening the cooling coil valves. This increases the chilled-water flow and heat transfer to the chilled water (i.e., the cooling demand).

The control of a hot-water heating system (Figure 2.2) is similar. As the heating demand increases, the zone temperature falls as energy gains to the zone air decrease. The zone controller responds to lower temperatures by opening a control valve and increasing the flow of hot water through the local reheat coil. Increasing water flow through the reheat coils reduces the temperature of the water returned to the boiler. With lower return water temperature, the supply water temperature drops, which causes the feedback controller to increase the boiler firing rate to maintain the desired supply water temperature.

In Europe, it is fairly common to have water-based distribution loops with radiant heaters. Water is circulated to the rooms and heat exchange happens through radiation and convection between the radiators and the room air rather than direct air exchange. The control architecture in this type of system is similar to the one used in air-based systems.

Set points and operating modes for HVAC equipment can be adjusted by the supervisory layer to maximize overall operating efficiency. In modern buildings, the control is performed in a computerized energy management systems (EMS) that aims at reducing utility costs. Standard supervisory control uses a collection of rules to determine the best operating points for the system. This is referred to as rule based control (RBC). The design of the rules is based on knowledge of the system, experience and tuning. As (i) the complexity of the system increases with the addition of extra equipment such as thermal storage, on site generation and shading control; and (ii) the objectives of the control system are becoming increasingly complex, for example with peak shaving or optimal response to dynamic pricing, the complexity of rule-based controllers also increases [25]. Tuning may be impractical and RBC altogether inadequate for these complex objectives.

Numerous researchers focus on optimization-based strategies for energy-optimal control of buildings. Early works such as [26] have used offline optimization to improve the operation of the system, in this case the night setback strategy. [24] provides an extensive list of such optimized strategies that can then be used in the rule-based controller to improve operation. Recent years have shown a surge of interest in dynamic optimization and in particular model predictive control (MPC) for energy-optimal control of buildings. The framework of MPC is particularly suitable for building control due to its capability to handle constraints and to account for future weather, occupancy, and electricity price predictions in the control formulation.

2.1.3 MPC for Building Control

Building control has been identified as a natural field for the application of MPC, due to various reasons, including its ability to handle constraints and complex objectives easily, the slow dynamics of buildings, and the fact that stability is not the primary concern of building control. The use of model predictive control has been explored extensively in the context of building control. Different objectives have been studied in the literature, such as total cost minimization [27], [28], [29], peak power reduction [30], [31], energy-optimal use of the building, and different types of demand response objectives [32], [33]. A variety of systems has been considered, including mixed-mode buildings [34], [35], storage systems [36], [37], [32], combined heat and power units [38], or passive solar systems [39].

It has been outlined that forecasts also play an important role, and have received special attention, in particular models for occupancy [40], [41] and the impact of weather on the building [42].

Specific efforts have been initiated in MPC theory to tackle building control problems, such as handling of periodic constraints [43] or stochastic MPC [42], [44].

It has been identified that MPC can help in understanding how to improve existing rule-based controllers. In [45], simplified operating rules are extracted from the results of the MPC simulations using data-mining procedures. Various factors influencing the energy saving potential of a building (utility rates, building mass, internal heat gains, efficiency of the HVAC system, and outside weather conditions) are studied in [46]. This study concludes that the factors affecting the energy use of a building do not necessarily influence its energy saving potential.

Summarizing the findings appearing throughout the literature, a few key advantages of predictive control for buildings are:

- The ability to utilize more information than classic techniques about the current and the future environment of the building when making control decisions. MPC offers a very natural way to feed forward information about weather, occupancy, and price forecasts into the control scheme, and use it to optimize the control objective.
- The possibility to specify complex control objectives and constraints in an intuitive manner.

Experimental at-scale implementations have also been conducted. Of particular interest are the works [37], [47] where a hierarchical MPC controller is designed to improve the operation of the cooling system of the University of California, Merced campus buildings. The high-level MPC controller manages the energy conversion systems, including chillers, a cooling tower, pumps and takes the building as a load. A lower-level MPC layer takes care

of the air handling units (AHU) and the variable air volume (VAV) boxes. An improvement of 19% of the average system COP is reported, resulting in significant savings. It lead to an improvement of the rule-based controller by 'imitation' of the optimal strategy deployed by the MPC controller. In other works, significant energy savings compared to the traditional rule-based controllers are reported in [48] and [49] for campus buildings in Europe, operated by reference tracking MPC controllers.

However, the key limiting factor to the deployment of MPC in buildings is usually the availability of a prediction model. An interesting contribution in this regard is [50] which reports that the identification, commissioning and installation costs for an MPC controller may in many cases outgrow its potential economic benefits. Therefore, efforts to facilitate the design of MPC controllers for building are still needed.

2.2 Building Simulation Tools

Various tools have been developed for building modeling, simulation and control design. Their strengths and weaknesses vary depending on the application. The most mature ones include Modelica, TRANSYS, ESPr, eQuest, and EnergyPlus [51]. Modelica is an equation-based modeling language that has a free open source building library which covers HVAC systems, multi-zone heat transfer and heat flow. It also enables real-time data exchange with building automation systems. TRANSYS provides a transient simulation environment and is well suited for the detailed analysis of solar systems, HVAC systems, renewable generation, and co-generation systems. ESPr is based on a finite volume, conservation approach and is powerful for simulating scenarios in different operating and environmental conditions. eQuest is a comprehensive building energy simulation tool and supports complex geometries, and many HVAC configurations. EnergyPlus is a very detailed complete building energy simulation software and includes many simulation capabilities.

The main differences between these tools lie in their simulation capabilities, modeling approach, the way they handle interior and exterior surface convection, solar gain, data exchange and the additional software they support. See [52] and Table 2.1 in [51] for a detailed comparison of these tools.

2.2.1 EnergyPlus

EnergyPlus [53] is a detailed building energy simulation software developed by the U.S Department of Energy (DOE) for the simulation of building, HVAC, lighting, occupancy, ventilation, and other energy flows in a building. It is typically used by architects, engineers, and researchers and helps to optimize the building design for energy and water usage.

EnergyPlus is a combination of many modules working together to determine the heating or

cooling energy requirement of a building. It include modules for shading computation, day lighting, window heat transfer, sky model, air loops simulation, zone equipment simulation, airflow network, and conduction transfer function. Each module simulates and determines its energy impact on the building and the HVAC system. The integrated simulation approach used in EnergyPlus means that all modules are simulated concurrently and a constant feedback between the modules ensures that a physically realistic solution is obtained.

Some of the key features of EnergyPlus include the integrated, simultaneous solution of the thermal zone conditions and HVAC system response, heat-balance based solution of radiant and convective effects, sub-hourly user definable time steps for interaction between the thermal zone and the environment, combined heat and mass transfer models, illuminance and glare calculations, component-based HVAC supporting both standard and novel configurations, a large number of built-in HVAC and lighting control strategies, import and export of data with other engines for co-simulation, and generation of detailed output reports with user defined time-resolutions[1].

EnergyPlus takes as inputs building description data and weather data as structured ASCII text files. The core of the software is script based and does not have any official GUI or user interface. Third-party software has been developed, e.g., OpenStudio [54] to interface with EnergyPlus. Generally, EnergyPlus, like most of the other detailed building simulation software, is not considered an easy-to-use tool and requires experience.

One of the strengths of EnergyPlus is that it allows the simulation of different types of environments, building types, HVAC types and configurations, and external weather conditions. It also enables the simulation of renewable, e.g., PV's and co-generation units. Another advantage is the free availability of a validated database of standard building models of different types and locations provided by the Reference Buildings database of the U.S. DOE [55]. It includes models for offices, warehouse, retail stores, malls, schools, supermarkets, restaurants, hospitals, hotels, and apartment buildings. This database is representative of approximately 70% of all the commercial buildings in the U.S. and is a good resource to carry out simulations with a wide variety of buildings.

EnergyPlus building models are generally of good quality, and are considered to be a reasonable representation of buildings. Various works have experimentally tested and validated EnergyPlus models [56], [57], [58], [59]. However, EnergyPlus models, because of their complexity, are not suitable as prediction models in optimization based control design. Therefore, there is a need to develop a systematic modeling procedure to obtain simple, yet representative models which can be used for control design.

[1] https://energyplus.net/

2.2.2 MLE+

MLE+ [60] is a MATLAB / SIMULINK toolbox for co-simulation with EnergyPlus. The toolbox provides an interface between EnergyPlus and MATLAB. It relies on BCVTB [61] to handle the communication of data between the two pieces of software. It is useful to carry out co-simulations where the building energy simulation is performed in EnergyPlus and the controller design and implementation is done in MATLAB. It also helps collecting data from EnergyPlus simulations for system identification or analysis purposes.

Using MLE+ requires the knowledge of EnergyPlus and involves manual processing for setting up the co-simulation which can be cumbersome when a large number of simulations are required.

2.3 Building Modeling

Building thermodynamic modeling can broadly be divided into three main categories - first principles physics-based (white-box), data-driven (black-box), and a combination of physics-based and data-driven (gray-box) modeling approaches [22], [62]. All these approaches have been studied in the literature and have their associated benefits and drawbacks.

First principles physics-based modeling methods [22], [62] involve constructing a detailed model of the building thermodynamics based on the principles of heat transfer through conduction, convection, and radiation. A Resistance-Capacitance (RC) network of nodes is constructed where each node represents the temperature in a specific zone, wall, surface, ceiling, or floor. The interconnection of nodes is defined by the physical geometry of the building. The model parameters (conduction, and convection coefficients, etc.,) are usually obtained from the knowledge of the construction material and architectural details. Constructing these types of models is time consuming (especially for large buildings) and requires expert knowledge of the building thermodynamics. The dimension of the model can be quite large depending on the size of the building, whereas the quality of the model is generally good.

Data driven modeling [63] approaches use experimental input-output data to learn a dynamical model of the building thermodynamics. The advantage of this method is that it does not require any knowledge of building construction or geometry, but the models obtained by this method lack any physical interpretation. The procedure can be applied to either the whole building or to a subsection of the building. Usually, a large data set is required to obtain models of reasonable accuracy which is difficult to obtain for an occupied building. Moreover, the identification data is also required to have a rich frequency content, which is difficult to obtain in a real building. Some authors have proposed to use the data from the energy simulation software, e.g., EnergyPlus. OpenStudio was used in [64] to perturb the EnergyPlus model and generate the experimental data which is then used to

fit a reduced-order linear model. The results demonstrated a model which was accurate enough for control and was used in simulation to design an MPC controller. Generally, there is no systematic method to select the structure and order of the model and it might take several trial-and-error rounds to obtain a reasonable model.

Grey-box modeling or hybrid modeling [65] approaches first choose a model structure based on the physical knowledge of the building and use parameter estimation techniques to identify the model parameters. Using a physical model structure reduces the requirement of a large training data set, and can provide a better quality model compared to black-box methods. [66] proposes a transfer function based model with parameters constrained to satisfy a physical representation for energy flows in the building. The model parameters were identified using simulation data from TRANSYS and field data from a test site, resulting in a satisfactory model quality. [67] presented a Monte-Carlo simulations based method to estimate the model parameters. [48] used subspace identification with data generated from EnergyPlus and divided the building into smaller parts to make sure that the estimation algorithm could be applied with the available computational power, and combined the identified parts together to obtain the complete model. The resulting model was validated successfully. [51] proposed using a parameter adaptive building model with time-varying parameters in a RC model to capture the time varying impact of the internal and external disturbances on zone temperatures. The parameters were then estimated online using an extended Kalman filter.

Experimental results have also been reported in the literature. [68] identified a low-complexity data-based model and an RC model of an entire floor of Sutardja Dai Hall, an office building on the University of California, Berkeley campus. Experiments were conducted and semi-parametric regression was used for data based modeling. The comparison results showed that the RC model was more accurate, but both models performed well for closed-loop control. [69] obtained two models of a single zone test office using system identification and physical modeling approaches and both the models showed a reasonable performance in predicting the room temperatures with the RC model being slightly more accurate at high frequencies. [70] used grey-box system identification methods to obtain a thermodynamic model for a building in Belgium for MPC operation.

All these methods are time consuming and often are difficult to generalize. The modeling and validation procedure needs to be repeated for every new building. Therefore, a systematic modeling approach is required which can be used with minimal effort to construct a good quality control-oriented model.

Remark 1. *Concurrently and independently to the development of OpenBuild, a similar effort was undertaken in the development of the BRCM toolbox [71]. This toolbox also helps to create discrete-time state-space (bi-)linear models for buildings using a physical modeling approach. The Toolbox is based on [72] and constructs a RC model of the building zones while the model parameters are provided by the user or can partly be obtained from*

EnergyPlus. The model validation with EnergyPlus shows a reasonable performance for the considered case. However, it does not provide input data compatible with the model for weather and usage description, and does not offer co-simulation capabilities.

2.4 MPC for Building Control

This section provides an overview of the ingredients used in MPC for buildings. It serves as reference for the rest of the thesis.

2.4.1 Optimization Problem

We start from a standard MPC problem formulation:

$$
\begin{aligned}
&\underset{x,u}{\text{minimize}} && J(\mathbf{u}) && (2.1)\\
&\text{subject to} && x_{i+1} = f(x_i, u_i, d_i) && (2.2)\\
& && y_i = g(x_i) && (2.3)\\
& && u_i \in \mathcal{U} && (2.4)\\
& && y_i \in \mathcal{Y} && (2.5)\\
& && i = 0, \ldots, N-1 &&
\end{aligned}
$$

The choice of the cost function (2.1) is discussed in section 2.4.4. Equations (2.2) and (2.3) embed the dynamics of the system and the effect of the disturbance and are discussed in section 2.4.2. Equation (2.4) gathers the input constraints and (2.5) represents the zone temperature constraints as discussed in section 2.4.3.

2.4.2 Model of the system

As we already mentioned, an MPC controller requires a model of the system. We usually consider discrete-time state-space models of the form

$$
\begin{aligned}
x^+ &= f(x, u, d)\\
y &= g(x)
\end{aligned}
\qquad (2.6)
$$

where x denotes the state of the system, u the controlled input to the system, d the vector of disturbances affecting the system and y represents the output of the system. In the case of buildings the output is usually the temperature in different zones of the buildings.

The inputs are the control variables of the HVAC system: depending on the type of HVAC, these inputs can be flow rates, supply temperatures, temperature setpoints, blind positions, or thermal power inputs, for example.

Buildings are affected by large disturbances coming from weather and internal gains, and it is crucial to model the effect of these disturbance in our model to have a good prediction quality. d typically regroups the effect of the outside temperature, sun irradiance, occupancy, and internal gains from equipment, lighting, etc.

We will see in Chapter 3 that the model in our approach is decoupled in two parts: the model for the thermodynamics of the building, which takes as inputs thermal power inputs to the zones and as outputs the temperatures inside the building, and the model of the HVAC system which is system dependent and takes as inputs the actual controlled inputs and outputs the resulting thermal flows to the rooms.

2.4.3 Constraints

One of the most advertised advantages of MPC is its natural ability to handle constraints on inputs and states of the problem. In the case of buildings, the constraint will typically include constraints on the inputs captured in (2.4) which model the operational limitations of the system, for example limits on power inputs, flow-rates, supply temperature, etc. In addition, it is frequent to impose comfort constraints, captured in (2.5). We usually define a comfort range for the zone temperatures as $[T_{\text{ref}} - \beta, T_{\text{ref}} + \beta]$ where T_{ref} is the optimal temperature and β is a parameter defining the size of the comfort range.

Notice that for commercial buildings, it is customary to relax the temperature during unoccupied hours in order to reduce the total energy consumption, a strategy referred to as night-time setbacks. In that case, the comfort range is extended during the night so that the constraint reads $y_t \in [T_{\text{ref}} - \beta_i, T_{\text{ref}} + \beta_i]$ with β_i a time-varying quantity.

2.4.4 Objective Function

Another advantage of MPC is the possibility to specify various types of objectives. Contrary to classical MPC setups, tracking is rarely the objective of MPC for buildings and quadratic costs are not common. Instead, economic performance is commonly specified as the objective of the problem. Assuming a relationship is known between the control inputs of the problem and the amount of energy used (electricity or other): e, a minimum energy objective reads

$$J(u) = \sum_{i=0}^{N} e_i$$

A minimum cost of energy objective is formulated as

$$J(u) = \sum_{i=0}^{N} c_i e_i$$

with c_i the time-varying cost of energy. Buildings are often subject to differentiated tariffs so that c_i changes according to a schedule, with alternating periods of peak demand with high cost of energy and periods of low demand with lower cost of energy. In other cases, the price is dynamic, and changes continuously. In this case, the cost of energy might need to be forecast.

A typical objective is also to reduce peak demand over predefined periods of time, as specified by a lot of utility tariff plans. The cost can then include a term of the form

$$J(u) = c_{\text{peak}} \max_{i \in [T_0, T_f]} p_i$$

with c_{peak} the cost of peak electricity consumption and p the power demand.

Beyond these classical costs, a multitude of Demand Response objectives can be computed. Event-driven Demand Response sometimes requires pre-specified power decrease upon request. For example, [11] studies such a problem and uses the following cost function

$$J = \sum_{i=0}^{N_{OC}-1} V_i^e - \delta_i V_i^{dr}$$

with $V_i^e = c_i e_i$ the cost of electricity consumption, $V_i^{dr} = c_i^d (B_{d,h} - p_{d,h})$, the payment from DR participation, where $B_{d,h}$ is the baseline consumption at time step i (day d, hour h) and c_i^d the payment for power reduction. The baseline consumption for an hour h is the average energy consumption during hour h over a set of previous days $\mathcal{S}_{d,h}$, and is given by

$$B_{d,h} = \beta_{d,h} \frac{1}{|\mathcal{S}_{d,h}|} \sum_{j \in \mathcal{S}_{d,h}} p_{d-j,h},$$

where $\mathcal{S}_{d,h}$ is the set of days used to compute the baseline, $\beta_{d,h}$ is a weather correction factor. δ_i is the binary variable indicating the status of DR participation at time step i.

An objective mixing different costs can be chosen and it is possible to penalize deviations from optimal comfort using one of the metrics introduced in Appendix B. Even when not directly using comfort metrics in the cost, a soft-constrained formulation is often used. In that case, extra decision variables s_i referred to as slacks are introduced and the temperature constraints are transformed into $y \in [T_{\text{ref}} - \beta_i - s_i, T_{\text{ref}} + \beta_i + s_i]$ while the slacks are

penalized in the cost so that

$$J(u) = \ldots + \rho(s)$$

with ρ a loss function.

2.5 Summary

Looking back at the MPC problem formulation (2.1)-(2.5), we see that when considering a particular building for control, the challenge is to gather and compile all the information necessary to build up the elements of the MPC problem, namely, the system model, the disturbance inputs to the model and the constraints description. In particular, we have outlined in the literature review a lack of systematic approaches to construct building models that are *appropriate for control and optimization*.

We introduce the OpenBuild toolbox in the next chapter: one of the main functionality of the toolbox is to construct automatically the model of the building thermodynamics together with the disturbance inputs corresponding to the simulated usage and weather.

3 The OpenBuild Toolbox

3.1 Introduction

3.1.1 Contributions of this Chapter

The primary objective of the OpenBuild toolbox is to facilitate the implementation, testing and validation of MPC controllers for buildings. It features the following novel elements:

- The OpenBuild toolbox enables the extraction of building models that are suitable for control and optimization purposes, based on available and standard building description data.

- The disturbance data affecting the building including weather, internal gains, and occupancy is also extracted with the toolbox.

- Through OpenBuild, users can access a large amount of data of existing buildings and realistic disturbance data to simulate various occupancy, weather and usage scenarios. This is possible because OpenBuild works in combination with the popular simulation environment EnergyPlus.

- It facilitates the design of controllers and observers, in particular predictive control algorithms, and their validation through co-simulation with EnergyPlus, by integrating the co-simulation interface MLE+. The user only requires input data files in EnergyPlus input format to create building models, without knowledge of modeling or EnergyPlus, and can co-simulate controllers from MATLAB. Therefore, the toolbox is particularly suited for control engineers and researchers interested in prototyping building controllers.

3.1.2 Structure of this Chapter

The rest of this chapter is organized as follows: Section 3.2 gives a very brief overview of the modeling principles used to derive the building thermodynamic models. Section 3.3 gives an overview of the components of the toolbox. Section 3.4 discusses the quality of the model extracted through OpenBuild. Section 3.5 gives a simple example that illustrates what a user needs to do to use the OpenBuild toolbox.

3.2 Building Thermodynamics Model

The goal of the modeling procedure is to obtain a model which is simple enough to be suitable for control (especially MPC), yet satisfactorily captures the dynamics of the building. A physical modeling approach is adopted. The following physical phenomena are modeled:

- Heat transfer through conduction
- Heat transfer through convection
- Long-wave radiation on all internal and external surfaces
- Internal gains (lighting, occupancy, equipment) on all internal surfaces
- Solar radiation on internal and external surfaces

We give in this section a brief overview of the modeling procedure, and refer the reader to Appendix A for a detailed description.

3.2.1 Modeling Fundamentals

The well-established RC modeling framework [72], [73] is used to model the thermodynamics of the building. It consists of representing the building as a set of thermal nodes in a graph where the temperature dynamics of each node is described by a linear differential equation. A parallel with electrical circuits illustrates best the concepts: temperatures of the zone air and of the building elements are represented by the voltages at each node of the RC network. The heat fluxes between the nodes are equivalent to the currents between the nodes of the RC network. Coefficients of heat conduction between the nodes and convection between the zone air and the building surfaces are modeled by resistances in the RC network. The thermal capacity of the zone air and of the layers in the building surfaces are modeled by the capacitors. Long wave radiation from outside and between surfaces are also linearized and represented by resistances.

3.2.2 Model Parameters

The computation of the parameters in the RC model is carried out using both the input data file and the post processed EnergyPlus data (surface view factors, convection coefficients, etc.). The thermal capacities and the conduction coefficients in the RC model depend on the physical properties of the materials used in the building construction, as described in the building data file. The convection coefficients in the RC model depend on the material properties, but also on other external factors including weather conditions. In EnergyPlus, the computation of convection coefficients can be carried out using different algorithms (see [74], pp. 64-74, 78-94), and yields time-varying convection coefficients. A constant time averaged coefficient is considered in the model extraction and is collected from the post-processed EnergyPlus data. The long-wave radiation from the external sources and between the internal surfaces of the building is characterized by a nonlinear function (see [74], pp. 76-77). This function is linearized, viewing factors are obtained from the post-processed EnergyPlus data and the physical properties of the construction material are obtained from the building data file. The solar radiation and the internal gains acting on the building surfaces are obtained from the post-processed EnergyPlus data and are applied to the corresponding nodes of the RC network. Lastly, EnergyPlus computes equivalent U-values capturing the overall heat transfer through windows, which are used by OpenBuild for window modeling.

3.2.3 Model Structure

Figure 3.1 gives an example of the RC structure created for a three zone building. The following energy flux balance equation is applied at each node of the RC model

$$C_n \frac{dT_n}{dt} = Q_c + Q_g + Q_r + Q_{\text{HVAC}}, \tag{3.1}$$

where C_n is the thermal capacity and T_n is the temperature of node n, respectively. Q_c combines the heat flux acting on the node due to conduction and convection, Q_g is the flux from solar and internal gains, Q_r is the flux due to radiation, and Q_{HVAC} is the flux from HVAC acting on the node. This results in a set of linear differential equations. The windows are a special case in the model, since they are assumed to have no thermal capacity: they are modeled by a set of algebraic equations (see [74], pp. 225-231). We use a linearized version of these equations to obtain explicit expressions of the window surface temperatures and substitute it in the differential equations of the rest of the temperature nodes.
This procedure provides a linear state-space model of the building which is discretized to obtain a model of the form

$$\begin{aligned} x_{i+1} &= Ax_i + B_u u_i + B_d d_i \\ y_i &= Cx_i \end{aligned} \tag{3.2}$$

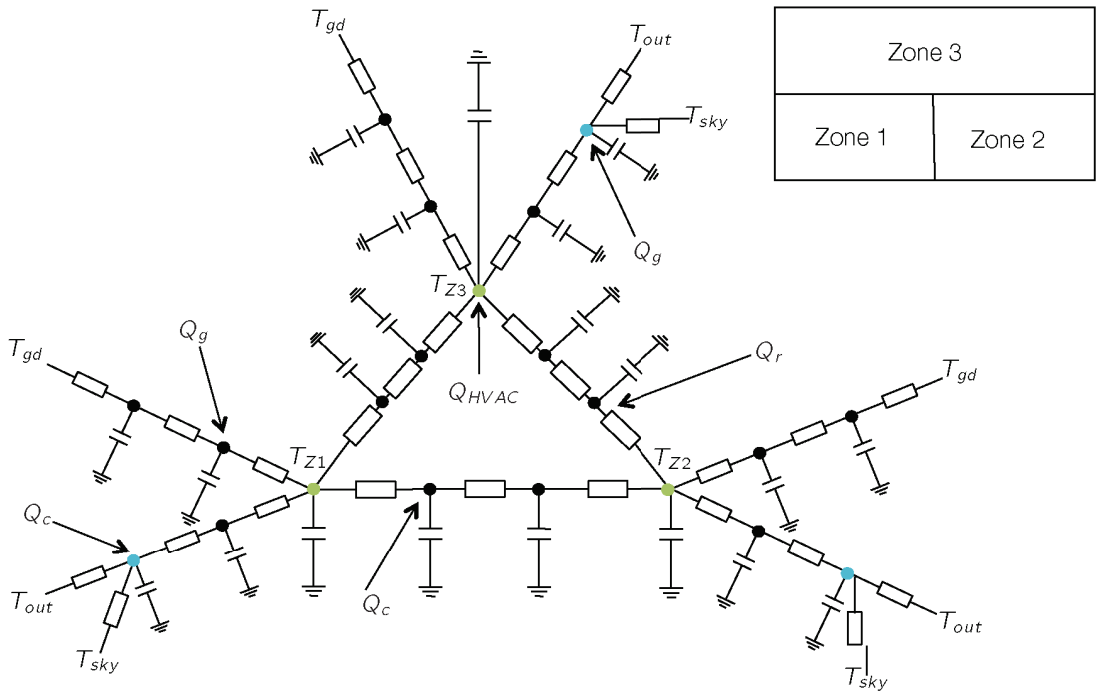

Figure 3.1 – Model Structure (green nodes: zone air, blue node: outside surfaces, black nodes: inside surfaces)

where $x_i \in \mathbf{R}^n$ is the state vector (containing the temperatures of all the zones, surfaces, and internal nodes), $u_i \in \mathbf{R}^{n_u}$ is the control input (Q_{HVAC}), and $d_i \in \mathbf{R}^{n_d}$ is the weather (*e.g.*, outside temperature and solar gains) and internal gains disturbance vector.

Remark 2. *The complete modeling procedure described in this section, including creating an RC network graph, computing of the model parameters, solving of algebraic equations and obtaining the linear model* (3.2) *is carried out automatically, taking as input only the building data description file and the weather description file.*

3.3 Code structure and simulation workflow

The main objective of OpenBuild is to enable the design and testing of advanced controllers, especially MPC controllers, in realistic simulation scenarios. It builds on the co-simulation interface MLE+ to provide control experts most of the tools and data required for controller design for buildings, as pictured in Figure 3.2. The OpenBuild toolbox helps to collect and construct these components, and streamlines their use in an integrated workflow.

Co-simulation is considered a valuable option for control design [75]. EnergyPlus is a widely used high-fidelity simulation environment, but it is not suited for complex controller design. Recent contributions [60] have enabled co-simulations between EnergyPlus and MATLAB,

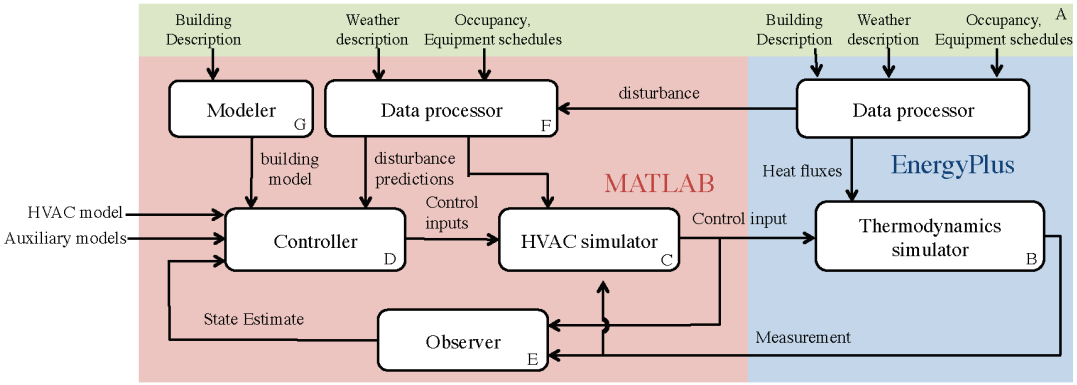

Figure 3.2 – Dataflow in OpenBuild co-simulations

where the controller is designed and simulated in MATLAB. However, co-simulations require a number of other elements including building description data, description of weather, occupancy and usage of the building. MPC design requires models of the building and HVAC system suitable for optimization. Simulations also require the conversion of weather and occupancy data to the actual inputs of the models used for control. This section details each of these components as they are included in OpenBuild. Figure 3.2 summarizes the different modules of OpenBuild with letter labels referring to the following subsections.

3.3.1 Building and weather data (A)

EnergyPlus allows the direct use of existing description data for buildings, such as the DOE reference buildings dataset [55]. In addition, tools are available to help users to easily create new models for EnergyPlus [54]. Lastly, conversion from other building description formats is often possible. EnergyPlus input data files include schedules of occupancy, equipment, lights, etc. that OpenBuild can directly interpret.

EnergyPlus takes standard weather data files as input. Typical weather data for numerous locations is readily available. Moreover, using EnergyPlus utility programs, additional weather files can be created based on measured or forecast weather data, also reconstructing missing or corrupted data. This is useful to construct predictions of the weather disturbances for an MPC controller. For example, a database of weather forecasts has also been collected: it can be used to test controllers with realistic historical forecasts, which are not easily found.

3.3.2 Thermodynamics simulator (B)

EnergyPlus can be used as the simulator for the thermodynamics of the building. It is possible to control some variables in EnergyPlus through an external interface, and [60]

provides ways to run co-simulations from MATLAB. However, two main difficulties arise: first the external interface lacks flexibility and requires knowledge of EnergyPlus and in some cases manual modifications of the files. Second, only specific variables are available for external control, mostly setpoints for thermostats. For most systems, no direct control of the low-level actuators and variables is possible (valve and damper positions, massflows, etc.). This issue is common to numerous building simulation software, which are generally not well suited for controller design. Note however, that setpoint control can prove sufficient for supervisory control purposes (and in many cases is actually more realistic than low-level control of components).

Therefore, to enable flexible HVAC simulation, OpenBuild typically uses EnergyPlus only for the thermodynamics of the building. From MATLAB's point of view, the inputs to the zones are heat fluxes to the rooms or surfaces of the building. This allows the decoupling of the simulation of the building and the HVAC. This is a reasonable setup since the thermodynamics of the building is mostly independent from the HVAC type.

Remark 3. *The models generated by OpenBuild can also be used to simulate the building in MATLAB without co-simulation.*

3.3.3 HVAC simulator (C)

Modeling the HVAC is a complex task, which is very difficult to perform automatically. The complexity of the HVAC descriptions in EnergyPlus are high, at a level of detail which is not required for controller design. Most works from the literature report targeted case-by-case modeling efforts for the HVAC, which is very time-consuming. In the perspective of large-scale simulations of building controllers, this motivates the use of HVAC models in MATLAB. These models map the actual input (such as electric power input, valve and damper positions or fluid flows) to the heat fluxes into the different rooms and surfaces. A framework is proposed to specify new HVAC system models easily. Some simple HVAC models have been developed and include simple forced-air systems, thermally activated building systems, electric boilers, heat pumps, and blind controls. In addition to simulating the HVAC, the HVAC simulator also computes appropriate inputs to the external interface of EnergyPlus. Additional modules such as batteries or storage tanks can easily be added and simulated together with the building. Notice that HVAC components can still be simulated in EnergyPlus in co-simulation but that requires manual processing of the files and good knowledge of EnergyPlus inner workings.

3.3.4 Controller (D)

Good controllers are imperative for the efficient operation of a building. OpenBuild focuses on MPC controllers. The controllers use a model of the dynamics of the system and solve a constrained optimization problem to compute an optimal input sequence. The performance

of MPC controller relies greatly on the quality of the model. OpenBuild can directly extract models for the thermodynamics of the building (*cf* Section 3.3.7) to facilitate the MPC setup. Section 2.4 details a typical MPC formulation for buildings.

3.3.5 Observer (E)

Full state information of the linear model is required for control with MPC, however it is not available from EnergyPlus (or in a real building). Observers are required to estimate the state of the building, HVAC system, and auxiliary systems attached to it. Observer design can be challenging because of model mismatch and disturbance issues. By combining an offset-free formulation [76] and Kalman filtering, good performance was generally achieved in our simulations. The Kalman filter is also designed using the model of the building. Examples of filters and controllers are available in the toolbox examples but tuning of the observers has been observed to have a significant impact on the quality of the estimation, therefore requiring a minimum effort from the user.

3.3.6 Data Processor (F)

Implementation of MPC controllers requires the prediction of the weather, including solar gains, occupancy, and internal gains. Occupancy and equipment use are usually specified in the form of schedules directly in the EnergyPlus file. Weather data comes in separate files which list temperatures, humidity ratios, weather conditions, solar irradiance, etc. This data needs to be interpreted to evaluate the impact of the weather on the building, *e.g.* through geometric computations to calculate the effect of the sun on each surface. EnergyPlus performs these computations, which we can directly exploit in OpenBuild. OpenBuild uses EnergyPlus as a pre-processing engine for the model. From only the building and weather description, it automatically runs the appropriate components of EnergyPlus to extract the corresponding weather and internal gain data compatible with the models. This is a key feature of OpenBuild which facilitates simulation greatly by requiring minimum user input.

3.3.7 Modeler (G)

When running simulations, EnergyPlus uses standard input files, describing the geometry and construction of the building, the heating system and simulation parameters. Based on the information in these files, it computes other quantities for the simulation, such as equivalent U-values of windows, viewing factors of internal surfaces, etc. This processed data is given out as an output of the simulations with EnergyPlus. OpenBuild automatically generates a linear state-space model of the building thermodynamics based on the input data files and the processed data from EnergyPlus. This automatic model generator is the backbone of the OpenBuild toolbox.

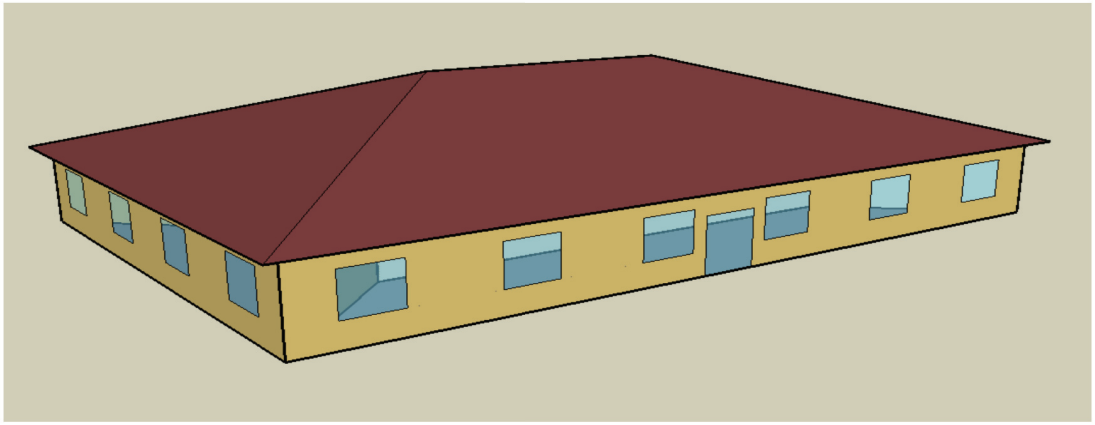

Figure 3.3 – Small Office

Table 3.1 – Characteristics of the Buildings

	Small Office	Warehouse
Floor Area (m^2)	511	4835
No. of floors	1	1
No. of zones	5	3
Window-to-wall ratio	21.2%	0.58%
Peak Occupancy (people/100m^2)	5.38	0.1
Exterior walls type	mass	metal
Roof type	attic	metal
Foundation Type	mass floor	mass floor

3.4 Validation of the building models

3.4.1 Data used for validation

One of the advantages of using EnergyPlus as the basis of our thermodynamic model extraction is the availability of a number of typical building models of different types from the Reference Building Database [55] of the U.S. DOE. The building models are in standard EnergyPlus input data format and come with typical schedules for occupancy, and internal gains (lighting, electrical equipment, etc.). They comply with ASHRAE standards for energy efficiency.

We selected two building models - Small Office, and Warehouse from this database for validating the quality of the models extracted using OpenBuild. The pictures of the two models are shown in Figure 3.3, and 3.4, and their characteristics are summarized in Table 3.1. These models together with their typical occupancy, internal gain patterns, and typical measurement year (TMY) weather data of Chicago are used for the validation experiments. Chicago has a large variation of temperatures over the year, allowing validating the models in both summer and winter conditions.

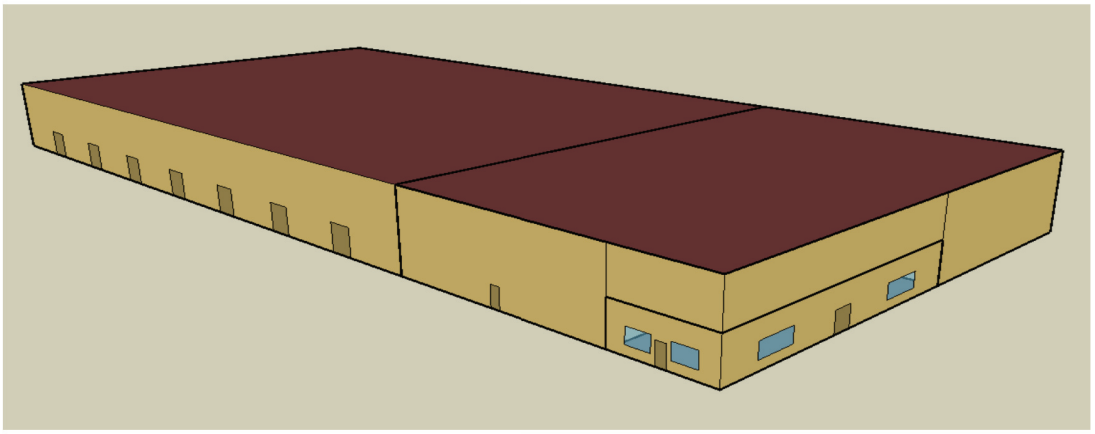

Figure 3.4 – Warehouse

3.4.2 Time-domain comparison

MPC based control schemes rely on the open-loop prediction models to generate the control inputs. We compare the time-domain prediction quality of the linear models with the original EnergyPlus models to evaluate the model quality. Two comparisons (open loop output and input) are performed.

Open loop Output comparison
The zone temperatures (output) of the two models are compared when excited with the same inputs. The EnergyPlus models are simulated using their default controllers with a sampling time of 15 minutes. The zone temperatures track specified setpoints according to the default schedules of the buildings. The thermal power input applied by the default controller in each zone of the building, and the associated disturbance input (occupancy, weather, etc.) are applied to the corresponding linear model in open loop. The zone temperature trajectories from both simulations are compared. The zone temperatures from the two simulations, for two of the zones of the small office model are shown in Figure 3.5 for a period of one week. The monthly RMSE for each building model is shown in Figure 3.6. The yearly maximum error, mean error, and RMSE for each building are reported in Table 3.2. The results show that the small office and the warehouse have a yearly RMSE of 1^oC, and 0.6^oC, respectively. It can be seen in Figure 3.6 that the RMSE is slightly higher in summer months for the office building due to the increased impact of the solar radiations. This effect is not seen in the warehouse model because it almost does not have windows. We emphasize that in this simulation the output temperature of the EnergyPlus model is the result of closed-loop control: it therefore appears very constant in simulation compared to the output of the linear model which is essentially an open loop profile. This is observed in Figure 3.5.

Open loop Input comparison
The thermal power input required to maintain the zone temperature at a specific level is

	Small Office	Warehouse
RMSE (^oC)	1.02	0.638
Max. Error (^oC)	4.75	5.528
Mean Error (^oC)	0.569	-0.132

Table 3.2 – Statistics of the open-loop output (zone temperatures) comparison

	Small Office	Warehouse
RMSE (kW)	1.30	13.93
Normalized RMSE	0.0588	0.0273
Max. Error (kW)	9.04	45.68
Mean Error (kW)	0.675	6.477

Table 3.3 – Statistics of the open-loop input (total thermal power) comparison

compared for the two models. The EnergyPlus model is simulated with its default controller to track a reference temperature of $T_{ref} = 23^oC$. Next, an open-loop optimization problem is solved for each month with the linear model to compute the trajectory of control input to achieve the same T_{ref} as output. The total thermal power input trajectories from the two simulations are compared. The two power trajectories for the small office model are shown in Figure 3.7 for a period of one week. The monthly normalized RMSE for each building model is shown in Figure 3.8. The power requirements of different buildings vary due to the difference in their sizes, therefore the RMSE of each building is normalized with respect to its peak thermal power consumption for comparison. The peak power consumption of the small office and the warehouse is $22kW$ and $510kW$, respectively. The yearly maximum error, mean error, RMSE, and the normalized RMSE for each building is reported in Table 3.3. The results show that the normalized RMSE values for the buildings are small. It can be seen in Figure 3.8 that the normalized RMSE has a similar trend as for the output comparison due to the effect of solar radiations. Overall, the models predict the thermal demand of the zones satisfactorily.

The two comparison results show that although the linear models have small errors compared to the EnergyPlus models, they still capture the thermodynamics of the buildings reasonably well, and are able to predict the thermal power requirements of the buildings in open loop.

3.4.3 MPC versus PID

Our intended use for the models is in optimal control applications. We have seen that the model captures the dynamics of the building quite satisfactorily but errors remain, in particular some steady-state drifts. We perform closed-loop simulations here to show how using the model generated with OpenBuild improves control. On one hand, a PI controller is designed for each zone in each building to provide good tracking performance. On the other hand, MPC controllers are also designed to track a reference temperature of $T_{ref} = 23^oC$.

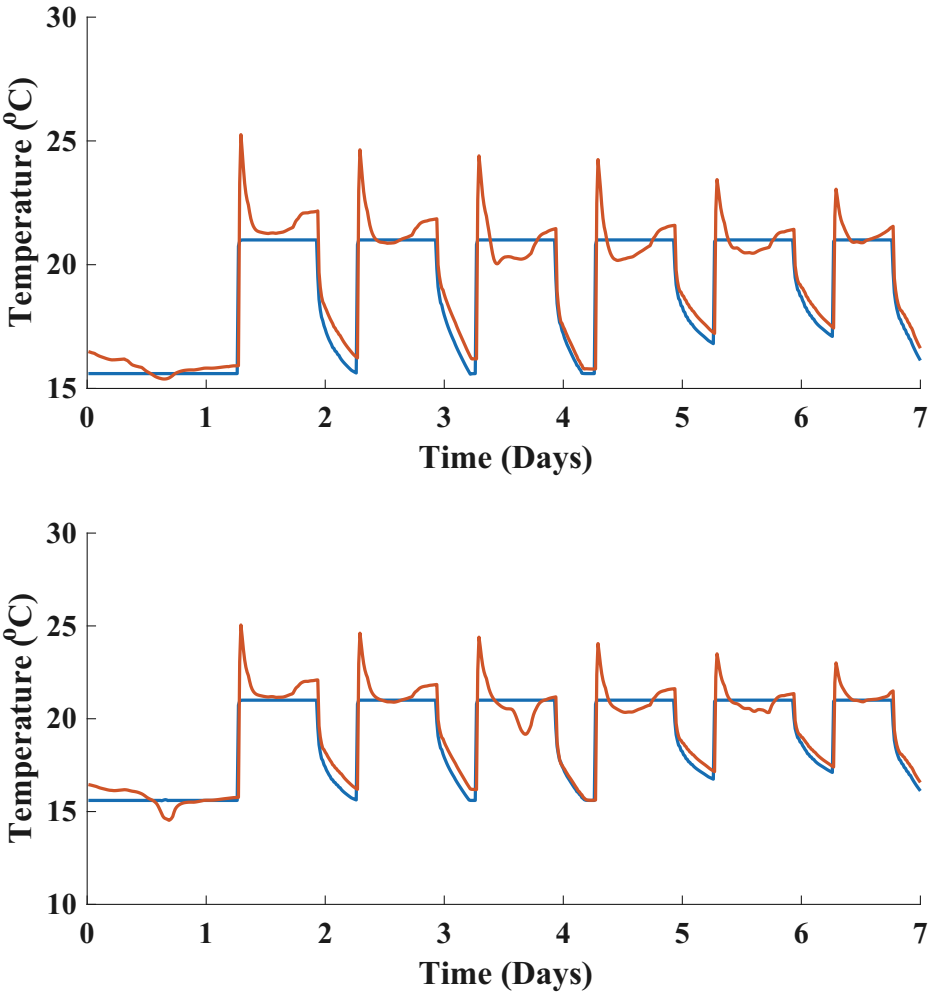

Figure 3.5 – Open loop output comparison - Small Office (zone 1 (top), zone 2 (bottom): EnergyPlus - Blue, OpenBuild model - Red)

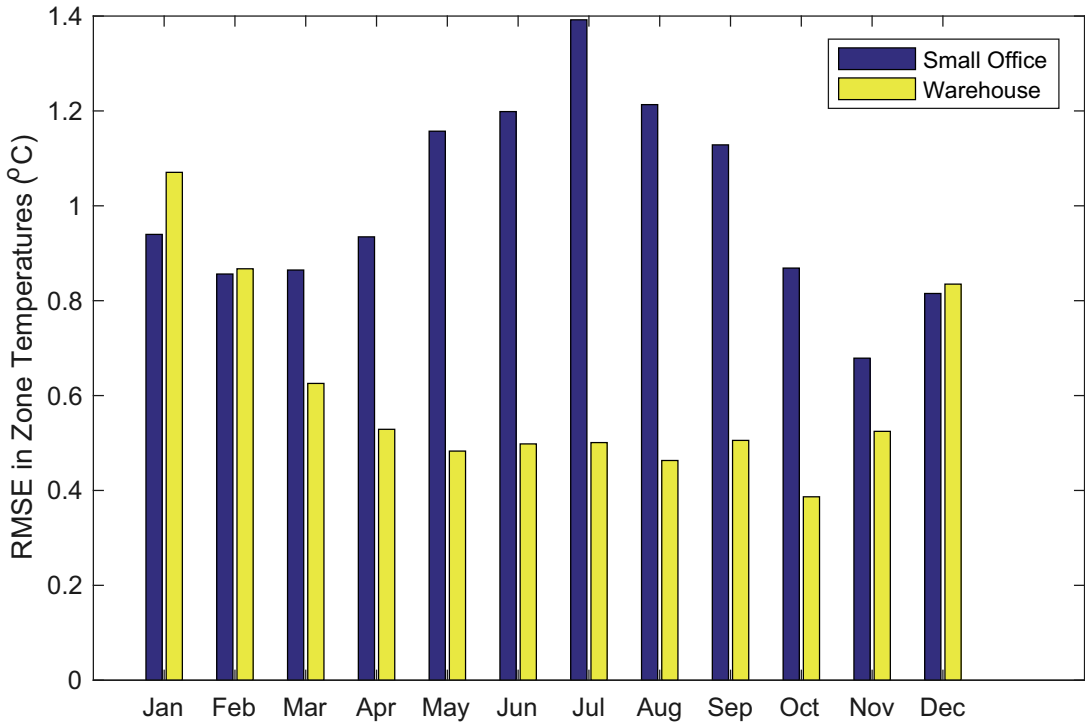

Figure 3.6 – Monthly open-loop zone temperature RMSE

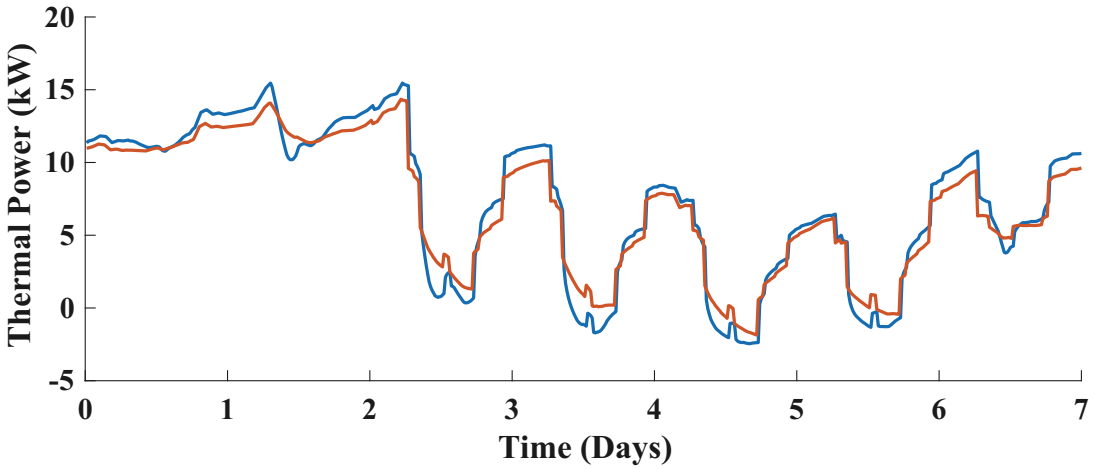

Figure 3.7 – Open loop input comparison - Small Office: EnergyPlus - Blue, OpenBuild model - Red)

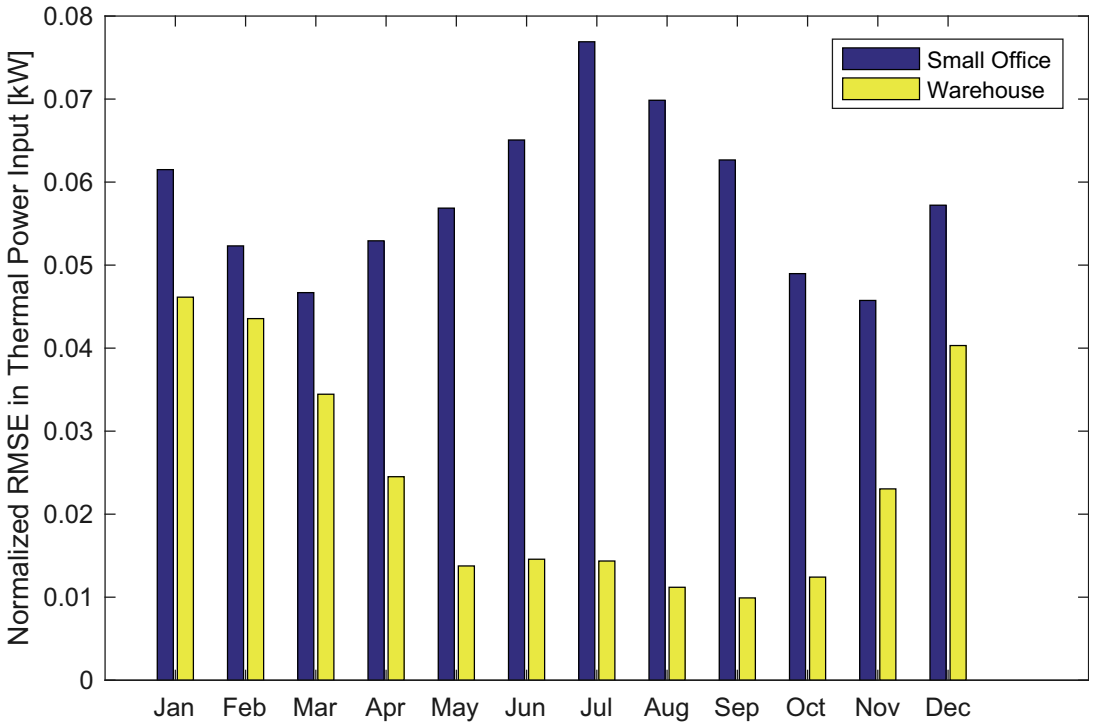

Figure 3.8 – Monthly open-loop total thermal power RMSE

This second controller does not introduce integral action to compensate for errors (coming from model mismatch for example). This can be mitigated by using a modified MPC controller where the model is augmented with a disturbance term affecting the system, and where the disturbance is estimated as part of the state estimation step. This third controller is referred to as the offset-free MPC (OFMPC). The output is augmented with a disturbance term so that $y = Cx + d$ and the disturbance vector d is estimated together with the state x. A Kalman filter has been tuned to estimate the state of the system for both MPC controllers. The global tracking quality is measured by means of the yearly root mean square error and maximum tracking error and reported in Table 3.4. We can observe that MPC outperforms a well-tuned PI controller and in particular the offset-free MPC improves the tracking significantly in all cases. We see that a large part of the prediction error of the model can be offset by proper disturbance estimation, which validates our objective to use the model for MPC applications.

To evaluate the impact of the weather on the quality of the model, we also reported monthly RMSE for each building in Figures 3.9, and 3.10. We can observe a seasonal pattern. For the office building, the quality of tracking is slightly worse in summer. This is probably due to the fact that the effect of higher solar irradiance causes larger prediction errors of the models. The warehouse does not have windows so the effect of sun is less crucial. Notice that the OFMPC manages in the case of the warehouse to mitigate the error more consistently all year round, which suggests a more persistent type of disturbance that the

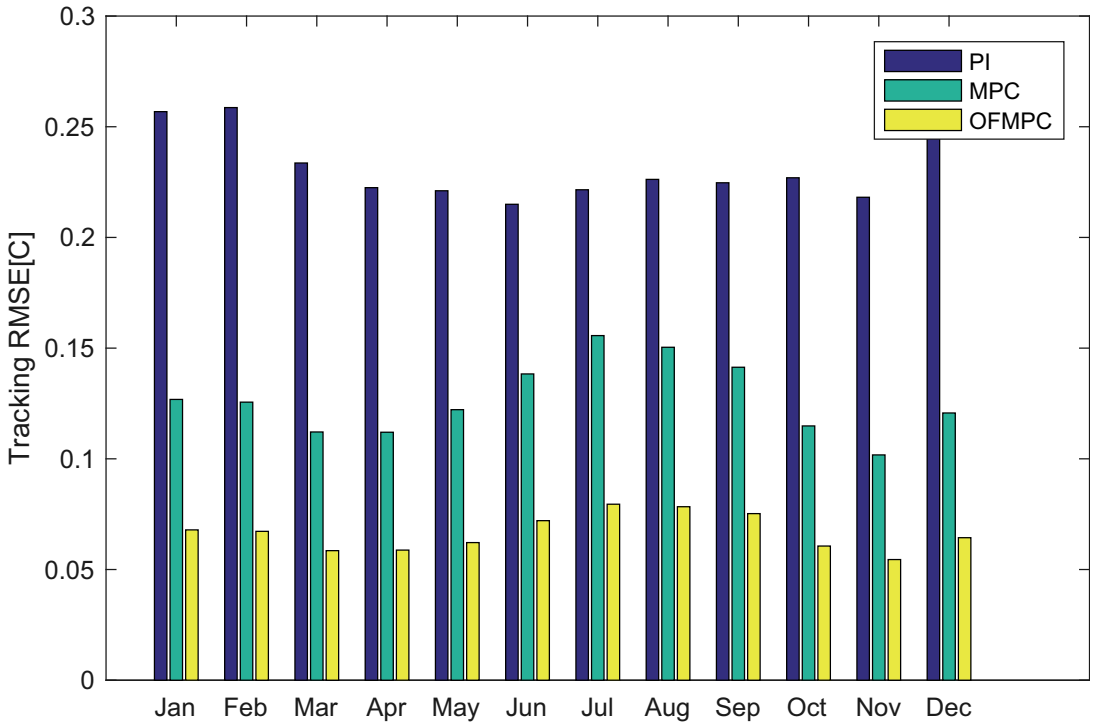

Figure 3.9 – Monthly tracking RMSE for the small Office

estimation counteracts more easily.

It would be possible to adapt the parameters of the model to different periods of the year but this was deemed unnecessary.

Remark 4. *As OpenBuild relies on a physical modeling approach, the quality of the model obtained is dependent on the particular building considered. EnergyPlus includes a very large quantity of objects that model different aspects of the building. The presence or absence of certain types of object may affect the building model prediction quality as we have observed in our investigations. We have continuously updated the toolbox to be able to generate accurate models for more buildings, but this is still an ongoing effort as we have observed that some models may perform significantly worse at times, usually due to*

Table 3.4 – Yearly statistics of the comparison

		RMSE(^oC)	Max Error(^oC)
Small Office	PID	0.231	1.44
	MPC	0.128	1.04
	OFMPC	0.0671	0.55
Warehouse	PID	0.23	1.11
	MPC	0.18	0.67
	OFMPC	0.052	0.34

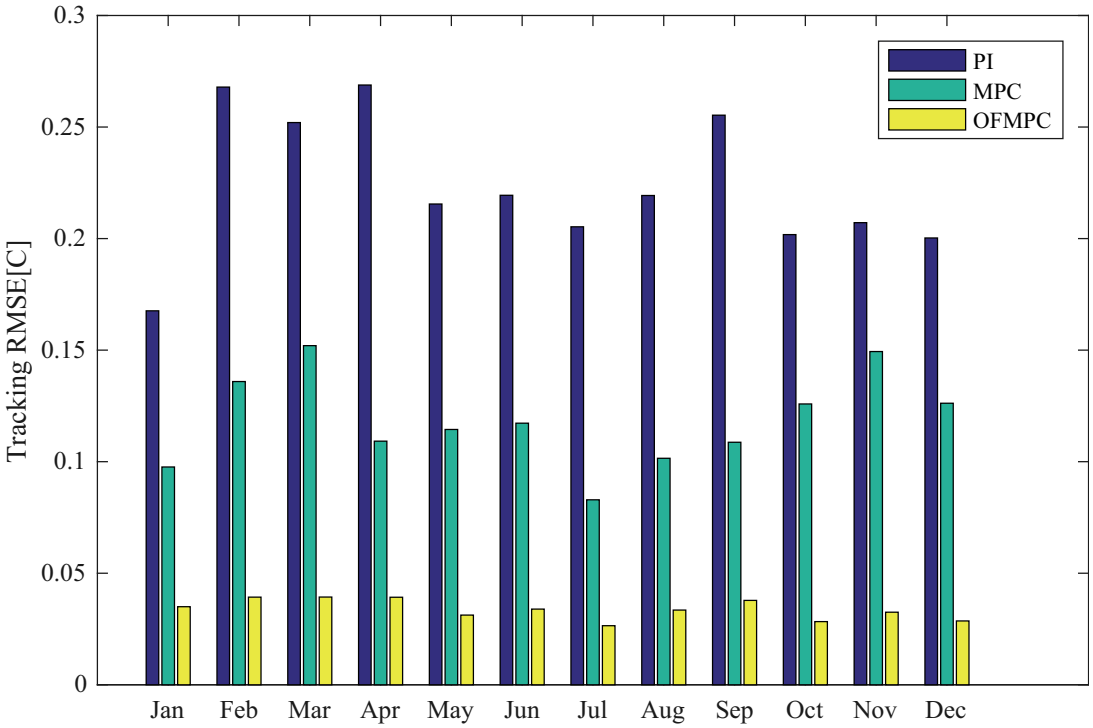

Figure 3.10 – Monthly tracking RMSE for the Warehouse

some part of the model not being processed or modeled as intended in EnergyPlus. An important aspect in this regard in that through the cosimulation interface, it is possible to validate the quality of the model automatically by comparing simulations of the EnergyPlus model and the extracted model, as described earlier in this section.

3.5 Example use of the OpenBuild toolbox

This section gives a step-by-step procedure to carry out a simulation study using OpenBuild, outlining how the toolbox helps the user performing the tasks easily. The study is purposefully simple and aims at illustrating how the OpenBuild toolbox can be used.

We consider a large twelve storey office building located in New York taken from the DOE Commercial Building Reference set [55]. The building has 19 zones served by a forced air heating and cooling system. We focus in this example on the use of a thermal storage for load shifting and minimization of the total cost of operation. We assume the building has a cold water tank which is supplied by an electrical heat pump. A step-by-step procedure to carry out this simulation using OpenBuild is given below

Step 1: A building object is initialized using as input the building data file and the weather data file. All required data is imported to MATLAB. During this process, EnergyPlus is first run once through OpenBuild and the processed data from the simulation is collected.

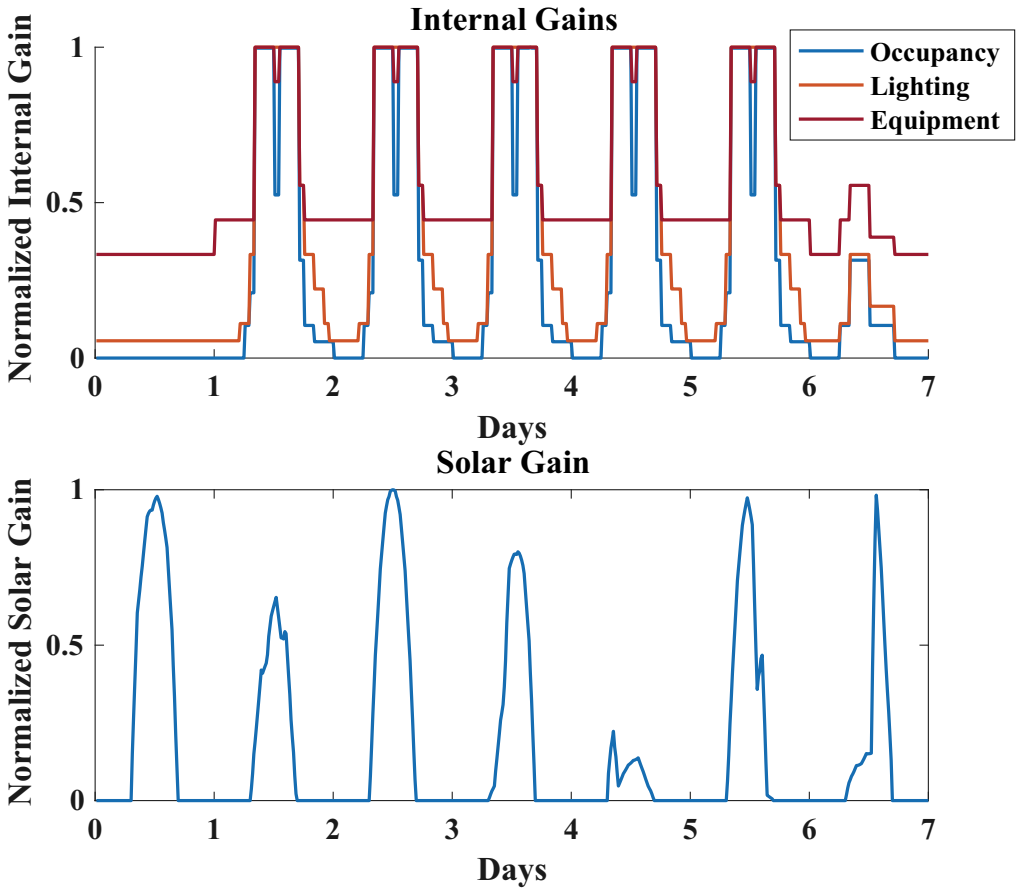

Figure 3.11 – Typical Internal and Solar Gains

Step 2: The building data is used to automatically generate a linear state-space model of the form of equation (3.2). At this point the inputs to the model are heat fluxes to each zone. For simplicity, it is considered here that each zone is served by an individual air handling unit which controls the heat flux to the room. The total cooling load of the building is given by $q_{load} = \sum_{k=1}^{n_u} u_k$ where u_k is the heat power input to zone k.
Step 3: A simulation engine object is initialized. This object handles the communication between the different objects simulated, either in MATLAB or in EnergyPlus. EnergyPlus is added as a simulator for the thermodynamics.
Step 4: A cold water tank is modeled in MATLAB and added to the simulation engine object. The tank is assumed to be perfectly stirred and the heat pump has a fixed coefficient of performance. Therefore, the tank dynamics model takes a very simple form:

$$C_p V \dot{T}_{tk} = \alpha(T_r - T_{tk}) - \eta_c P_e + q_{load} \tag{3.3}$$

where T_{tk} is the temperature of the cold water tank which stands in a room with constant temperature T_r. C_p is the heat capacity of water, V is the volume of the tank, and α is a coefficient representing heat leakage out of the tank. η_c is the coefficient of performance of the heat pump and P_e is the electrical power consumption of the heat pump. This model is created manually, and it is then added to the simulation engine automatically.
Step 5: This is the main step where user input is normally necessary. The user needs to implement a controller in MATLAB, possibly using the building model constructed by OpenBuild. In our case, the building model is discretized with a time-step of 30 minutes and is reduced using the Hankel-Norm based balanced truncation method. The resulting model is used as the prediction model along with the storage tank model in an MPC controller. The MPC controller is designed to minimize the total cost of operation in the presence of day-night electricity tariffs. An offset-free formulation [76] with soft comfort constraints is implemented. Night and weekend setbacks (time varying constraints) on the zone temperature are used (see Section 2.4). A prediction horizon of one day is considered. The following constraints are applied:

$$0 \leq P_e \leq P_{max} \tag{3.4}$$

$$u_{k,min} \leq u_k \leq u_{k,max} \tag{3.5}$$

$$T_{min} \leq T_{tk} \leq T_{max} \tag{3.6}$$

where P_{max}, $u_{k,min}$and $u_{k,max}$ are the maximum electrical power for the heat pump, and the minimum and maximal inputs, respectively. T_{min} and T_{max} represent minimum and maximal allowed temperatures in the storage tank.
Step 6: The models of the building and the storage are used to design the observer.
Step 7: Finally, the simulation engine runs the closed-loop simulation and the simulation data is saved. The simulation is run for a period of one week during the summer of 2012, using the real weather data of New York.

Figure 3.12 – Percentage decrease in the total cost with varying size of storage

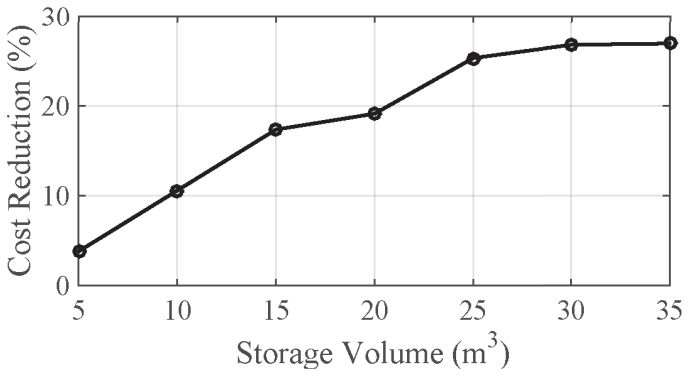

We refer to the OpenBuild manual [77] for a more comprehensive description of the toolbox use.

Remark 5. *The data for weather, occupancy, and internal gains required to simulate the linear models is also extracted from the EnergyPlus simulation output using OpenBuild. A typical profile of occupancy patterns, solar gain, and internal gains for a period of one week is shown in Figure 3.11.*

Simulations are performed for different sizes of the storage tank and the total electricity consumption of the building over a period of one week is compared. The results are cepicted in Figure 3.12. As seen in this figure, the percentage reduction in the total cost of electricity consumption compared to the case with no storage tank, increases with the size of the storage tank. This is due to the capability of the building to shift its electricity consumption to off-peak periods using the storage tank. The cumulative energy consumption over a period of one week for the case with no storage tank and with a $30m^3$ storage tank is shown in Figure 3.13. In this figure, the high tariff price periods have a shaded background. With the storage tank, the cumulative electrical energy consumption during the peak price periods is constant. Without storage the building consumes more electricity during the higher price periods, increasing the total cost of operation.

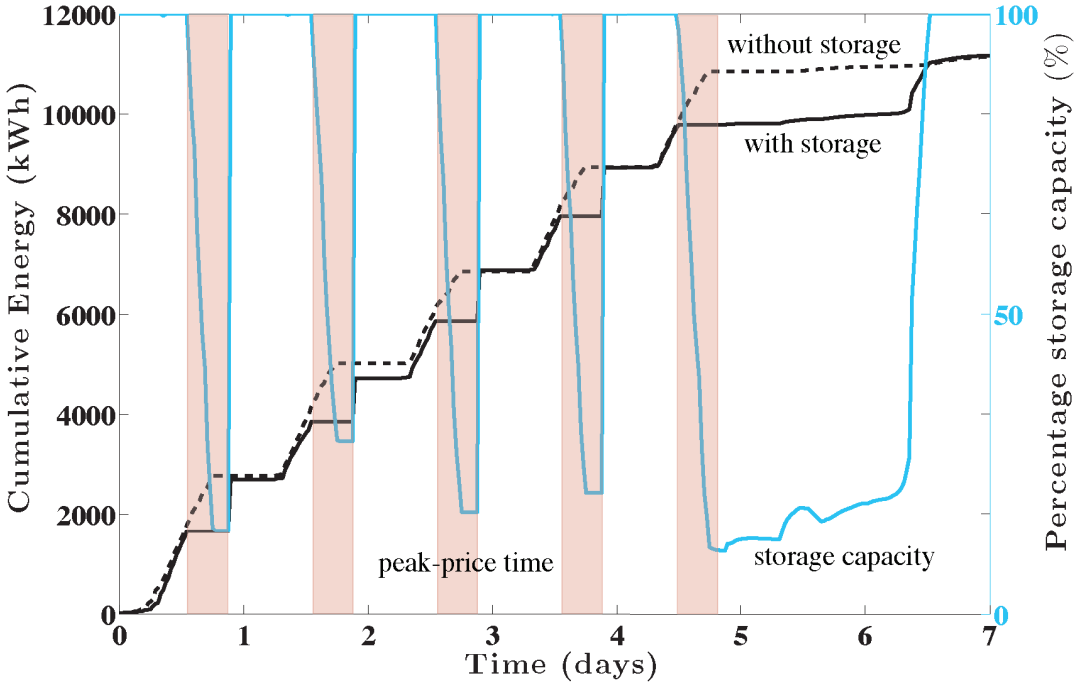

Figure 3.13 – Impact of storage ($30m^3$) on building's cumulative energy use

4 Use of the OpenBuild toolbox

OpenBuild has been developed to support our research and the research of our laboratory (Automatic Control Lab, EPFL) in general. OpenBuild is developed on open-source principles and is freely available for use of other labs and demonstrators, or for any entity or person interested in the operation and optimal control of buildings. OpenBuild has been proven in several contexts, and we present here all the contexts, to our knowledge, that OpenBuild has been utilized.

4.1 Research

OpenBuild research has been repeatedly used for different projects in our group to generate building models. The following papers have made use of data generated using OpenBuild:

- [11]: This paper studies the participation of buildings in the New-York system operator demand response program. Realistic data for an office building located in New York was generated using OpenBuild.

- [12]: An analysis of the participation of loads in the Swiss ancillary services market from the economic point of view.

- [9]: An extensive simulation of frequency regulation participation in Switzerland in the current market conditions.

- Theoretical papers [78], [79], and [80] include examples based on data from OpenBuild.

- OpenBuild has been used in combination with the *OpenBuildNet* software to perform grid scale simulation as reported in [13].

4.2 External Research

OpenBuild has also been used by other research laboratories for generating realistic building models. The following groups / projects have reported using OpenBuild:

- Energy Center, EPFL.
- Simulation examples based on the data generated from OpenBuild have been used in the Ph.D. thesis [81].
- The toolbox has been reviewed in [82], [83], and the book [84].
- OpenBuild have also been reported to be used by other research laboratories for master projects, e.g., the Institute for Dynamics System and Control, ETH, Zurich, and by the Ruhr University Bochum.

4.3 Teaching

OpenBuild has been used for a number of teaching projects in EPFL.

- The Eurotech winter/summer school, 'Energy Systems: From Physics to Systems' is a multidisciplinary two week course for PhD students covering a range of topics related to energy systems, including control. A mini-project on model predictive control for buildings was proposed and conducted by students participating to the school. The building description data was obtained using OpenBuild.
- One of the course projects for the master level class Model Predictive Control features energy-efficient control of buildings. The data for this project was extracted using OpenBuild.
- A number of semester and master projects have aimed at extending capabilities of OpenBuild, or have used OpenBuild to generate data:
  - *Demand Response parametric study* by Hervé Tommasi, aimed at generating multiple building models using OpenBuild in order to study the most important building features that influence its ability to provide demand response to the grid.
  - *Modeling and control of a building with a battery storage system* by Victor Saadé. This project explored the control strategy for the PV + battery system that will be installed in the EPFL solar decathlon building. The thermal model of the building was obtained through OpenBuild using an EnergyPlus description file for the planned building.

- *Semester project: Parameter Estimation of the thermal model of a building using OpenBuild and EnergyPlus* by Bertrand Buisson. This project was exploring the possibility to perform parameter identification for building modeling compared to standard system identification techniques. The basic idea of the project was to extract input data and a model structure from EnergyPlus through OpenBuild and perform system identification and parameter identification.
- *Data-based weather prediction models for control* by Marlène Dollfus. This project aimed at mitigating the effect of weather prediction error by using a filtering/prediction strategy for the forecast error for the upcoming time slots fusing forecast/local measurement and knowledge from past data. The effect of the strategy proposed was evaluated in a building control problem with data generated from OpenBuild.
- *Data-driven optimization for the Energy Bidding problem* by Tiago Morim. This project's goal is to explore different strategies to model the uncertainty in the uncertain energy regulation problem, in order to find the most effective way to use available samples of the uncertainty from historical data. The strategy was tested on an energy regulation problem for a building modeled through OpenBuild.

4.4 Other

The toolbox is available publicly online[1]. To date, it has been dowloaded more than 200 times.

[1] https://sourceforge.net/projects/openbuild/

[redacted] Appendix

A Detailed modeling

In this section, a fully detailed description of the modeling procedure is given. The modeling procedure was largely inspired by the EnergyPlus modeling framework, but significant differences are detailed when necessary. The RC modeling framework is employed. The RC modeling framework simplifies the partial differential equations describing heat transfer using a lumped parameter equivalent circuit. A number of thermal nodes are placed and an equivalent thermal capacitance C_i is associated to each node. The thermal capacitance represents the thermal mass present at that node and depends on the mass and material describing that node. Nodes in the network are connected with thermal resistors that have an equivalent thermal resistance R_{ij}. This resistance models the potential for heat transfer between this nodes. Finally, a forcing term Q_i at each node represents extra contribution of heat transfer at that node and includes heat transfer through internal gains, from solar radiation, from the heating system, etc. For each node a differential equation describes the heat transfer and takes the from

$$C_i \dot{T}_i = \sum_{j \in \mathcal{N}_i} \frac{1}{R_{ij}} (T_j - T_i) + Q_i \tag{A.1}$$

where T_i is the temperature at node i in degree Celsius, C_i the thermal capacitance of node i in $J/^oC$, R_{ij} the thermal resistance between node i and j in $^oC/W$, $\mathcal{N}_i$ the set of nodes neighbouring i and Q_i the thermal forcing term in W. Note that despite being primarily designed to represent thermal conduction, thermal resistances simply induce a linear differential equation structure and can therefore be used to model any exchange phenomena that has a linear dependence on temperature difference (that might be the case after linearization). We used thermal equivalent resistances to model thermal conduction, convection and longwave radiations, as detailed in the subsequent subsections.

A.1 Thermal node placement

Following recommendations and assumptions of EnergyPlus, one core assumption is that the building is divided in thermal zones. A thermal zone usually designates a part of the building served by a single terminal HVAC unit. The basic assumption concerning thermal zones is that the temperature is uniform in that zone (in other words the air in that zone is "well-stirred"). Each thermal zone can therefore be represented by a single node on the thermal graph. The capacitance associated to that zone directly corresponds to the thermal capacitance of the air in the zone. Following [74], pp.7, the expression of the thermal capacitance is:

$$C = C_p \rho_{air} V * c_z \tag{A.2}$$

with V the volume of air in the zone and C_p the zone air specific heat. The density of air is taken as in standard conditions with $\rho_{air} = 1.204 kg/m^3$. At typical value of humidity ratio of 50% and temperature of 25^oC, an average value of the air specific heat of $1.02 kJ/kg^oC$ is taken. The computation of the volume is performed by EnergyPlus and collected from output data files. Finally, c_z is a zone multiplier and may be added in EnergyPlus for technical reason.

Next, nodes are placed in surfaces. To evaluate heat conduction inside surfaces, a state-space model approach is also used in EnergyPlus. As detailed in [74], pp.37, a number of nodes are placed across the surface, and conduction is modeled using lumped parameter values. Although the precision of the method grows with the number of nodes a good compromise was found positioning nodes at each interface between two materials inside the surface.

Each layer of the surface has a total thermal capacitance which is computed as $C = \rho C_p l A$ with A the surface area in m^2, C_p the specific heat capacity of the material in J/kg^oC, l the width of the layer in m, and ρ the density of the material in kg/m^3. The conductive resistance between adjacent nodes is computed as $R = \frac{l}{kA}$ with k the thermal conductivity of the material in $W/^oCm$. By assumption the thermal capacitance of a node at the interface of layers i and j takes half of the total capacitance of layers i and j, so that $C = \frac{C_i + C_j}{2}$.

A.1.1 Special case of no mass materials

In EnergyPlus, some materials are specified as having no mass. They are treated slightly differently as per [74], pp.40-41. Two cases may occur:

- If the no-mass layer is stuck between two "massive" layers, then the previously proposed approach still works: the interface nodes will simply receive a zero mass contribution

from both. If several no-mass layers are together, they are transformed into one equivalent no-mass layer first

- If the surface starts or ends with a no-mass layer, then the no-mass layer will be given the same properties as air.

A.1.2 Remarks on EnergyPlus conduction modeling

Two notable differences can be noted between our approach and EnergyPlus. The first is that EnergyPlus establishes a state-space model first with a number of nodes varying between 6 and 18 per layer of material, which is much larger than in our cases. Using a large number of nodes is also possible in our case but would inflate the state-space size drastically, which was not deemed necessary considering the small benefit in terms of prediction quality. Secondly, EnergyPlus transforms the state-space model into a model that does not make explicit use of internal nodes temperatures. It is converted instead into a model that takes as inputs previously observed temperatures at the surfaces on the outside and inside faces of the surfaces. While this has the advantage of eliminating the need for an observer later on, the procedure to produce the CTF coefficient is reported to become unstable when the time step shrinks too much (see discussion in [74], pp.38). On the other hand, using state-space models is standard in control and well understood, which led us to keep that representation.

A.1.3 Particular cases of surfaces: Adiabatic surfaces

Some surfaces are modeled using the adiabatic boundary condition. As detailed in [74], pp.93, adiabatic boundary conditions are applied to two surface types in EnergyPlus: 1) Surfaces with adiabatic outside boundary conditions 2) Internal Mass objects. For both surface types, EnergyPlus will apply the same boundary conditions to each side of the construction so that there is no temperature difference across the surface. In this case, all heat transfer into the surface is a result of the dynamic response of the construction to varying inside boundary conditions. The surface will store and release heat only at the inside face of the surface (it is assumed that the outside face is not within the zone). Adiabatic boundary conditions are dealt with by short circuiting the inside face and outside face node of the surface considered. The heat balance at each point should not be applied directly. It should appear from the point of view of the outside face that energy comes from the inside face, but not the other way around.

A.1.4 Particular cases of surfaces: Ground connection

Some surfaces have a ground boundary condition. This appears in simulations where heat exchange with the ground can be quite significant especially for single story buildings. A

temperature for the ground is computed as detailed in [85] on pp. 81. To achieve that, the outside face temperature node is forced to the ground temperature which becomes a new input to the building. Usually the ground temperature is quite consistent across the year and it can be recovered from the EnergyPlus run. Forcing the node to the ground temperature is like having a voltage source in the equivalent RC electrical network.

A.2 Convection

EnergyPlus proposes a number of models to take into account thermal convection from the surfaces to the air, one of which can be explicitly specified in the input file. Convection takes a form similar to conduction.

$$Q_{conv} = h_c(T_a - T_s) \tag{A.3}$$

where T_a is the temperature of the air, T_s the temperature of the surface, and h_c a time-varying convection coefficient which is computed based on various factors (temperature in the room, humidity, etc), depending on the calculation method selected. Note that methods to compute inside and outside convection are different. See [74], pp.76-92 to learn more on the convection coefficient computation for inside convection and [74], pp.62-72 for outside surface convection. In our case, a time invariant average of the convection coefficient is extracted from simulation. Note that convection coefficients display typically a periodic pattern so different models could be learnt for daytime and nighttime for example, but a time invariant model was deemed more convenient and sufficiently accurate.

A.3 Internal longwave radiation

Internal longwave radiation describes the thermal exchange of fluxes in the building between internal surfaces. It has been observed that this represents a significant part of the heat exchange in EnergyPlus and has therefore been modeled separately. As per [74], pp.74-75, the thermal longwave radiation exchange is governed by equation:

$$q_{i,j} = A_i F_{i,j}(T_i^4 - T_j^4) \tag{A.4}$$

with A_i the area of surface i, T temperatures in K and $F_{i,j}$ the 'scriptF' factor from surface i to j. ScriptF factors are exchange coefficient between pairs of surfaces and take into account all possible paths between these surfaces. For implementation in the model a linearization is taken around typical conditions.

A.4 External longwave radiation

The outside surface of the building also exchanges thermal radiation with the surrounding environment, namely the air, the sky and the ground. The total long wave radiation exchange hence takes the form, per [74], pp.57-59:

$$Q_{LWR} = \epsilon\sigma F_{gnd}(T_{gnd}^4 - T_s^4) + \epsilon\sigma F_{sky}(T_{sky}^4 - T_s^4) + \epsilon\sigma F_{air}(T_{air}^4 - T_s^4) \tag{A.5}$$

where ϵ is the long-wave emittance of the surface and is collected from input data, σ is the Stefan-Boltzmann constant and the F's are the view factor to air temperature, sky temperature and ground surface temperature respectively. As in EnergyPlus, air and ground surface temperature are taken to be the same. The expressions of the view factor are taken to be:

$$\begin{aligned} F_{gnd} &= 0.5(1 - cos\phi) \\ F_{air} &= 0.5(1 - \beta)(1 + cos\phi) \\ F_{sky} &= 0.5\beta(1 + cos\phi) \\ \beta &= \sqrt{0.5(1 + cos\phi)} \end{aligned}$$

where ϕ is the tilt angle of the surface.

A similar linearization procedure is taken around average temperatures, as for internal convection. Note that the sky temperature then becomes an input to the model whereas it is not something directly measurable. EnergyPlus computes what the sky temperature is as a function of outdoor temperature, cloud coverage and humidity ratio. Value for the sky temperature is usually close but lower than outdoor temperature, especially in clear sky conditions. Note that some cooling systems exploit the fact that sky temperature is low by using a roof pool to cool down the water at night.

A.5 Solar heat gain rate

A large part of the gains affecting the system come from the sun. Detailed geometric computations are performed in EnergyPlus to compute the global horizontal and normal irradiance (GHI and NHI), as well as the resulting irradiance on each surface, outside and inside the building. Total solar radiation heat gain rate are available for every surface in the building and are collected and used as inputs to the model. While this has the benefit of leveraging the whole computational power of EnergyPlus, it adds a new input for every surface exposed to the sun in the building. Several improvements or alternatives could be brought to the model. The difficulty of modeling solar radiation is that their effect is time-varying (actually periodic with a period of one day and slow drift over the year), but linear if the input is taken as the normal horizontal irradiance. It has been observed that

clustering all solar inputs in one yields a model which is too rough. The question is then if linear time-invariant model with a large number of inputs is more convenient than a linear time-varying model with a single input. A reasonable compromise can be to reduce the number of inputs to a few significant ones (mostly depending on the main directions of incidence. This would cause some inaccuracies, especially for indoor surfaces but would probably yield a good approximating model. A data driven approach was adopted to cluster disturbances that are very similar.

A.6 Internal gains

Different types of objects in EnergyPlus input files allow one to describe different types of internal gains in the rooms, including gains from electric equipment, lights, and people. Each piece of equipment produces a heat flux affecting the building, with a convective part (which directly affects the room air), a latent part (through evaporation, this part is un-modeled in our building) and a radiative part. This split is described in the EnergyPlus object, and a schedule describes the total heating rate for that object. This processed data is used as inputs to our models. As described in [74], pp.1020, radiative gains are distributed on surfaces in proportion to the value of their surface absorptance.

Remark 6. *Gains from people are specific in the sense that they depend on indoor conditions. It is a reasonable assumption that they are constant provided the zones are air conditioned. In addition, internal gains from people usually represent a relatively small share of internal gains. See [74], pp.1016-1020 for more details on internal gains computations.*

A.7 Windows

Windows are modeled in great detail in EnergyPlus as explained in [74], pp.217-233. Two modeling methods are employed. The first one models windows layer by layer, and is the one implemented in EnergyPlus. The second, simpler, reuses the layer-by-layer approach but converts first an arbitrary window performance into an equivalent single layer. OpenBuild uses the second method for its computation. The first step is to recover the equivalent U-value for that window. Following [74], pp.221-226, we have

$$\frac{1}{U} = R_{i,w} + R_{l,w} + R_{o,w}$$

where $R_{i,w}$ is the inner film resistance, $R_{o,w}$ the outer film resistance and $R_{l,w}$ the layer resistance, all in m^2K/W. From U all values can be computed using equations:

$$R_{i,w} = \begin{cases} \frac{1}{0.395073\ln(U)+6.949915} \text{ for } U < 5.85 \\ \frac{1}{1.788041U-2.886625} \text{ for } U \geq 5.85 \end{cases}$$
$$R_{o,w} = \frac{1}{0.025342U - 29.163853}$$

A two layer model of the window is used, in the same fashion as other surfaces. The layer resistance is used to specify the conduction between the two layers. Inside and outside convection coefficients are recovered from the EnergyPlus run average value. A different type of solar heat gain is affecting the window. It is computed in EnergyPlus under the name 'Surface Window Total Glazing Layers Absorbed Solar Radiation Rate' which is assumed to be spread between the two layers equally. The window layers obey the same type of differential equation that describe their temperature evolution, but the main difference with other walls is that they are assumed to have no thermal inertia. This transforms equation (A.1) in an algebraic equation by setting the left hand side part to zero. This algebraic equation allows to express the temperature of the window layers as a function of the temperature at the other nodes and the disturbance and substitute in the rest of the differential equations.

$$C_{wall}\dot{T}_{wall} = A_{11}T_{wall} + A_{12}T_{windows} + B_1u$$
$$0 = A_{21}T_{wall} + A_{22}T_{windows} + B_2u$$

which gives $T_{windows} = -A_{22}^{-1}A_{21}T_{wall} - A_{22}^{-1}B_2u$ and after substitution:

$$C_{wall}\dot{T}_{wall} = (A_{11} - A_{12}A_{22}^{-1}A_{21})T_{wall} + (B_1 - A_{12}A_{22}^{-1}B_2)u$$

A.8 Infiltration

Infiltration is described by some specific objects in the EnergyPlus input files. As detailed in [74], pp.360-361, infiltration describes any outdoor air that unintentionally enters the zones by way of infiltration (that is, not through mechanical ventilation). It is assumed to be instantaneously mixed with the zone air. The amount of energy that is exchanged between the zone and the outside air is described by the equation

$$Q_{\text{inf}} = \dot{m}C_{air}\rho_{air}(T_o - T_z) \tag{A.6}$$

where $\dot{m}$ is the mass flow rate exchange in m^3/s, C_{air} the thermal capacitance of air in $J/K/kg$, ρ_{air} the density of air in kg/m^3, T_o the outside temperature and T_z the zone

temperature. According to the documentation, the mass flow rate is computed as

$$\dot{m} = I_{inf} F_{sch}(A + B|T_o - T_z| + Cv + Dv^2) \tag{A.7}$$

where I_{inf} is the design maximum flow rate, F_{sch} a scheduled value that controls the flow rate as a function of time, v the wind speed and A, B, C, and D user-chosen coefficients. Default value in EnergyPlus is (1,0,0,0) so that the mass flow rate does not depend on outside conditions. Even in that case, the flow rate is usually time-varying. For convenience, we chose not to use a time-varying infiltration. Two options are available. The first introduces a new input to the model which is the energy exchange through infiltration. Values from the simulation can be used and should be relatively consistent if the indoor temperature is not too far from the simulation temperature. It also allows to cascade the system with a more detailed model for infiltration if desired. Otherwise, a constant mass flow rate needs to be fixed: the average flow rate in simulation can be used.

B Comfort Modeling

One of the most important objectives of building control is to maintain or improve occupant comfort. Comfort is a human's perception of his environment, and therefore is difficult to measure. This perception of comfort is different for different people and might also vary for the same person at different times. Various measures of comfort have been reported in the literature, e.g., the Predicted Mean Vote (PMV), the Predicted Percentage of Dissatisfied (PPD), etc. PMV is based on the model developed by Fanger [17] and is the predicted mean point rated by a large group of people. It is based on heat balance equations and empirical data that rates how a person would feel about a thermal condition. PPD is a function of PMV and analytical equations have been developed for this relationship [86]. The analytical equations defining PMV and PPD are complicated and are a function of many parameters, e.g., operative temperature, relative humidity, air velocity, metabolic activity, and clothing resistance, etc. Therefore, it makes them difficult to use for control design.

Another similar, but slightly simpler measure developed by ASHRAE via a logistic regression analysis performed on the data collected in the ASHRAE RP-884 database is called ASHRAE Likelihood of Dissatisfied (ALD) [86] and is defined in literature as

$$ALD(T) = \frac{e^{0.008T^2+0.406T-3.050}}{1+e^{0.008T^2+0.406T-3.050}} \in [0.05, 1.00) \tag{B.1}$$

where $T = |T_{zone} - T_{comfort}|$, T_{zone} is the zone temperature, and $T_{comfort}$ is the optimal comfort temperature. Unlike, PMV and PPD, ALD is only a function of the absolute difference between the zone temperature and the optimal comfort temperature.

All these measures are for a specific building zone and for a specific point in time. A measure called Long-term Percentage of Dissatisfied (LPD) has been proposed for an average value of comfort throughout the building [86]. It accounts for the hourly-predicted ALD calculated for each zone and is weighted by the number of people inside the zone, and over time and

is given as

$$LPD(ALD) = \frac{\sum_{t=1}^{T}\sum_{z=1}^{Z}(p_{t,z}ALD_{t,z})}{\sum_{t=1}^{T}\sum_{z=1}^{Z}(p_{t,z})} \tag{B.2}$$

where $ALD_{t,z}$ and $p_{t,z}$ are the ALD and normalized occupancy of the zone z at time t.

Although ALD is only a function of zone temperatures and is simpler than PMV and PPD, it is still difficult to use for control design because it is non-linear. In most of the MPC based control design found in the literature, the comfort is usually defined by a bound of temperatures around the optimal comfort temperature resulting in convex constraints for the MPC optimization problem. However, ALD together with LPD can easily be used in the post-processing to evaluate the occupant comfort.

Ancillary Services Part II

5 Ancillary Services Provision: Theory

5.1 Introduction

5.1.1 Ancillary Services

Power grid operators are required to balance electricity production and consumption to guarantee the stability of the power system and the quality of the power output. However, the actual consumption is uncertain and the load demand is difficult to predict in advance causing imbalance of production and consumption. To cover these imbalances, the transmission system operator (TSO) procures reserve generation capabilities called Ancillary Services (AS). The purpose of this reserve capacity is to act as a backup to meet the real-time mismatch between production and consumption, when required. AS allow for efficient system operation, provide resilience to uncertainties and establish safeguards against unprecedented events. The TSO procure such standby capacity from Ancillary Services Providers (ASP). Traditionally, those have been generating units, while today flexible loads or storage systems can also act as ASPs [87].

The heart of AS is the frequency control service that responds to power grid contingencies at various time scales [88], and is designed to regulate the system frequency at 50Hz. The deviation of frequency from this value is an indication of surplus or shortage of energy in the network, i.e., a value of frequency above 50Hz is a result of surplus energy in the network and vice versa. Frequency control services are divided into three main categories - primary, secondary, and tertiary depending on the timescales.

Primary Frequency Control

Primary frequency control is the fastest responding layer and is required to be fully active within 30 seconds of a contingency according to European regulations. Primary control is usually provided by the generating units and is decentralized. It is essentially a proportional

controller which reacts to the changes in the system frequency by increasing or decreasing the power generation within certain limits.

Secondary Frequency Control

Secondary frequency control is slower than primary control and is activated to relieve the primary control resources. Its effect is evident after about 30 seconds of the disturbance and ends within 15 minutes. Secondary control is a centralized controller which computes a regulation signal indicating the desired increase or decrease in power generation. This regulation signal is transmitted to the secondary frequency control reserves which are required to react accordingly.

Tertiary Frequency Control

Tertiary frequency control is the slowest of the three categories, and is activated to relieve the secondary frequency control reserves. It reacts after about 15 minutes, and consists of semi-automatic or manual changes in the power production setpoints of large generating units to account for any serious contingency.

5.1.2 Motivation

Recently there has been an aggressive shift in policy around the world towards electricity generation from clean renewable sources. Increasing the share of intermittent power sources (wind, solar, etc.) in the grid create new challenges in maintaining safe grid operation [2], [89]. Traditionally, only loads were stochastic, while now the production is also becoming more and more uncertain. Therefore, an increasing amount of reserve power is required for grid stability [3]. Since this trend is expected to continue, efficient and economic dispatch of AS will be a crucial part of modern power systems.

This has compelled grid operators to look beyond traditional (generators) ancillary service providers (ASP) to demand-side resources [4], i.e., loads providing AS. The potential of demand-side resources have been identified in literature, and many operators have started encouraging the participation of loads by adapting their rules [90]. Loads are expected to provide AS at reduced financial and carbon costs.

5.1.3 Why buildings?

The loads, while providing AS, have to maintain an appropriate quality of service and achieve their primary objectives [4]. Therefore, only loads with flexible demands can provide AS. Different types of loads have been identified as suitable for providing AS, e.g.,

thermostatically controlled loads (TCL's) [5], [91], plug-in hybrid electric vehicles (PHEV's) [2], [6], and interruptible industrial and domestic loads [7] etc. Electric batteries are also suitable for providing flexibility to the grid, but have some drawbacks, e.g, they are expensive, not environmentally friendly and have a limited functional life.

Building heating ventilation and air-conditioning (HVAC) systems are particularly suited for providing demand-side services because they consume significant amounts of electricity, and have flexible demand. Moreover, most commercial buildings are also equipped with a building management system which makes it easy to run advanced control strategies needed to provide ancillary services.

The primary objective of building control is to maintain occupant comfort, while minimizing the operational costs. The thermal capacity of a building makes it possible for its electricity demand to be flexible. This flexibility can be used to either shift the consumption of the building from peak to off-peak hours or to directly provide flexibility (e.g., secondary frequency control service) to the grid.

5.1.4 Main Idea

The key idea is for the buildings to act as virtual storages in the electricity grid. Controlling the buildings appropriately can allow the buildings to be ASP's. This will not only help the grid, but will also result in a financial benefit for the buildings.

This idea of buildings acting as virtual storage has also been validated in experiments [10] and the result is shown in Figure 5.1. In this figure, the top plot shows the measured temperature trajectories in four offices, while the second plot shows the total power input in each office (in different colors) and the nominal consumption of the building (dotted blue line). The energy content (integral) of the extra power (above or below the nominal consumption) applied to the building is shown in the bottom plot in Figure 5.1. It can be seen that there is a correlation between the zone temperatures and the energy content of the extra power applied to the building. In other words, the extra power is stored in the building thermodynamics and is retrieved by consuming less than the nominal power. It validates the concept of a building acting as a virtual storage which can be charged or discharged to provide secondary frequency control service to the grid.

The basic idea of secondary frequency control for loads is to modify the electric power consumption according to the requirements of the grid. In real-time operation the grid sends the regulation signal which indicates the desired change in consumption. The loads are required to increase or decrease their consumption proportional to the power capacity which the loads agree in advance. The reward of this service is a payment proportional to this capacity. The change in consumption is with respect to a pre-specified baseline power over the regulation period.

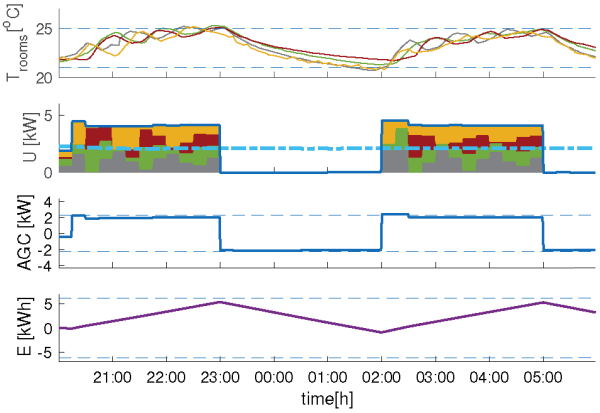

Figure 5.1 – Validation of virtual storage concept. (Upper: Zone temperature (different colors denote the temperatures in different zones), Middle Up: Power distribution among zones (different colors denote the distribution of power in different zones), and nominal consumption (dotted blue), Middle Down: Extra power input to the building with respect to the nominal consumption, Lower: Energy content of the extra power input to the building)

The control challenge is divided into two phases - bidding and online operation. The bidding phase is at the beginning of the activation period and at this point the building needs to specify a baseline power and an offered capacity over the activation period. During online operation the building is required to track the received regulation signal (in proportion to the declared capacity) with the difference of its consumption compared to the declared baseline.

5.2 Literature Review

This section gives an overview of the existing works in literature.

5.2.1 Demand response using buildings

Many studies have been performed to explore the potential of using buildings for providing demand response (DR) services. The existing demand response programs vary in different countries, but the fundamental ideas are similar, i.e., to vary the consumption of the building to help the grid. DR programs can be categorized in two major groups - price based methods, and direct load control.

In price based methods, the response of the loads is modulated by incentivizing the use of energy at certain hours of the day. Day-night tariffs, time-varying electricity prices, and peak-power reduction are examples of such schemes. Various studies have demonstrated the ability of buildings to shift their power consumption from peak to off-peak hours without sacrificing occupant comfort [30]. Several studies have explored the benefits of buildings

participating in electricity markets, usually by adapting to the variations of electrical price to achieve a less costly operation by shifting load.

Direct load control schemes are usually more complicated and often require the loads to declare a baseline power consumption before hand. The loads are incentivized to reduce their consumptions at certain times of the day and the remunerations are usually proportional to the amount of reduction they can offer. [11] investigated participation of an office building in New York's DR program using model predictive control. [33] studied DR for residential buildings coupled with extra storage. These approaches mostly optimize the operation of the building without a-priori promises to the grid operator. Other approaches require the buildings to declare the offered capacity in advance, e.g., secondary frequency control.

5.2.2 Ancillary services

Ancillary service provision requires more sophisticated control because of the need to declare the capacity and baseline power consumption over the whole regulation period in advance and strict online tracking requirements. Recently, different solutions have been proposed for this problem. This section presents a review of the works proposing using building HVAC systems for providing ancillary services to the grid. The existing literature can be divided into two main categories - theoretical, and experimental (or realistic simulations). The theoretical works focus on developing methods to characterize flexibility, and to allow buildings to provide flexibility to the grid. The experimental and simulation based works focus on demonstrating the feasibility of buildings providing ancillary services.

Theory

This section summarizes the recent developments in the control of buildings for the provision of ancillary services.

Some of the recent works have proposed using model-based approaches and robust optimization to characterize building flexibility. In [92], the authors propose an approach to determine the flexibility of buildings using min-max robust MPC. Upward and downward flexibility and a nominal consumption are computed for a single zone building (SISO system). A robust optimization based hierarchical control scheme was presented in [93] enabling an aggregation of commercial buildings providing ancillary services to the grid. The approach was generalized with stochastic comfort constraints and a linear approximation of the heat pump providing thermal power to the building in [94]. [95] discussed a contract design problem for aggregators providing AS. A method based on robust optimization to characterize a building's consumption flexibility as a virtual battery, enabling it to offer it to the grid was presented in [78] and was generalized in [79]. The key idea of the approach is to certify the ability of a building to track any reference drawn from a polytopic set on a

finite time horizon using methods from robust model predictive control. A parameterization of the set of reference signals is optimized to compute the largest set of trackable signals of a certain class. The approach is demonstrated in simulations to compute a nominal consumption and flexibility over a finite time horizon. [96], and [97] also proposed methods based on robust programming concepts to compute flexibility.

Some works have proposed using analytical and heuristic based methods to estimate building flexibility. [98] proposed a feed-forward control architecture to inject a filtered regulation signal as input to a fan. Simulations were conducted and it was estimated that about 15% of fan power capacity can be deployed for regulation purposes with minimal effect on occupant comfort. A drawback of the method is the lack of systematic approach for computing the flexibility and the nominal power consumption. Design of a multirate MPC controller to manage the provision of both regulation and demand-response services to compensate for demand-supply imbalances was discussed in [99]. However, the reference signal was considered to be know in advance and simplistic models were used in simulations. Two methods were proposed by [90] to control the consumption of a HVAC system by varying the speeds of the main fans indirectly either by varying the fan duct pressure or the zone temperatures and tested the approach in simulations.

Some recent works have also proposed to aggregate the flexibility of a group of flexible loads to act as a virtual battery, [91], [100]. [101] investigated the ability of a homogeneous collection of deferrable energy loads to behave as a battery by absorbing and releasing energy in a controllable fashion.

Participation in the intraday energy market, while providing AS, gives the capacity to the building to change its contracted power consumption during the course of the day. By doing so, the building may effectively charge / discharge its stored energy. [87] proposed a method to charge / discharge the storage system (acting as an ASP) at a frequency slower than the tracking signal using intraday market, bilateral agreements, or pooling with a power plant such that a smaller storage size is required to provide frequency tracking services.

Experiments

This section gives an overview of the recent experimental works demonstrating the ability of buildings to provide ancillary services.

Most of the experimental works are based on using heuristic methods to determine the flexibility. The power flexibility of a university building is empirically estimated in [102], and [92]. The flexibility in the power consumption of the main supply fan is estimated by indirectly varying its consumption by modulating the supply duct pressure. At-scale experiments are performed to show that the occupant comfort is not affected by the intermittent fluctuations in the air mass flow. [103] also proposed to provide the power tracking by modulating the

fan power consumption. Experiments were conducted on a 40,000 sq. ft. office space for a duration of 40 minutes, and a filtered regulation signal was tracked with respect to a baseline determined by a pre-existing controller. [104] experimentally demonstrated using simple control of a chiller (by manipulating the cooling water setpoint) to provide secondary frequency control for the Pennsylvania-Maryland interconnection (PJM) test regulation signals.

Our work [10] was the first experimental demonstration of using formal model-based methods to determine the baseline and capacity of a building at the beginning of the regulation period and to track the received regulation signal in real-time. The methods developed in [9] and [79] were used for flexibility computation, and laboratory-scale experiments were performed using electric heaters. Some of these experiments are also a part of this thesis and are discussed in more detail in Chapter 7. The initial work was extended by incorporating the participation in the intraday market and a thorough analysis of the affect of providing ancillary services on occupant comfort was performed in [14].

Another experimental work using model-based methods to compute flexibility was presented by [105]. Experiments were performed in a single zone unoccupied test facility equipped with a standard HVAC system in Lawrence Berkley National Laboratory.

5.2.3 Contributions of this Chapter

This chapter presents the control problem of a building providing secondary frequency control service to the grid, while also participating in the intraday energy market. The two phases - online and offline of secondary frequency control provision are introduced and the control problem for both of them is formulated. The offline phase bidding problem is formulated as a multi-stage uncertain optimization problem. An approximate solution method based on a novel intraday control policy and two-stage stochastic programming is proposed. A closed loop control algorithm based on a stochastic MPC controller is proposed for the online phase of operation. The efficacy of the proposed control solution is demonstrated in simulations.

5.2.4 Structure of this Chapter

The rest of the Chapter is structured as follows. The preliminaries of loads providing ancillary service and the two phases of the secondary frequency control provision are introduced in Section 5.3. The formulation of the bidding problem is presented in Section 5.4, followed by the proposed approximate solution method in Section 5.5. The controller and algorithm for the closed loop operation is presented in Section 5.6, and the simulation results demonstrating the effectiveness of the control approach are discussed in Section 5.7. Finally, the conclusions are drawn in Section 5.8.

Notation: Bold letters denote sequence of vectors over time, the length of which is clear from context, e.g., $\mathbf{e} = [e_0^T, e_1^T, ..., e_{N-1}^T]^T$.

5.3 Concept of ancillary service provision

Ancillary services are required by the grid to maintain safe operation and are procured from ancillary service providers (ASP's) which can either be energy producers or consumers. For example, for surplus energy in the grid, a generator ASP can help the grid by decreasing production or equivalently a load ASP can help by increasing consumption. The ASP's are paid in exchange for providing this service.

Ancillary services can be divided into various categories [88], [106] and frequency control is one of them. Frequency control is further divided into primary, secondary, and tertiary services based on the time scales.

This chapter focuses on the control of building thermodynamics for the provision of secondary frequency control service to the grid. The regulations for secondary frequency control provision differ slightly in different countries, but the fundamentals are similar. The presentation here is based on Swiss regulations, but can easily be modified for other markets.

5.3.1 Secondary Frequency Control

The grid operator procures secondary control reserve capacity in an auction from a set of pre-qualified ASPs before the beginning of the regulation period. The acquired reserve capacity is activated by sending a real-time regulation signal to all the ASPs. The regulation signal for each ASP is proportional to its accepted capacity and is a scaled version of the normalized regulation signal which is called the automatic generation control (AGC) signal in Switzerland. By convention, a positive AGC signal refers to loads consuming more and vice versa.

There are two phases - offline and online for an ASP providing secondary frequency control service to the grid.

5.3.2 Offline Phase

The offline (bidding) phase is at the beginning of the regulation period. During the offline phase, the building is required to specify a baseline power $\bar{\mathbf{e}}$ and a flexibility γ around the baseline that the building agrees to provide to the grid over the regulation period. These two quantities are fixed in advance over the whole regulation period. The baseline is the nominal power consumption of the building which it consumes when it is not providing any regulation services, while the offered capacity γ represents the maximum deviation in power

consumption around the baseline that the building is willing to track.

5.3.3 Online Phase

During the online phase, the grid operator sends a normalized AGC signal **a** to the building. The magnitude of the receievd AGC signal indicates the desired increase or decrease in consumption of the building compared to its baseline. The building needs to track the received AGC signal in proportion to the offered capacity γ, i.e., the building needs to make sure that its total consumption is close enough to the sum of the baseline and the scaled AGC signal $\gamma\mathbf{a}$.

Moreover, the building can also modify its pre-declared baseline power by participating in the intraday market. The building can buy or sell energy **m** for any 15 minutes interval of the day, at least one hour before the time of interest. The delay in the intraday market means that the building cannot modify its baseline instantaneously. For example at 3 p.m., the building can buy or sell energy in the intaday market for any 15 minute time-slot after 4 p.m., till the end of the day. Participation in the intraday market is optional and its impact on the provision of ancillary services will be discussed in detail in the next chapters.

The tracking error during online operation is defined as the difference between the total power consumption of the building e_i and the sum of the total baseline $(\bar{e}_i + m_i)$ and the scaled AGC signal γa_i, and is given by

$$\epsilon_i = e_i - \bar{e}_i - m_i - \gamma a_i \tag{5.1}$$

where ϵ_i is the tracking error, $\bar{e}_i$ is the day-ahead baseline, and m_i is the modification in the day-ahead baseline by participating in the intraday market. During online operation, the building is required to modify its total power consumption such that the tracking error stays within an allowed range m_e as defined in the regulations.

$$|\epsilon_i| \leq m_e \tag{5.2}$$

5.4 The Bidding Problem

The bidding problem is the optimization problem that the building needs to solve at the beginning of the regulation period to declare the baseline and the offered capacity over the regulation period. This section presents the formulation of the bidding problem.

5.4.1 Building Thermodynamics

A state space model of the building thermodynamics is extracted from an EnergyPlus model using the MATLAB toolbox OpenBuild as explained in Chapter 3. The OpenBuild toolbox extracts all relevant data and constructs a linear continuous-time state space model of the thermodynamics. The continuous-time linear model obtained from OpenBuild is approximated using the standard Hankel-Norm model reduction method and is discretized to obtain a model of the following form

$$\begin{aligned} x_{i+1} &= Ax_i + B_u u_i + B_d d_i \\ y_i &= Cx_i \end{aligned} \tag{5.3}$$

where $x_i \in \mathbb{R}^n$ is the state, $u_i \in \mathbb{R}^m$ is the thermal power input to each zone of the building, $d_i \in \mathbb{R}^p$ is the disturbance input (outside temperature, solar gain, internal gains, etc.), and $y_i \in \mathbb{R}^q$ is the temperature in each zone at time step i.

The temperature in each zone influences occupant comfort, and therefore it is controlled to stay within certain acceptable bounds. This is incorporated as a linear constraint on the output of the system. The comfort constraint of level θ_i, at time step i, is defined by $|y_i - T_{\text{ref}}| \leq \theta_i$, where T_{ref} is the optimal zone temperature, and θ_i is the deviation from the optimal temperature. The thermal input to each zone of the building is constrained by the physical limits of the HVAC system which translates into an input constraint.

The *set of admissible thermal power trajectories* is defined as the set of all the possible thermal power inputs that the building can consume, over a horizon N, while meeting the comfort requirements and actuator limitations, and is given as

$$\mathcal{U}(x) = \left\{ \mathbf{u} \;\middle|\; \begin{array}{l} x_{i+1} = Ax_i + B_u u_i + B_d d_i \\ |Cx_i - T_{\text{ref}}| \leq \theta_i \\ u_i \in \mathbb{U} \\ x_0 = x, \quad \forall i = 0, \ldots, N-1. \end{array} \right\} \tag{5.4}$$

where x is the initial state of the building and $\mathbb{U}$ is the set defining the actuator limits.

5.4.2 HVAC System

The electrical power consumption of the building e_i is a function of the thermal power supplied to the building zones u_i. This relationship depends on the type of the energy conversion (or the HVAC) system. In many cases it is reasonable to approximate this function by a linear (constant or time-varying) coefficient-of-performance (COP) of the HVAC system. Therefore, the relationship between e_i and u_i is assumed to be linear and is

given by

$$e_i = h(u_i) \tag{5.5}$$

5.4.3 Bidding Problem

The objective of the bidding problem is to select the capacity bid γ and the baseline power consumption $\bar{\mathbf{e}}$ over the regulation period which minimizes the expected operational cost, while satisfying operational constraints, AGC tracking requirement, and maintaining occupant comfort with a high probability. The operational constraints are expressed by (5.2), (5.4), and (5.5). The bidding problem is formulated as the following optimization problem

$$\begin{array}{ll} \underset{\gamma,\bar{\mathbf{e}},\pi_u,\pi_m}{\text{minimize}} & \mathbb{E}_{\mathbf{a}} J(\gamma, \bar{\mathbf{e}}, \mathbf{e}, \mathbf{m}, \mathbf{a}) \\ \text{s.t.} & \mathbf{u} \in \mathcal{U} \\ & \mathbf{e} = h(\mathbf{u}) \\ & \|\mathbf{e} - \bar{\mathbf{e}} - \mathbf{m} - \gamma \mathbf{a}\|_\infty \leq m_e \\ & \gamma \geq 0 \\ & \mathbf{u} = \pi_u(\mathbf{a}), \quad \mathbf{m} = \pi_m(\mathbf{a}) \end{array} \tag{5.6}$$

where the AGC signal $\mathbf{a}$ is uncertain, and the decision variables are the baseline power consumption $\bar{\mathbf{e}}$, the capacity bid γ, the total electrical power consumption $\mathbf{e}$, the intraday transaction $\mathbf{m}$, and the the thermal power consumption of the building $\mathbf{u}$. The cost function J captures the total cost of operation and depends on the realization of the AGC signal, therefore, its expectation is taken over $\mathbf{a}$. Whereas, the constraints can be formulated as robust or stochastic depending on the assumptions on uncertainty. Typically, the comfort constraints are formulated as chance constraints while the operational and tracking constraints are handled in a robust fashion.

At the time of the decision, the AGC signal is unknown and is revealed progressively, therefore (5.6) is a multi-stage uncertain optimization problem [107]. Note that the problem has $N + 1$ stages according to how often the uncertainty is revealed and the control decision readjusted. The total duration of the regulation period N is fixed and is known in advance. The problem uncertainty is revealed at different stages, and it is possible to re-adjust the control actions $\mathbf{u}$, and $\mathbf{m}$ accordingly. The capacity γ and the baseline over the regulation period $\bar{\mathbf{e}}$ are the first stage variables, while $\mathbf{u}$ and $\mathbf{m}$ are the subsequent stage variables. Therefore, for subsequent stage variables, the goal is to optimize over the control policies $\mathbf{u} = \pi_u(\mathbf{a})$, $\mathbf{m} = \pi_m(\mathbf{a})$, rather than a fixed trajectory over the whole horizon. Furthermore, the policies must be causal, i.e., the decision at time step i depends only on the realization of uncertainty until time i.

Multi-stage uncertain optimization problems are known to be intractable [107], thus obtaining

an exact solution of the bidding problem (5.6) can become challenging especially for long time horizons.

5.4.4 Cost Function

The cost function J of the bidding problem typically has two parts - deterministic J_1 and uncertain J_2. The building needs to pay for the baseline purchased in the day-ahead market, while it gets rewarded for the capacity offered to the grid. These two cost components are a function of the first stage variables and therefore are deterministic. On the other hand, the cost of intraday transactions and the penalty of not being able to track the received AGC signal in accordance to grid's requirements are functions of the subsequent stage variables and the uncertainty, and therefore, are uncertain. More details on the cost function are given in Section 6.3.2.

5.5 Approximate Solution Method

An approximate solution method for the bidding problem (5.6) is presented in this section. The key idea is to separate the intraday control policy from the bidding problem and to optimize it independently. Then, the pre-defined intraday control policy is fixed and the rest of the problem is approximated by a two-stage stochastic optimization problem. It is important to note that the intraday actions cannot be fixed at the time of the bid and are required to be taken during the course of the day. A multi-stage control policy is required for the intraday trades, and therefore, standard two-stage stochastic optimization cannot be used directly to approximate the bidding problem (5.6).

First, the proposed causal intraday control policy which is a function of previously received AGC is presented followed by the approximation of the bidding problem.

5.5.1 Intraday Control

This subsection describes the proposed intraday control policy and explains how it can be used to reduce to size of the virtual storage needed to track a given AGC.

The energy content of the received AGC signal is defined by the integral (or cumulative sum) of the AGC. If the energy content of the AGC reaches a large positive or negative value, it means that the AGC is biased positively or negatively over extended periods of time. It is quite common for the AGC mean to exhibit a considerable bias in either direction for short time horizons. Tracking such AGC signals is challenging since they require the loads to store or release significant amounts of energy. In other words, a larger virtual storage (building capacity) will be required to track an AGC signal with higher energy content,

since extra energy will be consumed or removed from the building compared to its baseline (nominal) consumption.

The building may decide to participate in the intraday market to counteract such temporal deviations of AGC from zero mean. Through the use of intraday trades, it is possible to reset the energy content of the effective regulation signal close to zero by applying an appropriate control policy. This implies that the building may re-adjust its baseline (declared) power consumption, depending on its current state and the energy content of the AGC. For example, if the cumulative sum (energy content) of the AGC signal on a certain day is positive, i.e., the building consumed extra energy to track the AGC, then, it may compensate for that by reducing its future baseline consumption. Thus, by participating in the intraday market, the building may effectively offer a higher tracking capacity to the grid for the same virtual storage size.

Residual Tracking Signal

The residual tracking signal is defined as the sum of the received AGC and the intraday transaction, i.e., the signal required to be tracked by the building after making the intraday adjustments to the baseline power consumption. The residual tracking signal is the effective regulation signal with respect to the original day-ahead baseline power consumption. The normalized residual tracking signal is given as

$$\mathbf{r} = \mathbf{a} + \bar{\mathbf{m}} \tag{5.7}$$

where $\bar{\mathbf{m}}$ is the normalized intraday transaction. $\bar{\mathbf{m}}$ denotes the intraday transaction corresponding to the received normalized AGC signal $\mathbf{a}$. Total intraday transaction $\mathbf{m} = \gamma\bar{\mathbf{m}}$ is a scaled version of $\bar{\mathbf{m}}$.

Control Policy

The objective of the intraday control policy is to minimize the expected value of the cumulative sum (energy content) of the residual tracking signal. The key idea of using such a control policy is to reduce the size of the building (virtual) storage required to track a given AGC. The main steps involved in the proposed intraday control policy are to measure the energy content (cumulative sum) of the residual tracking signal, and then to choose a future intraday control action, such that the expected cumulative sum of the future residual tracking signal is minimized. This strategy attempts to reset the energy content of the residual tracking signal to zero at every time step, but is affected by the intraday market delay of one hour.

The proposed causal control policy of intraday transaction $\bar{\mathbf{m}} = \pi_m(\mathbf{a})$ is formulated, such that the residual tracking signal has a smaller bias (cumulative sum) over the horizon, and

a mean closer to zero. The cumulative sum of a signal $\mathbf{a}$, from time step j to k is defined as $\hat{a}_j^k = \sum_{i=j}^{k} a_i$. The intraday control policy is given by

$$\pi_{\bar{\mathbf{m}}}(\mathbf{a}) = \left\{ \bar{\mathbf{m}} \;\middle|\; \begin{array}{ll} \bar{m}_{i+1} = & \\ \underset{\bar{m}_{i+1}}{\text{argmin}} & |\hat{r}_0^i + \bar{m}_{i+1} + \mathbb{E}_a[\hat{a}_i^{i+1}]| \\ \text{s.t.} & \hat{r}_0^i = \hat{r}_0^{i-1} + \bar{m}_i + \hat{a}_{i-1}^i \\ & \hat{r}_0^{-1} = 0, \bar{m}_0 = 0, \hat{a}_{-1}^0 = 0 \\ & \forall i = 0, ..., N-1. \end{array} \right\} \tag{5.8}$$

where $\bar{m}_i$ is the normalized intraday action at time step i, $\hat{r}_0^i$ is the cumulative sum of the residual tracking signal from time step 0 to i, and $\hat{a}_i^{i+1}$ is the cumulative sum of the AGC signal received between time step i and $i+1$. Note that (5.8) is a causal multi-stage control policy. At time step i, the control policy (5.8) measures the cumulative sum of the received AGC signal in the interval $i-1$ to i and updates the cumulative sum of the residual tracking signal $\hat{r}_0^i$ using the previously optimized intraday action $\bar{m}_i$. Then, the intraday action for the next time step $\bar{m}_{i+1}$ is optimized by minimizing the expected value of the cumulative sum of the residual tracking signal at the next time step. The AGC signal at the next time step is not yet realized and is uncertain. This procedure is repeated recursively, as the uncertainty is revealed. The expected value in the cost function can be estimated at each step using scenarios of the AGC signal.

Remark 7. *The actual tracking signal is a scaled version of* $\mathbf{a}$*. Similarly, the actual intraday transaction is* $\mathbf{m} = \gamma\bar{\mathbf{m}}$*, and the resulting residual tracking signal required to be tracked by the building after making intraday adjustments is a scaled version of* $\mathbf{r}$*.*

Remark 8. *The intraday transaction will incur a cost. Note that this part of the total cost in the bidding problem is now a function of* γ *only, since* $\bar{\mathbf{m}}$ *is already fixed with the intraday policy* (5.8)*.*

Remark 9. *Note that given the scenarios of the normalized AGC signal over the horizon* $\mathbf{a}^j$*, the control policy* (5.8) *can be used to obtain the resulting scenarios of the intraday action* $\bar{\mathbf{m}}^j$*, and the residual tracking signal* $\mathbf{r}^j$*.*

5.5.2 Two-stage Stochastic Approximation

Once the intraday control policy is fixed, the bidding problem is approximated by a two-stage stochastic optimization problem.

The multi-stage structure of the optimization problem (5.6) is reduced to two stages. The causality requirements are relaxed, and it is assumed that after the first stage variables are selected, the uncertainty is revealed over the whole horizon in the second stage, and it is possible to re-adjust the second stage control actions after the uncertainty is realized. The first stage variables are γ and $\bar{\mathbf{e}}$ over the regulation period, while $\mathbf{u}$ is the second

stage variable. Instead of the multi-stage policy $\mathbf{u} = \pi_u(\mathbf{a})$, a two-stage control policy is used. The intraday control policy $\mathbf{m} = \pi_m(\mathbf{a})$ is already fixed (5.8) as a function of the uncertainty, and is not an optimization variable anymore. Moreover, the received AGC signal is transformed to the residual tracking signal $\mathbf{r}$ using (5.8).

If the first stage variables (γ and $\bar{\mathbf{e}}$) are fixed, the best strategy is to minimize the second stage (uncertain) cost J_2, subject to the comfort requirements and the operational constraints. The optimal value of the second stage cost is defined as J_2^*, given that the first stage variables are fixed and the operational constraints are satisfied and is given as

$$\begin{aligned} J_2^*(\gamma, \bar{\mathbf{e}}, \mathbf{a}) := \quad & \underset{\mathbf{e},\mathbf{u}}{\text{minimize}} \quad J_2(\gamma, \bar{\mathbf{e}}, \mathbf{e}, \mathbf{m}^*(\mathbf{a}), \mathbf{a}) \\ & \text{s.t.} \qquad \mathbf{u} \in \mathcal{U} \\ & \qquad\quad \mathbf{e} = h(\mathbf{u}) \\ & \qquad\quad \|\mathbf{e} - \bar{\mathbf{e}} - \mathbf{m}^*(\mathbf{a}) - \gamma\mathbf{a}\|_\infty \leq m_e \end{aligned} \tag{5.9}$$

where the intraday control action is already fixed using (5.8) and is a function of the offered capacity and the uncertain AGC, i.e., $\mathbf{m}^* = \gamma\pi_{\bar{\mathrm{m}}}(\mathbf{a})$.

The approximate bidding problem is given as

$$\begin{aligned} & \underset{\bar{\mathbf{e}},\gamma}{\text{minimize}} \quad J_1(\gamma, \bar{\mathbf{e}}) + \mathbb{E}_{\mathrm{a}}[J_2^*(\gamma, \bar{\mathbf{e}}, \mathbf{a})] \\ & \text{s.t.} \qquad \gamma \geq 0 \end{aligned} \tag{5.10}$$

The optimizer of (5.10) is the AGC tracking capacity γ^* and the baseline power consumption $\bar{\mathbf{e}}^*$ over the regulation period.

Solution Method

The two-stage stochastic optimization problem (5.10) can be solved using the well-known sample averaged approximation method [107] where the expectation in the cost function is approximated using historic samples of the uncertain AGC. An implicit policy of the second stage decision variables is defined by having separate trajectories of the second-stage decision variables corresponding to each sample of the uncertain variable $\mathbf{a}$, resulting in the following optimization problem

$$\begin{aligned} & \underset{\bar{\mathbf{e}},\gamma}{\text{minimize}} \quad J_1(\gamma, \bar{\mathbf{e}}) + \tfrac{1}{N_s} \sum_{j=1}^{N_s} [J_2(\gamma, \bar{\mathbf{e}}, \mathbf{e}^j, \mathbf{m}^*(\mathbf{a}^j), \mathbf{a}^j)] \\ & \text{s.t.} \qquad \mathbf{u}^j \in \mathcal{U} \\ & \qquad\quad \mathbf{e}^j = h(\mathbf{u}^j) \\ & \qquad\quad \|\mathbf{e}^j - \bar{\mathbf{e}} - \gamma\mathbf{r}^j\|_\infty \leq m_e \\ & \qquad\quad \gamma \geq 0, \qquad\quad \forall j = 1, ..., N_s \end{aligned} \tag{5.11}$$

where N_s is the number of samples of the normalized AGC signal $\mathbf{a}$ and the corresponding samples of the normalized residual tracking signal $\mathbf{r}$. Note that the normalized residual tracking signal is a function of the uncertain AGC only, thus a sample of $\mathbf{r}$ can be obtained corresponding to each sample of $\mathbf{a}$ using (5.8). Moreover, as already described $\mathbf{m}+\gamma\mathbf{a} = \gamma\mathbf{r}$. The superscript j defines the second-stage decision variable corresponding to the j^{th} scenario of the uncertain parameter. Note, that for each sample of the uncertain parameter $\mathbf{a}^j$ there are separate trajectories of the second stage optimization variables $\mathbf{e}^j$ and $\mathbf{u}^j$, also implicitly defining separate trajectories for the state variables.

The original bidding problem (5.6) is a multi-stage uncertain optimization problem and is known to be intractable [107]. Problem (5.10) is the two-stage stochastic optimization problem defining the approximate solution of the bidding problem using the intraday control policy (5.8). Problem (5.11) is the scenario based tractable solution of the two-stage stochastic optimization problem (5.10), and can easily be transformed into a linear programming problem, and thus large scale problems can be solved efficiently using standard software tools.

5.6 Real-time Operation

During the real-time operation phase, the building is required to track the AGC signal received from the grid. The baseline power consumption $\bar{\mathbf{e}}^*$ and the offered capacity γ^* are already fixed during the bidding phase. The intraday trades are also a function of the received AGC as defined by (5.8). The only decision left during the online operation phase is to choose the thermal power input to each zone of the building u_i at each time step, such that the operational constraints and the AGC tracking requirements are satisfied. A two-stage stochastic optimization based MPC controller is proposed to achieve the goals of the real-time operation phase.

5.6.1 Stochastic MPC controller

This section describes the proposed MPC controller to track the received regulation signal from the grid, while maintaining occupant comfort and operational constraints.

Set of admissible thermal power trajectories

The building controller is required to maintain occupant comfort, which is defined as a band of deviation of the zone temperatures from an ideal value T_{ref} (5.4). In practice, small deviation of zone temperatures outside the comfort bounds is usually allowed for a short time and may even be unnoticed by the occupants. Therefore, the MPC problem is formulated using soft comfort constraints, i.e., maintaining high comfort levels whenever

possible while allowing small temperature deviations outside the comfort bounds if it is necessary to meet the grid requirements. Soft comfort constraints also helps to maintain the recursive feasibility of the resulting MPC controller, i.e., the MPC optimization problem is feasible at every time step.

The *set of admissible thermal power trajectories* over the horizon N (5.4) is modified with the addition of slack variables in the comfort constraints, and is given as

$$\mathcal{U}_N^{\delta}(x,\delta) = \left\{ \mathbf{u} \;\middle|\; \begin{array}{l} x_{i+1} = Ax_i + B_u u_i + B_d d_i \\ |Cx_i - T_{\text{ref}}| \leq \theta_i + \delta_i \\ u_i \in \mathbb{U} \\ x_0 = x, \quad \forall i = 0, \ldots, N-1. \end{array} \right\} \tag{5.12}$$

where x is the initial state of the building and δ_i is the slack variable at time step i.

Stochastic Controller

The objective of the online phase controller is to track the received AGC signal while maintaining occupant comfort and operational constraints. The control input at each time step is the thermal power input to each zone u_i. The AGC over the complete horizon (regulation period) is not realized at the time of the decision and is uncertain. The MPC control problem is formulated as a two-stage stochastic optimization problem where the control input for the first time step is the first stage variable, while the control inputs from the second step onwards until the end of the horizon are the second stage decision variables.

If the first stage variable at time step t (u_t) is fixed, the best strategy is to minimize the violation of comfort bounds from time step $t+1$ onwards until the end of the horizon, subject to the operational and AGC tracking constraints. The optimal comfort violation from time step $t+1$ to N is defined as V^*, given that the first stage variables are fixed and the operational constraints are satisfied and is given as

$$\begin{array}{rlll} V^*(x_{t+1}, \mathbf{r}) := & \underset{\mathbf{u}}{\text{minimize}} & V_\delta(\delta) & \\ & \text{s.t.} & \mathbf{u} \in \mathcal{U}_{N-t-1}^{\delta}(x_{t+1}, \delta) & \\ & & \mathbf{e} = h(\mathbf{u}) & \\ & & \|\mathbf{e} - \bar{\mathbf{e}}^* - \gamma^* \mathbf{r}\|_\infty \leq m_e & \end{array} \tag{5.13}$$

where V_δ is a penalty on the slack variables, and $\mathbf{r}$ is the residual tracking signal from time step $t+1$ to N and is uncertain. The horizon of the problem (5.13) is from time step $t+1$ to N.

With V^* defined, the proposed MPC control problem for time step t is formulated as

$$\begin{aligned} V(x_t, r_t) := \quad & \underset{u_t}{\text{minimize}} \quad V_\delta(\delta_t) + \mathbb{E}_{\mathbf{r}}[V^*(x_{t+1}, \mathbf{r})] \\ & \text{s.t.} \qquad u_t \in \mathcal{U}_1^\delta(x_t, \delta_t) \\ & \qquad\quad e_t = h(u_t) \\ & \qquad\quad \|e_t - \bar{e}_t^* - \gamma^* r_t\|_\infty \leq m_e \end{aligned} \tag{5.14}$$

where x_t is the initial state of the building, and r_t is the residual tracking signal corresponding to the measured AGC a_t at time step t. The AGC from time step $t+1$ to the end of the horizon N is uncertain, and thus an expectation is taken over $\mathbf{r}$ in the cost function. $\bar{e}_t^*$, and γ^* are the baseline and the capacity fixed during the bidding phase. The horizon of the MPC problem (5.14) is from time step t to N.

The MPC control problem (5.14) is a two-stage stochastic optimization problem and its exact solution is known to be intractable [107]. A scenario based approximate solution method is presented next.

5.6.2 Approximate Solution Method

An approximate solution of the proposed MPC control problem (5.14) can be obtained using the standard sample averaged approximation method [107] where the expectation in the cost function is approximated using the conditional scenarios of the AGC and the resulting residual tracking signal. An implicit policy of the second stage decision variables is defined by having separate trajectories of the second-stage decision variables corresponding to each sample of the uncertain variable from time step $t+1$ to N, resulting in the following optimization problem

$$\begin{aligned} \tilde{V}(x_t, r_t, \tilde{\mathbf{r}}^j) := \quad & \underset{u_t}{\text{minimize}} \quad \tfrac{1}{Ns} \sum_{j=1}^{N_s} [V_\delta(\delta^j)] \\ & \text{s.t.} \qquad u_t \in \mathcal{U}_1^\delta(x_t, \delta_t) \\ & \qquad\quad \mathbf{u}^j \in \mathcal{U}_{N-t-1}^\delta(x_{t+1}^j, \delta^j) \\ & \qquad\quad x_{t+1}^j = x_{t+1} \\ & \qquad\quad e_t = h(u_t) \\ & \qquad\quad \mathbf{e}^j = h(\mathbf{u}^j) \\ & \qquad\quad \|e_t - \bar{e}_t^* - \gamma^* r_t\|_\infty \leq m_e \\ & \qquad\quad \|\mathbf{e}^j - \bar{\mathbf{e}}^* - \gamma^* \tilde{\mathbf{r}}^j\|_\infty \leq m_e \qquad \forall j = 1, ..., N_s \end{aligned} \tag{5.15}$$

where x_t is the initial state of the building and r_t is the residual tracking signal at time step t. $\tilde{\mathbf{r}}$ denote the scenarios of the residual tracking signal corresponding to the conditional scenarios of the AGC from time step $t+1$ to N, and N_s is the number of scenarios. The superscript j defines the second-stage decision variable corresponding to the jth scenario of the uncertain parameter. Note, that from time step $t+1$ to N there are separate

trajectories of the second stage optimization variables $\mathbf{e}^j$ and $\mathbf{u}^j$ corresponding to each sample of the uncertain parameter $\tilde{\mathbf{r}}^j$. u_t is the first stage variable and is the control input applied to the building at time step t.

5.6.3 Closed-Loop Control

The proposed MPC controller (5.15) is applied with a shrinking horizon at each time step, and the intaday trades are computed using the intraday control policy (5.8). The steps of the closed-loop control of the building during the online phase are given below:

1. Measure the state of the system x_t and the received AGC signal a_t at time step t.

2. Compute the intraday control action $m_{t+\Delta}$ and the corresponding residual tracking signal $r_{t+\Delta}$ for Δ time steps ahead using the control policy (5.8), where Δ is the intraday market delay.

3. Generate scenarios of the AGC $\tilde{\mathbf{a}}$ from time step $t+1$ to N. It has been shown in [12] that the AGC is a time-correlated signal, at least up to few hours ahead. A stochastic predictor[1] for the AGC over the prediction horizon can be obtained exploiting the time-correlation properties of the AGC over short timescales.

4. Use the intraday control policy (5.8) to compute the corresponding scenarios of the residual tracking signal $\tilde{\mathbf{r}}$ from time step $t+1$ to N.

5. Compute the control input u_t by solving the optimization problem (5.15) using x_t, r_t, and the scenarios of $\tilde{\mathbf{r}}$.

6. Apply the computed control input to the building and go back to step 1) at next time step.

Remark 10. *The participation in the intraday market is optional, and a building may decide not to modify its day-ahead declared baseline by trading in the intraday market. In this case, the presented offline and online control methodology can be used with small modifications. The intraday control policy is not required and the intraday trade* $\mathbf{m}$ *is zero. As a result, the residual tracking signal* $\mathbf{r}$ *is equal to the received AGC* $\mathbf{a}$*. The bidding problem* (5.11) *and the online phase MPC control problem* (5.15) *can be solved using the scenarios of the AGC signal without the need of computing the residual tracking signal. The closed-loop control algorithm is modified by skipping steps 2 and 4, while the AGC scenarios are used instead of the residual tracking signal in step 5.*

[1] An AGC predictor was developed in the lab for generating scenarios of future AGC using methods similar to [108].

5.7 Simulations

This section presents the simulation results demonstrating the efficacy of the proposed control scheme.

The building model for simulations is taken from [10] and the weather data of Lausanne is used. The building has four zones, and a peak power consumption of 8kW. The AGC signal is obtained from Swiss Grid, the transmission system operator (TSO) of Switzerland. The closed loop control is implemented with a sampling time of 15 minutes, and 15 minutes averaged AGC is used in simulations. The length of the regulation period is assumed to be one day, resulting in $N = 96$.

The bidding problem (5.11) is solved using 100 historic scenarios of the AGC and the corresponding residual tracking signal at the beginning of the regulation period. Since, the purpose of the simulation is to demonstrate the effectiveness of the control method, a simplified objective function of maximizing flexibility, i.e., $J = -\gamma$ is used. The solution of the problem results in a capacity bid of ± 2.49kW and a baseline consumption for a period of one day.

5.7.1 Closed-Loop Simulation

During the online phase, the building is controlled using the stochastic MPC controller (5.15) and the closed loop algorithm described in Section 5.6.3.

The result of the closed loop simulation for a particular day is depicted in Figure 5.2. This figure shows that the received AGC signal is tracked by the building, while the zone temperatures stay within the comfort bounds. The distribution of the total power in each zone is also shown with different colors in the second plot. The received AGC on this particular day is almost zero mean, and therefore the intraday trades are also in both directions, buying and selling energy over the course of the day.

The closed loop simulation result for a different day is shown in Figure 5.3. It can be seen in this figure that on this day the received AGC is biased in the positive direction, i.e., the building is consistently required to consume extra energy to track the AGC. In this case, the intraday control policy acts by selling energy in the intraday market over the course of the day, thus reducing the effective baseline and making it easier for the building to track the AGC.

5.7.2 Closed-Loop Yearly Simulation

The closed loop simulation is repeated 365 times, each time to track the AGC signal of a different day of the year 2014. The yearly results are depicted in Figure. 5.4. The

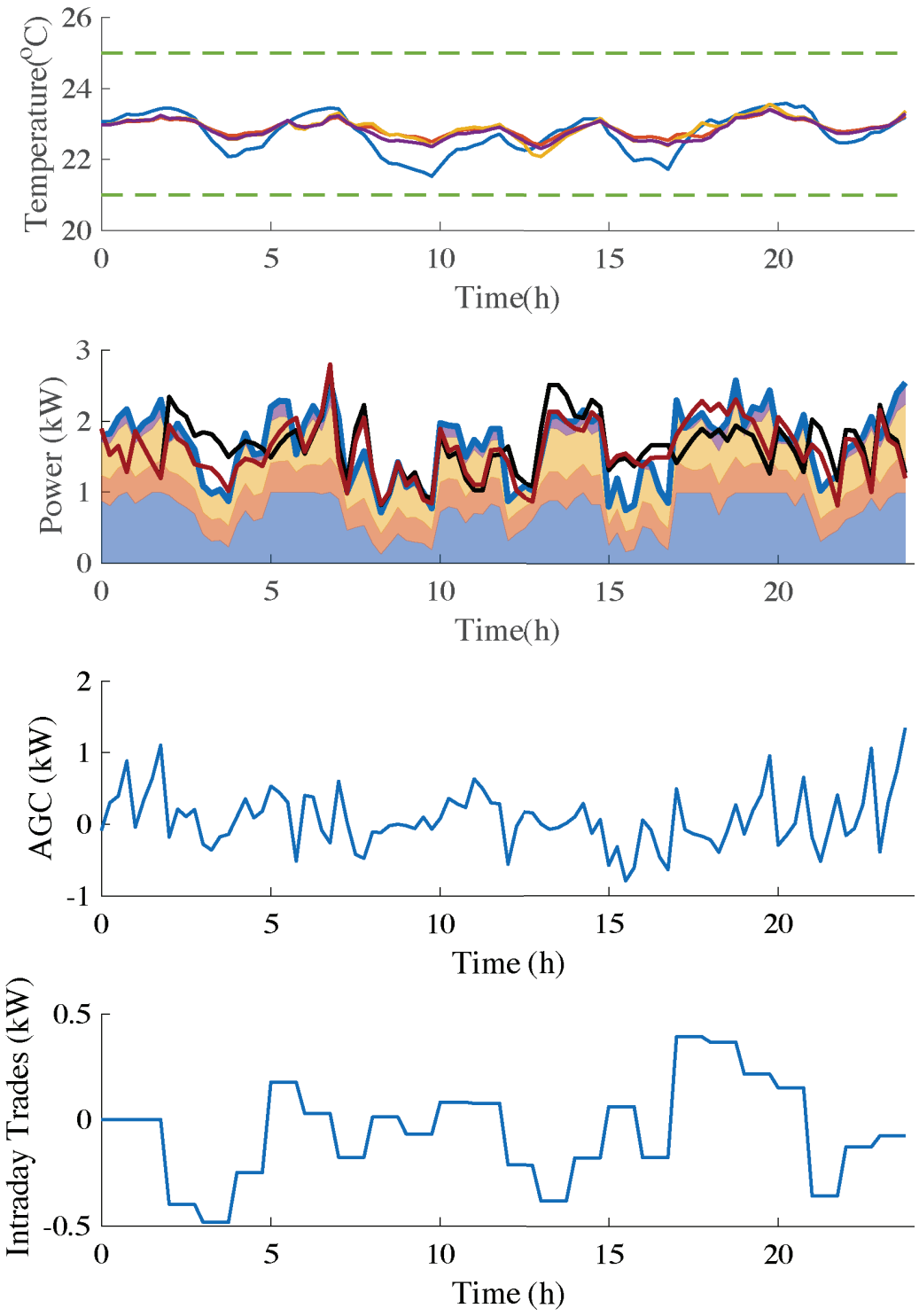

Figure 5.2 – Closed Loop Control for AGC Tracking - day 1 (top: zone temperatures - different colors correspond to temperatures in different zones, middle up: total power $\mathbf{e}$ (blue), original baseline $\bar{\mathbf{e}}$ (black), modified baseline $\bar{\mathbf{e}} + \gamma\bar{\mathbf{m}}$ (red), middle down: AGC $\gamma\mathbf{a}$, bottom: intraday trades $\gamma\bar{\mathbf{m}}$.

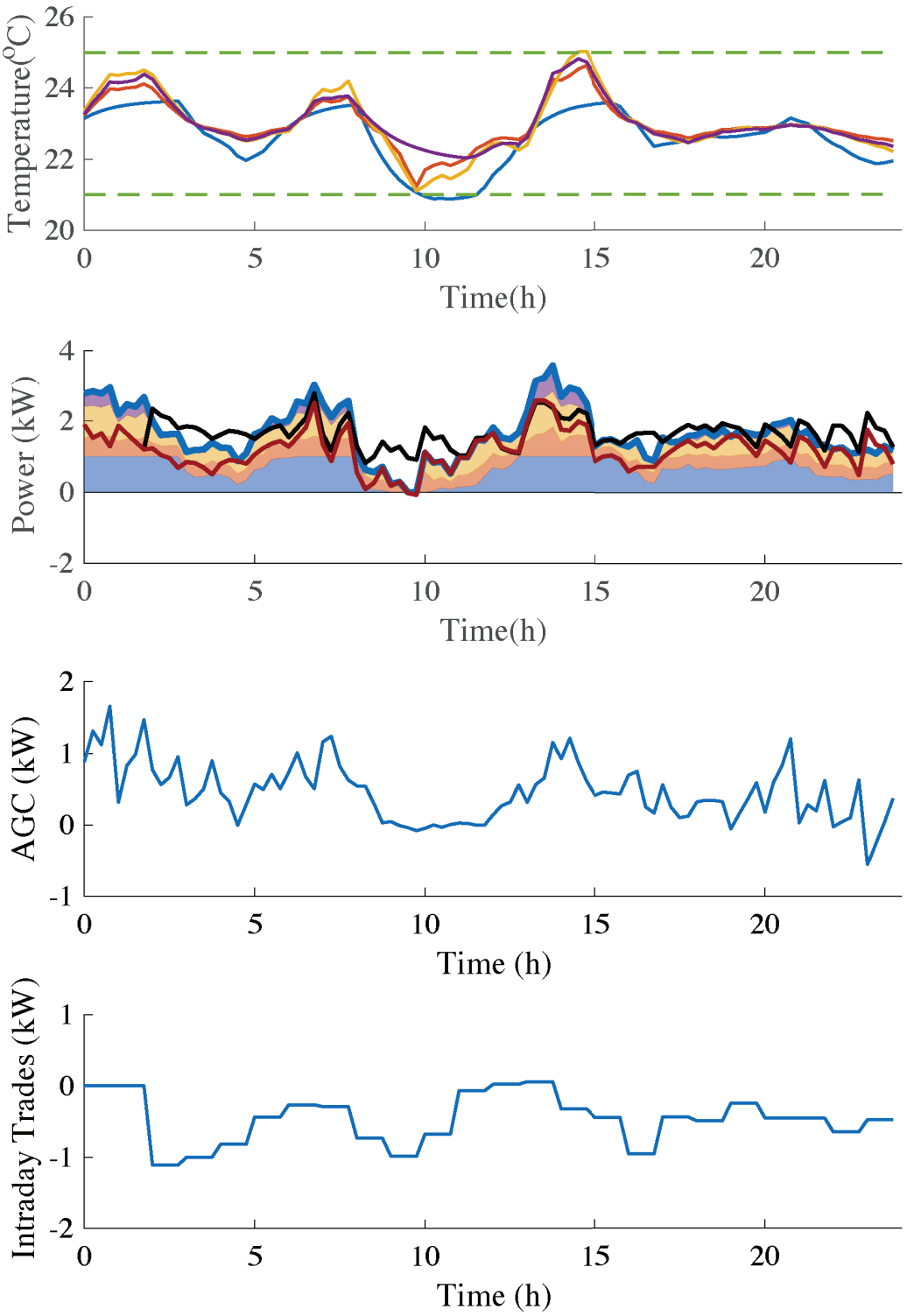

Figure 5.3 – Closed Loop Control for AGC Tracking - day 2 (top: zone temperatures - different colors correspond to temperatures in different zones, middle up: total power $\mathbf{e}$ (blue), original baseline $\bar{\mathbf{e}}$ (black), modified baseline $\bar{\mathbf{e}} + \gamma\bar{\mathbf{m}}$ (red), middle down: AGC $\gamma\mathbf{a}$, bottom: intraday trades $\gamma\bar{\mathbf{m}}$.

resulting closed loop zone temperature trajectories for tracking all the daily AGC signals are within the comfort bounds most of the time with small violations for short amounts of time. The original day-ahead baseline, total power consumption, the received AGC, and the corresponding intraday transactions for all the days of 2014 are also shown. The results show that the controller is robust enough to track various different regulation signals.

5.8 Conclusion

This chapter presented the control problem of a building providing secondary frequency control service to the grid. The two phases (offline and online) of ancillary services provision were introduced. The bidding problem for the offline phase is formulated as a multi-stage uncertain optimization problem. An approximate solution method for the bidding problem based on a novel intraday control policy and two-stage stochastic programming is proposed. A closed loop algorithm based on a stochastic MPC controller is proposed for the on-line phase.

Simulation results showed that it is indeed possible for a building to act as a virtual storage and provide flexibility to the grid. The proposed controller showed satisfactory performance in simulations, and the building was able to track the received AGC, while satisfying the comfort requirements.

The control scheme presented in this chapter is used in Chapter 6 to carry out a comprehensive financial analysis of buildings providing secondary frequency control services in Switzerland. The efficacy of the proposed control algorithm is also tested in experiments and the results are discussed in Chapter 7.

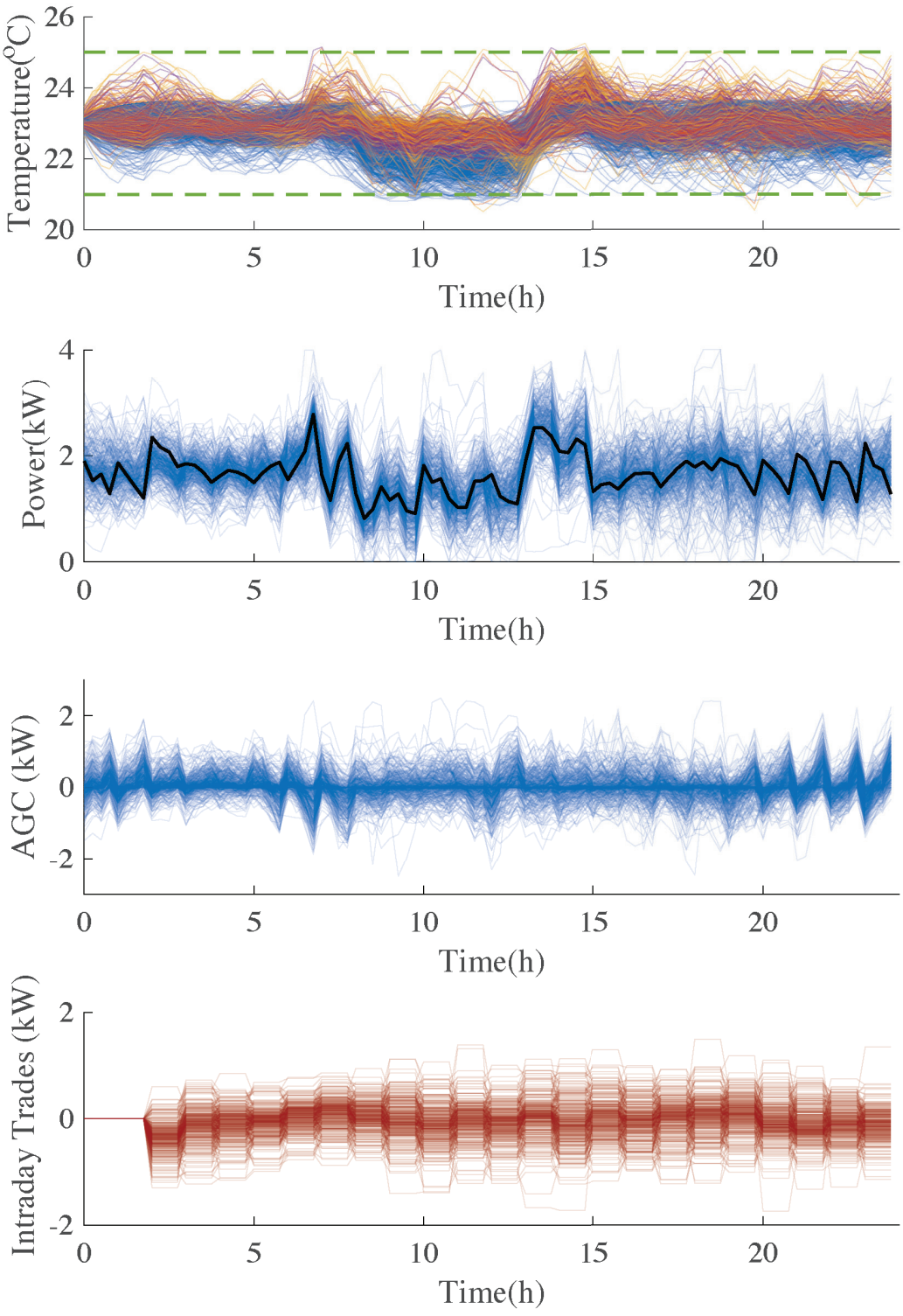

Figure 5.4 – Closed Loop Control for AGC Tracking - yearly (top: zone temperatures on different days of the year - different colors correspond to temperatures in different zones, middle up: original baseline $\bar{\mathbf{e}}$ (black), total power consumption on different days of the year $\bar{\mathbf{e}} + \gamma\mathbf{r}$ (blue), middle down: AGC $\gamma\mathbf{a}$, bottom: intraday trades $\gamma\mathbf{m}$.

6 Ancillary Services Provision: Economics

6.1 Introduction

As discussed in Section 5.2, most of the works in literature focus on the technical capability of buildings providing AS, without assessing the economic feasibility or taking into account a realistic market structure, while the solution of the bidding problem does not consider participation on the intraday energy market. Finally, no analysis on how to optimize financial performance by incorporating all mechanisms (weekly bids, day-ahead auctions, intraday market) of the energy and AS market has been performed.

6.1.1 Contributions of this Chapter

This chapter presents a simulation based financial analysis for a typical office building providing secondary frequency control service to Swissgrid, the Swiss Transmission System Operator (TSO). The operation of the Swiss ancillary services, electricity spot, and intraday markets is summarized, and all the costs and rewards associated with the provision of ancillary services in Switzerland are considered. The control methodology presented in Chapter 5 is adapted for the particular building, HVAC models, and the Swiss market remuneration structure and is used in this study.

Extensive simulations are carried out with real data for energy prices, ancillary service bids, meteorological records and the frequency control signals for the year 2014 (as transmitted by Swissgrid) to answer the following research questions:

- **Economic benefit for a building providing AS:** What is the economic benefit for an office building participating in the Swiss secondary frequency control market, and the additional financial value of participating in the intraday energy market?
- **Impact of AGC tracking on occupant comfort:** How is occupant comfort affected when the building is providing ancillary services to the grid?

- **Sensitivity of the benefits to the price of electricity:** How sensitive is the economic benefit (of providing ancillary service) to the price of electricity?

All the above research questions are answered for a typical Swiss office building, both with and without a thermal storage in its HVAC system.

6.1.2 Structure of this Chapter

The structure of the markets and the different costs and rewards involved in the provision of ancillary services in Switzerland is discussed in Section 6.2. The formulation of the particular problem considered in the study is presented in Section 6.3. The statistical properties of the regulation signal in Switzerland are presented in Section 6.4, and the benefits of participating in the intrady energy market are illustrated in Section 6.5. The simulation study, and the analysis is presented in Section 6.6. Finally, the conclusions are drawn in Section 6.7.

Notation: Bold letters denote sequence of vectors over time, the length of which is clear from context, e.g., $\mathbf{e} = [e_0^T, e_1^T, ..., e_{N-1}^T]^T$.

6.2 Swiss Ancillary Services and Spot Market

This section introduces the different markets involved in the provision of ancillary services in Switzerland. The interaction of ASPs with different markets and the associated costs and rewards are also discussed.

As described in Section 5.3, the ASPs participate in the provision of the secondary frequency control service in two phases (offline and online). During the offline phase in Switzerland, an auction is conducted every week, where all ASPs declare their available flexibility γ, for the upcoming week, in reference to their nominal (baseline) power consumption $\bar{\mathbf{e}}$. The flexibility is offered as the maximum scaling of AGC signal $\mathbf{a}$, the ASP will be able to track, at a specific price. The baseline consumption is declared either in the day-ahead or intraday energy market. During the online phase, an AGC signal is propagated from Swissgrid, which all ASPs are required to track according to the requirements published by Swissgrid.

The details of the costs, benefits and structure of the two phases and the energy markets are discussed below.

6.2.1 Offline / Bidding Phase

During the bidding phase, the ASP interacts with the secondary frequency control market and the electricity spot market, the details of which are given below.

Weekly AS Capacity Auction

Every week, the ASP bids a certain capacity γ MW in the secondary frequency control market. This is the flexibility in terms of maximum deviation from the baseline power consumption that the ASP can offer to the grid, and in turn, receives a reward

$$R_{capacity}(\gamma) := c_{capacity}\gamma \tag{6.1}$$

where $c_{capacity}$ is the bid price of the ASP.

Day Ahead Auction

Each day, the ASP participates in the day-ahead spot market to buy the baseline power profile $\bar{\mathbf{e}}$ MWh for each 15 min increment of the next day. Its cost is defined as

$$C_{baseline}(\bar{\mathbf{e}}) := \mathbf{c}_{electricity}^{T}\bar{\mathbf{e}} \tag{6.2}$$

where $\mathbf{c}_{electricity}$ is the electricity price which is the sum of the day-ahead spot market price, distribution charges, and taxes. Note, that the distribution charges and taxes may differ depending on the physical location of the ASP within Switzerland and the level of the distribution network at which it is connected to the grid.

6.2.2 Online Phase

During online operation, the ASP interacts with the intraday market, and tracks the AGC signal received from Swissgrid, the details of which are given below.

Intraday Transaction Cost

As the day progresses, the ASP can re-adjust its baseline power consumption in the intraday market. The ASP can buy or sell energy $\mathbf{m}$ MWh for any hour of the day, at least 75 minutes[1] before the hour-of-interest, from other market participants. This means that the ASP can still modify its predefined baseline power schedule. Participation in the intraday market is optional and the ASP may decide not to alter its baseline. The cost of intraday transactions is defined as

$$C_{intraday}(\mathbf{m}) := \mathbf{c}_{intraday}^{T}\mathbf{m} \tag{6.3}$$

where $\mathbf{m}$ is the intraday power and $\mathbf{c}_{intraday}$ is the intraday transaction price. Note that the intraday transaction price may vary with the time of purchase of the intraday power, however,

[1] Minimum lead time of 75 minutes was applicable in 2014. Since 16 July 2015 this has been reduced to 60 minutes.

all intraday transactions are considered to be exactly 75 minutes before the time-of-interest. $\mathbf{c}_{intraday}$ can be higher or lower compared to the electricity price $\mathbf{c}_{electricity}$. The intraday cost $C_{intraday}$ may be either positive or negative, depending on net buying or selling of energy.

AGC Tracking

Swissgrid remunerates the ASP by measuring its total power consumption e_i every 15 minutes. Financial adjustments are made based on the 15 minutes measurements, and have two parts, (i): The AGC Tracking Reward - Incentivizing the price of energy consumed / produced by AGC tracking, and (ii): Tracking Error Penalty - penalizing the tracking errors.

AGC Tracking Reward

If the received AGC signal is positive, the ASP increases its consumption. This extra energy is charged at a reduced price $\mathbf{c}_{AGC}$ as a bonus. Similarly, for tracking a negative AGC signal, the ASP decreases its consumption, and in turn, receives a rebate at a price $\mathbf{b}_{AGC}$ on unused energy. The total reward received by the ASP for tracking the AGC signal $\gamma\mathbf{a}$ is therefore given as

$$R_{AGC}(\gamma, \mathbf{a}) := -\mathbf{c}_{AGC}^T \max\{\gamma\mathbf{a}, 0\} + \mathbf{b}_{AGC}^T \max\{-\gamma\mathbf{a}, 0\} \tag{6.4}$$

where $\mathbf{c}_{AGC} \leq \mathbf{c}_{electricity} \leq \mathbf{b}_{AGC}$.

Tracking Error Penalty

The tracking service provided by the ASP, during the online tracking phase, is the difference between the total power consumption $\mathbf{e}$, and the net baseline schedule $\bar{\mathbf{e}} + \mathbf{m}$, and the tracking error ϵ as defined in (5.1) is given as

$$\epsilon = \mathbf{e} - \bar{\mathbf{e}} - \mathbf{m} - \gamma\mathbf{a} \tag{6.5}$$

Swissgrid imposes penalties $C_{penalty}$ on ϵ to maintain tracking quality. Different penalties are paid for positive and negative tracking error and the total penalty is given as

$$C_{penalty}(\epsilon) := \mathbf{c}_{penalty}^T \max\{\epsilon, 0\} - \mathbf{b}_{penalty}^T \max\{-\epsilon, 0\} \tag{6.6}$$

where $\mathbf{c}_{penalty}$ is the cost, and $\mathbf{b}_{penalty}$ is the rebate paid for tracking errors.

The Swissgrid regulations require the tracking errors to be smaller than a predefined ratio q of the offered capacity γ, i.e., $m_e = q\gamma$ in the tracking constraint (5.2).

Readers are referred to [109] for more details of the Swiss AS market.

6.3 Problem Formulation

This section describes the offline (bidding phase) and the online (closed-loop AGC tracking) control for the economically optimal operation of a building participating in the Swiss ancillary services market. The building considered in this study is assumed to have a thermal storage in its HVAC system.

6.3.1 HVAC System and Thermal Storage

This sub-section describes the HVAC system and the thermal storage of the building considered in this study.

Thermal storage constitutes an integral part of modern HVAC systems in large commercial buildings. Storage systems are installed for two main reasons. Firstly, to reduce the operational cost by shifting electrical power consumption from expensive peak hours to cheaper off-peak hours. Secondly, to reduce the size of the heating / cooling system required to meet the peak thermal load. A generic thermal storage model takes the following form

$$s_{i+1} = \alpha s_i + \beta_{in} e_i - \beta_{out} p_i \tag{6.7}$$

where $s_i \in \mathbb{R}$ is the state of the storage, $e_i \in \mathbb{R}$ is the electrical power consumed, and $p_i \in \mathbb{R}$ is the thermal power out of the storage at time step i. Moreover, α is the dissipation rate of the storage, β_{in} is the coefficient of performance (COP) of the HVAC system, and β_{out} is thermal power loss in discharging the storage. The COP of the heating / cooling system is defined as the net efficiency of converting electrical power to thermal power.

The storage state is constrained by the physical size of the storage ($s_i \in \mathbb{S}$), and the electrical power input is constrained by the power rating of the installed (heating / cooling) equipment ($e_i \in \mathbb{E}$). We define the set of all the possible electrical and thermal power consumption trajectories, over a horizon N, as the *set of admissible electrical and thermal power* which is given as

$$\mathcal{S}(s) = \left\{ (\mathbf{e}, \mathbf{p}) \;\middle|\; \begin{array}{l} s_{i+1} = \alpha s_i + \beta_{in} e_i - \beta_{out} p_i \\ s_i \in \mathbb{S} \\ e_i \in \mathbb{E} \\ s_0 = s, \quad \forall i = 0, \ldots, N-1. \end{array} \right\} \tag{6.8}$$

where s is the initial state of the storage.

Thermal storage is assumed to be in parallel operation with the building and at the output

of the HVAC. Thus, the electrical heating / cooling system can either provide the thermal power to the building directly, or charge the thermal storage. On the other hand, the building can use both the storage and the heating / cooling system to meet its thermal load. This implies that the total thermal power consumed by the building is equal to the thermal power output of the storage and is expressed as the following linear constraint

$$\mathbf{p} = \Gamma \mathbf{u} \tag{6.9}$$

where $\mathbf{u}$ is the thermal power input to the building as defined in (5.4), $\Gamma := I_N \otimes \mathbf{1}^T$, with I_N an identity matrix of size N, and $\otimes$ is the Kronecker product.

6.3.2 The Bidding Problem

The bidding problem for the offline phase is formulated as in (5.6) with the general HVAC constraint ($\mathbf{e} = h(\mathbf{u})$) replaced by the following two operational constraints of the particular HVAC system (with storage) considered in this study

$$(\mathbf{e}, \mathbf{p}) \in \mathcal{S} \tag{6.10}$$

$$\mathbf{p} = \Gamma \mathbf{u} \tag{6.11}$$

Cost Function

The total cost of operation J in (5.6) is the sum of all the costs and rewards introduced in Section 6.2 and is given by

$$J = C_{baseline}(\bar{\mathbf{e}}) - R_{capacity}(\gamma) + \mathbb{E}_{\mathrm{a}}[C_{penalty}(\epsilon) - R_{AGC}(\gamma, \mathbf{a}) + C_{intraday}(\mathbf{m})] \tag{6.12}$$

The cost of buying baseline and the reward of providing capacity are the deterministic part of the cost, while the AGC tracking penalty, reward, and the intraday costs are a function of the uncertain AGC and are uncertain. Therefore, expectation is taken over $\mathbf{a}$ for the uncertain part of the cost.

6.3.3 Approximate Solution

The bidding problem is solved using the approximation method described in Section 5.5 using the intraday control policy and two-stage stochastic programming. The intraday policy (5.8) described in Section 5.5.1 is used, while the particular formulation of the two-stage stochastic programming ((5.9), (5.10), and (5.11)) is slightly different due to the particular cost function and the HVAC considered in this study and is presented next.

Two-stage Stochastic Approximation

Once the first stage variables (capacity γ and the baseline power consumption $\bar{\mathbf{e}}$) are fixed in the first stage (the intaday transaction $\mathbf{m}$ is also defined using (5.8)), the best strategy is to minimize the tracking error penalty $C_{penalty}$, subject to the comfort requirements and the operational constraints. The optimal value of the tracking penalty is defined as $C^*_{penalty}$, given that the first stage variables are fixed and the operational constraints are satisfied

$$\begin{aligned} C^*_{penalty}(\psi, \phi) := \quad & \underset{\mathbf{e},\mathbf{u}}{\text{minimize}} \quad C_{penalty}(\mathbf{e} - \psi) \\ & \text{s.t.} \qquad \mathbf{u} \in \mathcal{U} \\ & \qquad\quad (\mathbf{e}, \mathbf{p}) \in \mathcal{S} \\ & \qquad\quad \mathbf{p} = \Gamma \mathbf{u} \\ & \qquad\quad \|\mathbf{e} - \psi\|_\infty \leq q\phi \end{aligned} \tag{6.13}$$

The approximate bidding problem is given as

$$\begin{aligned} \underset{\bar{\mathbf{e}},\gamma}{\text{minimize}} \quad & C_{baseline}(\bar{\mathbf{e}}) - R_{capacity}(\gamma) \\ & + \mathbb{E}_{\mathbf{a}}[C^*_{penalty}(\bar{\mathbf{e}} + \gamma \mathbf{r}, \gamma) - R_{AGC}(\gamma, \mathbf{a}) + C_{intraday}(\gamma \bar{\mathbf{m}})] \\ \text{s.t.} \quad & \gamma \geq 0 \end{aligned} \tag{6.14}$$

where $\mathbf{r}$ is the normalized residual tracking signal defined by (5.7) and $\bar{\mathbf{m}}$ is the normalized intraday transaction defined by (5.8). The optimizer of (6.14) is the AGC tracking capacity γ^* and the baseline power consumption $\bar{\mathbf{e}}^*$ for the whole week.

The two-stage stochastic optimization problem (6.14) can be solved using the sample averaged approximation method [107], as described in Section 5.5.2, resulting in the following scenario based optimization problem

$$\begin{aligned} \underset{\bar{\mathbf{e}},\gamma}{\text{minimize}} \quad & C_{baseline}(\bar{\mathbf{e}}) - R_{capacity}(\gamma) \\ & + \tfrac{1}{N_s} \sum_{j=1}^{N_s} [C_{penalty}(\mathbf{e}^j - \bar{\mathbf{e}} - \gamma \mathbf{r}^j) - R_{AGC}(\gamma, \mathbf{a}^j) + C_{intraday}(\gamma \bar{\mathbf{m}}^j)] \\ \text{s.t.} \quad & \mathbf{u}^j \in \mathcal{U} \\ & (\mathbf{e}^j, \mathbf{p}^j) \in \mathcal{S} \\ & \mathbf{p}^j = \Gamma \mathbf{u}^j \\ & \|\mathbf{e}^j - \bar{\mathbf{e}} - \gamma \mathbf{r}^j\|_\infty \leq q\gamma \\ & \gamma \geq 0, \qquad\qquad \forall j = 1, \ldots, N_s \end{aligned} \tag{6.15}$$

where N_s is the number of samples of the normalized AGC signal $\mathbf{a}$ and the corresponding samples of the normalized residual tracking signal $\mathbf{r}$. The superscript j defines the second-stage decision variable corresponding to the j^{th} scenario of the uncertain parameter.

The offline phase bidding problem is approximated by (6.15) which can be solved using the historic scenarios of the AGC signal and the corresponding residual tracking signal. Readers

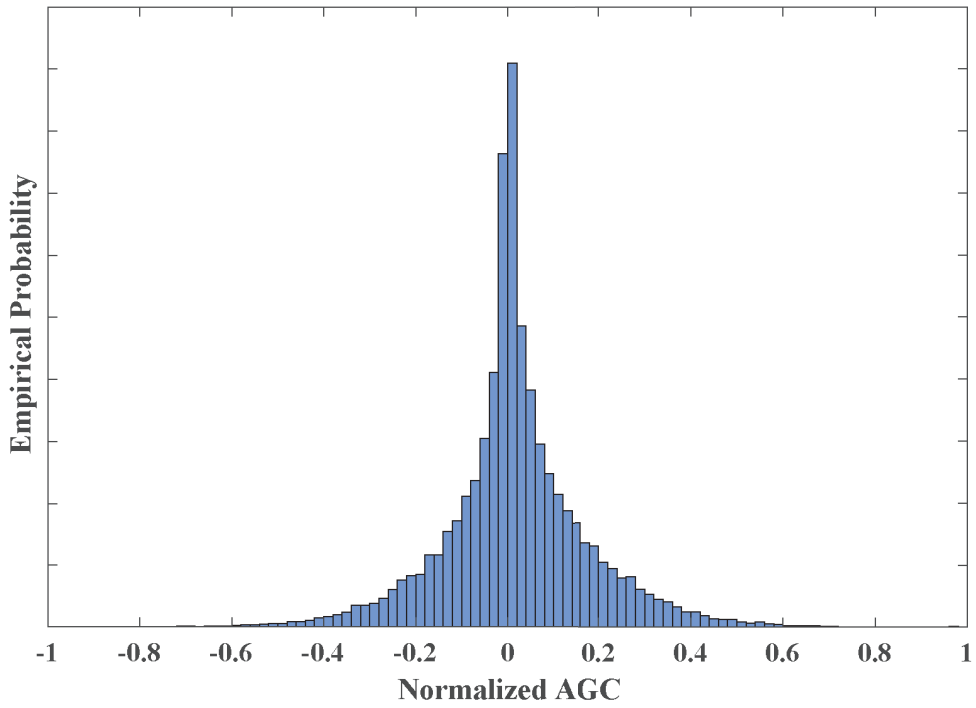

Figure 6.1 – Empirical distribution of the normalized AGC signal

are referred to Section 5.5 for more details on the approximate solution of the bidding problem.

6.4 Statistical Properties of the AGC signal

Important elements of the regulation signal can be captured by analyzing the statistics of the AGC provided by Swissgrid.

The empirical distribution of the AGC throughout 2014 is depicted in Figure 6.1. The magnitude of the AGC is between -1 and 1. The regulation signal is almost zero mean with a small positive bias of 0.0182 over a period of one year which means that the building is required to consume extra energy on average while tracking the AGC. However, this varies every week and especially every day (there exist days for which the AGC is almost entirely positive or entirely negative). The probability distribution of the AGC shows that there are very few significant outliers, while the mass of the signal is concentrated close to zero and the 99^{th} percentile of the signal is only 0.512. This means that 99% of times Swissgrid asks the ASPs to provide only about 51% of the total offered capacity γ.

The daily mean of the AGC signal throughout 2014 is shown in Figure 6.2. The AGC shows a daily pattern in its mean. On average the AGC is slightly positive or negative at certain

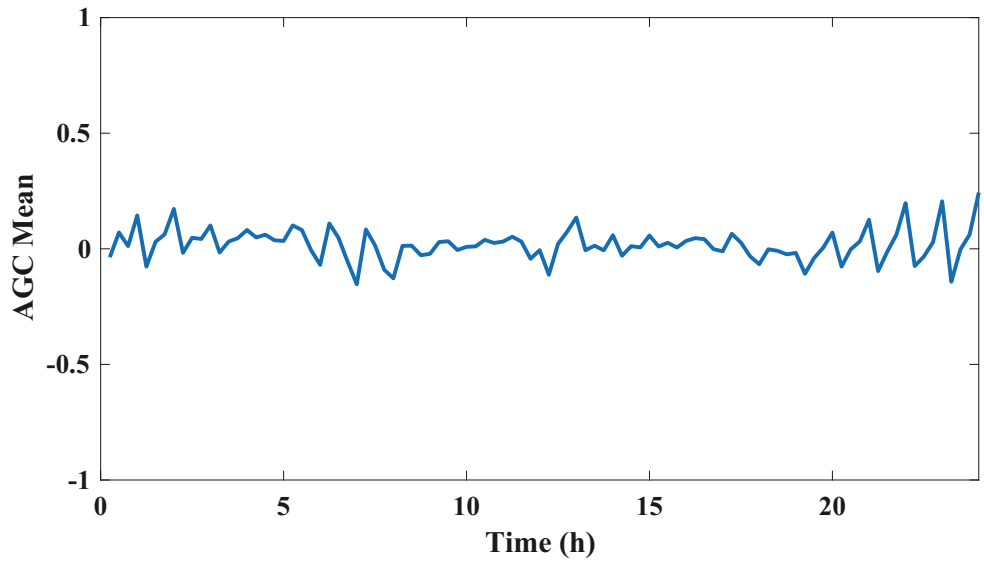

Figure 6.2 – Daily mean of the normalized AGC signal

times of the day.

The scenario based solution to the bidding problem proposed in Section 5.5 uses the historic samples of the AGC. Therefore, it can exploit the distribution and the daily pattern of the historic AGC to optimize the economic performance of the building.

6.5 Benefits of Intraday Participation

This section demonstrates the benefit of participating in the Intraday market, and gives an insight into the operation of the Intraday control policy described in Section 5.5.1.

The power and energy content of an AGC signal and the corresponding residual tracking signal obtained using the control policy (5.8) is shown in Figure 6.3. In this figure, the AGC signal for a particular week is shown in blue in the top plot, and the intraday trades computed using (5.8) is shown in green. The sum of these two signals is the residual tracking signal which is shown in the middle plot in this Figure. The bottom plot shows the energy content (cumulative sum) of the AGC (purple), and the residual tracking signal (blue) over a period of one week. It can be seen that the maximum power level of the original AGC and the residual tracking signal is almost the same, while the energy content of the residual tracking signal is reduced by participating in the intraday market using the presented control policy.

A similar result can be seen in Figure 6.4 which shows the empirical probability distribution of the AGC and the corresponding residual tracking signal obtained using the control policy

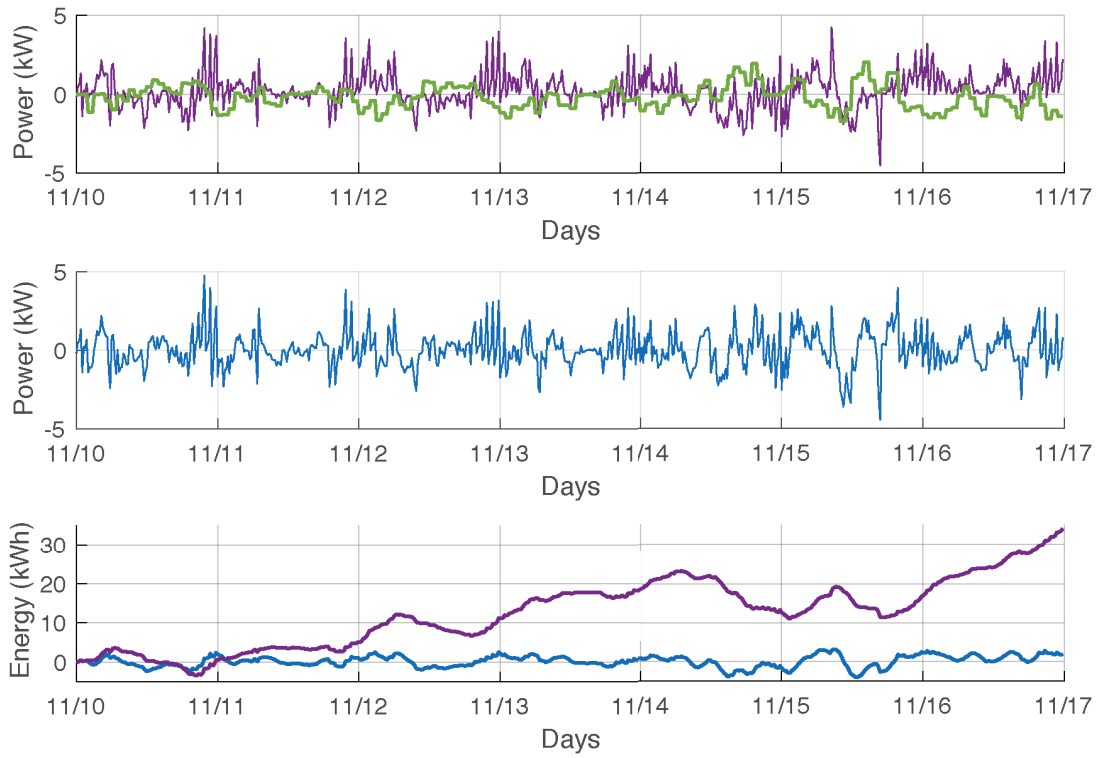

Figure 6.3 – Power and energy content of the AGC signal and the residual tracking signal (top: AGC signal (purple), Intraday trades (green), middle: residual tracking signal, bottom: energy content (cumulative sum) of the AGC (purple), and the residual tracking signal (blue)).

(5.8) over a period of one day. It can be seen in this figure that the worst-case energy content of the residual tracking signal is much less than that of the original AGC. The 99^{th} percentile of the energy content of the AGC is 4.52 kWh/kW, while for the residual tracking signal, it is reduced to 1.12 kWh/kW.

The statistical analysis shows the ability of the proposed intraday control policy (5.8) in reducing the energy content of the effective tracking signal. As a result, a smaller virtual storage will be required to provide a similar tracking capacity.

6.6 Simulations and Analysis

This section presents the simulation study of a building providing secondary frequency control services in Switzerland. The simulation cases and setup is presented first followed by the analysis of the results.

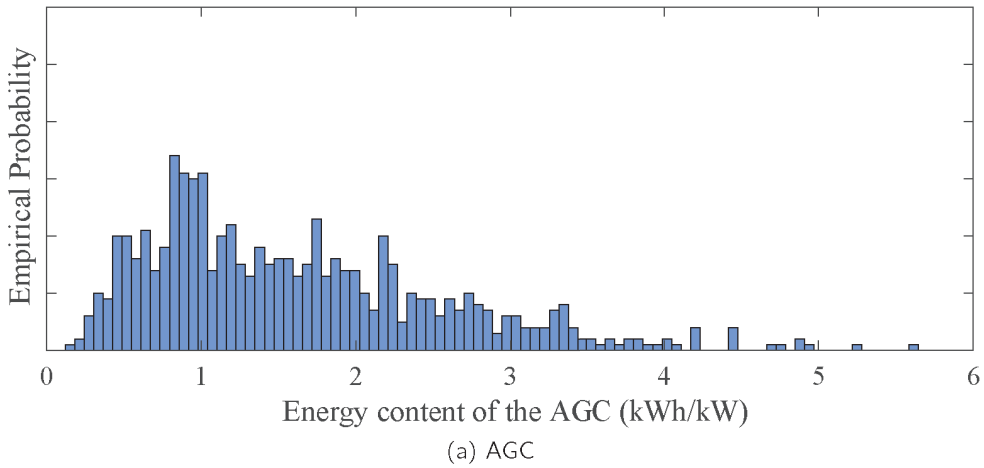

(a) AGC

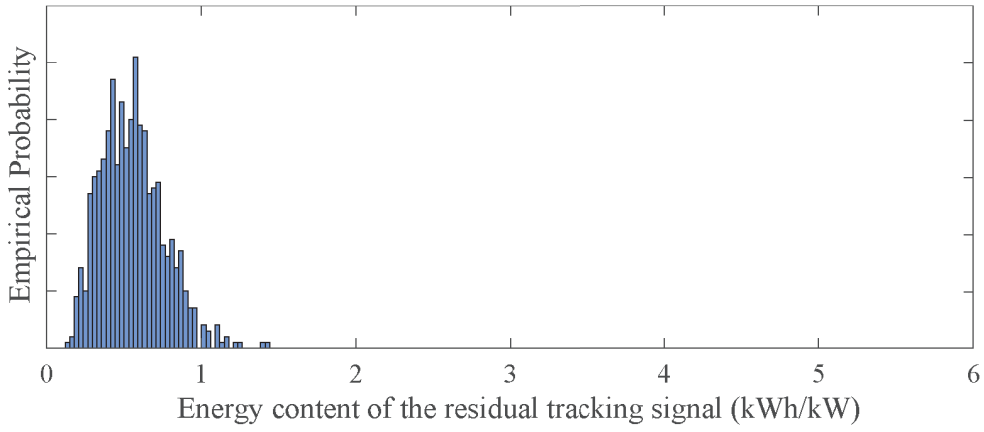

(b) Residual tracking signal

Figure 6.4 – Empirical probability distribution of the energy content (cumulative sum) of the daily AGC signal scenarios and the corresponding residual tracking signal scenarios. The values of the cumulative sum are given as kWh per kW of capacity offered.

Building	
Floor Area (m^2)	511
No. of Zones	5
Peak Occupancy (people/100m^2)	5.4
Maximum thermal power input (per zone)	3.6 kW
Thermal Storage	
Dissipation rate α	1
Average COP β_{in}	2.4
Maximum electrical power consumption of the heating / cooling system	7.5 kW
Maximum thermal energy capacity	150 kWh
Full charge / discharge time	8.3 h
Comfort	
Optimum ALD comfort temperature T_{ref}	23 °C
Temperature variation (office hours)	2 °C
Temperature variation (excl. office hours)	4 °C

Table 6.1 – Building and Simulation Parameters

6.6.1 Simulation Cases

Following simulation cases are defined to carry out the analysis:

- **Minimum Cost - No AGC tracking:** The building minimizes its total energy cost of operation without participating in the AS market. A minimum cost MPC controller is used for this case which has been widely studied in previous literature.
- **AGC Tracking - No Intraday:** The building minimizes its total cost of operation while providing the AGC tracking service, without participation in the Swiss intraday market.
- **AGC Tracking - Intraday:** The building minimizes the total cost of operation while providing the AGC tracking services to the grid and participating in the intraday energy market.

For comparison, all the above cases are repeated with and without a thermal storage tank in the HVAC system. The base cases are taken to be the minimum cost operation with and without thermal storage tank, respectively.

6.6.2 Simulation Setup

The building employed in all simulations is the ASHRAE standard EnergyPlus model of a five zone office from the reference database of the U.S. department of Energy [55]. The

building model is provided with typical usage patterns of electrical equipment, lights and occupancy schedule. The heating / cooling system and the thermal storage tank is sized using EnergyPlus. An ideal thermal storage is considered. For winter, this represents a hot water storage tank, while for summer an ice storage system. Main simulation parameters are given in Table 6.1. The assumptions of our simulations are listed below:

- Simulations are carried out for winter (weeks 2 to 10, and 45 to 52) and summer (weeks 24 to 35) 2014.
- Recorded weather data of Lausanne for 2014 are used.
- Real energy prices for Lausanne for 2014 are used. The spot ($\mathbf{c}_{electricity}$) and intraday index price ($\mathbf{c}_{intraday}$) of electricity is obtained from the European Power Exchange (EPEX) [110].
- The average weekly capacity price ($c_{capacity}$), AGC tracking bonus ($\mathbf{c}_{AGC}$, $\mathbf{b}_{AGC}$) and deviation penalty ($\mathbf{c}_{penalty}$, $\mathbf{b}_{penalty}$) for the year 2014 are obtained from Swissgrid.
- The intraday market is assumed to be liquid at all times.
- The historic normalized AGC signal (obtained from Swissgrid) is split into weekly signals which are used as scenarios. $N_s = 45$ random scenarios of the weekly AGC signal are drawn to solve the two stage program (6.15). N_s is limited by the computational complexity of the resulting optimization problem, however, sensitivity studies suggest that the number is still representative of the underlying probability distribution.
- The AGC signal of the year 2014 is obtained from Swissgrid and is used in our simulations.

Simulation Run

The bidding problem (6.15) is solved with a horizon (regulation period N) of one week (as required by Swissgrid), yielding the weekly capacity bid γ and the baseline power consumption $\bar{\mathbf{e}}$. As the AGC signal arrives for the concerned week, in the real time phase, it defines the total power consumption of the building, i.e., the sum of the baseline power consumption and the scaled version of the received AGC signal. An open loop optimization problem determines the optimal distribution of thermal power in each zone of the building, while respecting the operational constraints. This gives the resulting state trajectories. For the case where the building participates in the intraday market, the control policy (5.8) is used to obtain the intraday actions as described in Section 5.5.

The simulation result for week 46 is shown in Figure 6.5 to demonstrate the effect of the proposed methodology. The received AGC signal is tracked while the zone temperatures

stay within comfort bounds. The received AGC signal, the residual tracking signal, the intraday transaction and their respective cumulative sum are also shown in Figure 6.5. It can be seen that the causal intraday control policy (5.8) is effective in limiting the cumulative sum of the residual tracking signal.

Comprehensive simulation results are presented in Section 6.6.3 to study the financial aspect and benefit of participating in the Swiss AS program.

Remark 11. *Building thermodynamics are slow, and are modeled with a sampling time of 15 minutes. From a comfort point-of-view applying a fast thermal input signal is equivalent to applying a 15 minutes average of the fast signal. Moreover, most commercial HVAC systems (except electric heaters, and fans) cannot be controlled at rates faster than 15 minutes. Furthermore, all financial remuneration is cleared by Swissgrid using the 15 minutes average signals. Therefore, we use 15 minutes average data (including AGC signal) in our simulations. A device with fast dynamics (e.g. electric battery) will be required in practice to alter the consumption with high frequency. The size of the electric battery required to support AGC tracking at high frequency is determined by the worst-case energy content and power of the difference between the AGC signal received every second and the* 15 *minutes average AGC. This worst-case is estimated using historic AGC scenarios and the analysis suggests that only a small supporting electric battery with power limit of* $\pm 1kW$*, and a capacity of* $0.04kWh$ *is required when following the remaining of the AGC building tracked signal of* $\pm 1kW$ *at a frequency of* $1s$*.*

Quality of Stochastic Programming Solution

This section describes the solution quality of the bidding problem (6.15).

The quality of the approximate stochastic programming solution is evaluated by numerically estimating the dispersion of the optimal cost of (6.15). Approximate two-stage stochastic program (6.15) is solved 20 times (for each case) for week-3 using different sets of randomly drawn historic AGC scenarios. The estimated coefficient of variation (ratio of standard deviation to expected value) of the optimal cost is 0.028, and 0.0122 for AGC Tracking with, and without intraday participation and without additional storage, while it is 0.0019, and 0.0208 for the case of additional storage. The coefficient of variation close to zero indicates that the dispersion of the optimal cost is small.

Next, the two-stage stochastic program (6.15) is also solved (for each case) with a larger number of AGC scenarios ($Ns = 100$). The optimal cost with additional scenarios, in all cases, is within 2.6% of the average optimal cost from the first study. Re-solving the optimization problem with extra AGC scenarios do not improve the optimal cost significantly.

Both these results show that the solution of (6.15) is a reasonable estimate of the stochastic programming problem.

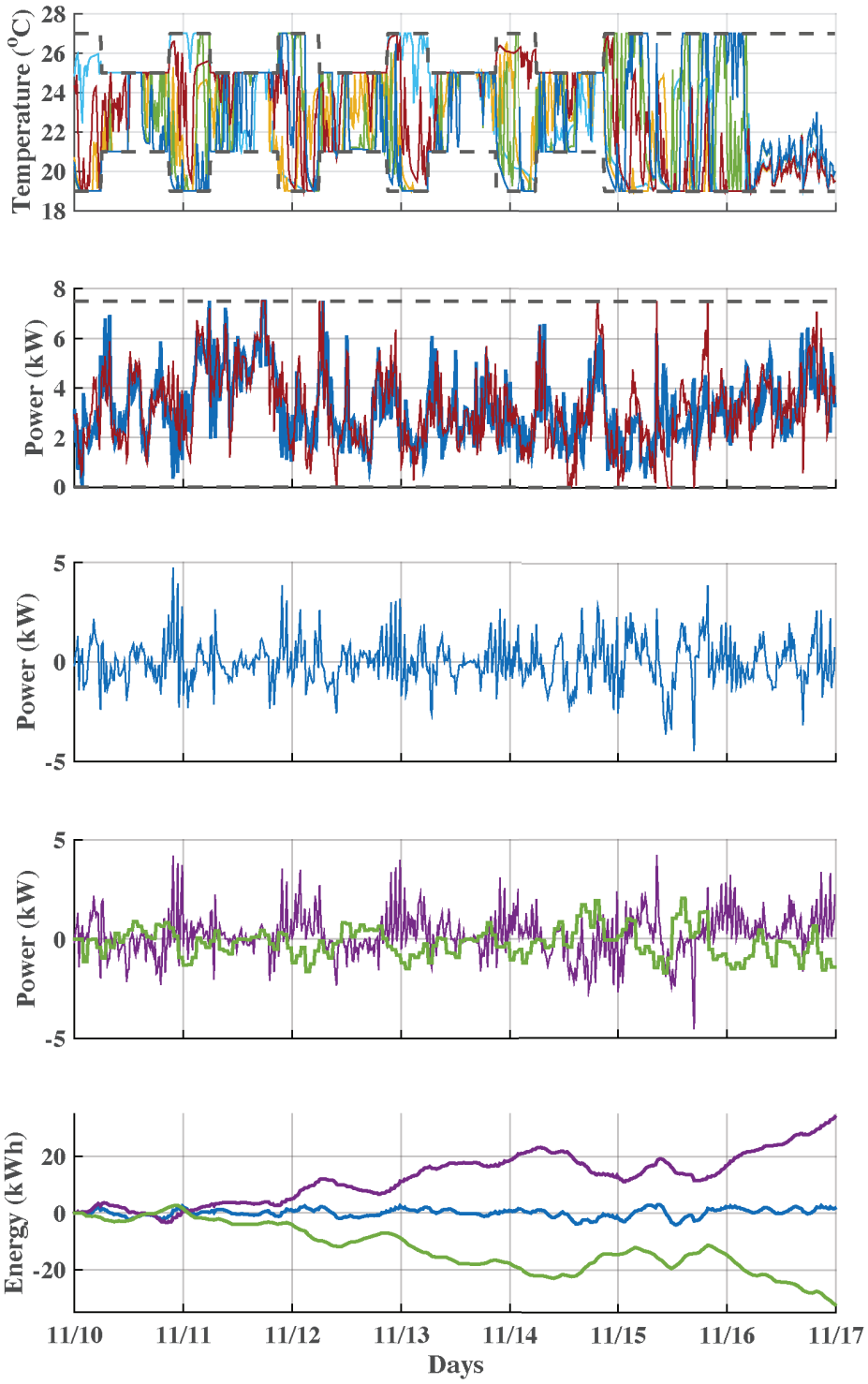

Figure 6.5 – Simulation result for week 46 (2014). Upper: Zone temperatures. Middle Up: Baseline power consumption $\bar{\mathbf{e}}$ (blue), total power consumption $\mathbf{e}$ (red). Middle: Residual tracking signal $\gamma\mathbf{r}$. Middle down: Received AGC signal $\gamma\mathbf{a}$ (purple), intraday transaction $\mathbf{m}$ (green). Lower: Cumulative sum of AGC (purple) / residual tracking signal (blue) / intraday transaction (green).

Computations

The simulations are performed in MATLAB. The two-stage stochastic optimization problem (18) is formulated as a linear program using the YALMIP [111] toolbox for mathematical modeling and is solved using the Gurobi solver. It takes 40 minutes on average to solve the weekly bidding problem.

Comfort Measure

The *ASHRAE Likelihood of dissatisfied* (ALD) is used as a measure of occupant comfort. ALD is a function of the deviation of zone temperature from the ideal temperature as described in Appendix B. ALD calculation is as a post-processing step and not a part of the optimization problem. *Long-term percentage of dissatisfied* (LPD) which is a function of ALD and the occupancy rate is used to evaluate the average comfort per week (for more details see [86]).

6.6.3 Analysis of results

Economic Benefit

The building participating in the Swiss AS, can reduce on average 13% its operational costs, while participating in the intraday energy market reduced them by 29.5%. A building without extra storage saves on average 8.3% without, and 11.1% with intraday market participation. The percentage reduction in operational cost for all cases is depicted in Figure 6.6. The percentage savings vary every week depending on the outside weather condition, electricity price, etc.

On average, participating in the intraday market is advantageous for the building (solid line is above dotted line for most of the weeks). However, it is important to note that on any specific week, e.g., week 45, the saving may be reduced by participating in the intraday market. This is because the intraday transaction cost for any specific week might be larger than the benefit of having a residual tracking signal with low energy.

Comparing the total cost of operation when providing the ancillary service to the grid, with and without thermal storage, suggests that having thermal storage reduces the operating cost of the building on average 27.5% with, and 12.4% without intraday market participation.

Figure 6.7 illustrates the various components of the operational cost. The two most important parts are the baseline cost and the capacity bonus, both of which are the deterministic part of the cost function. Both, the tracking bonus and the intraday transaction cost may be positive or negative depending on the received AGC signal. The tracking error penalty is negligible, and not shown in this figure.

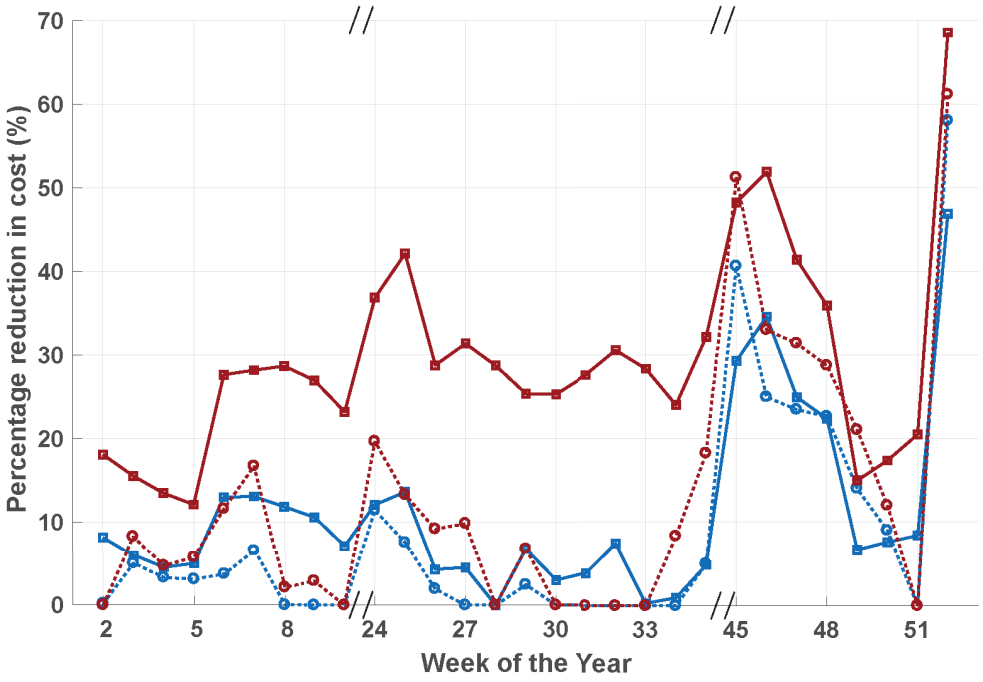

Figure 6.6 – Percentage reduction in weekly operation cost compared to the base case of minimum cost without AGC tracking. Solid lines: AGC Tracking - Intraday case, Dotted lines: AGC tracking - No Intraday case. Red: Additional thermal storage, Blue: No additional thermal storage.

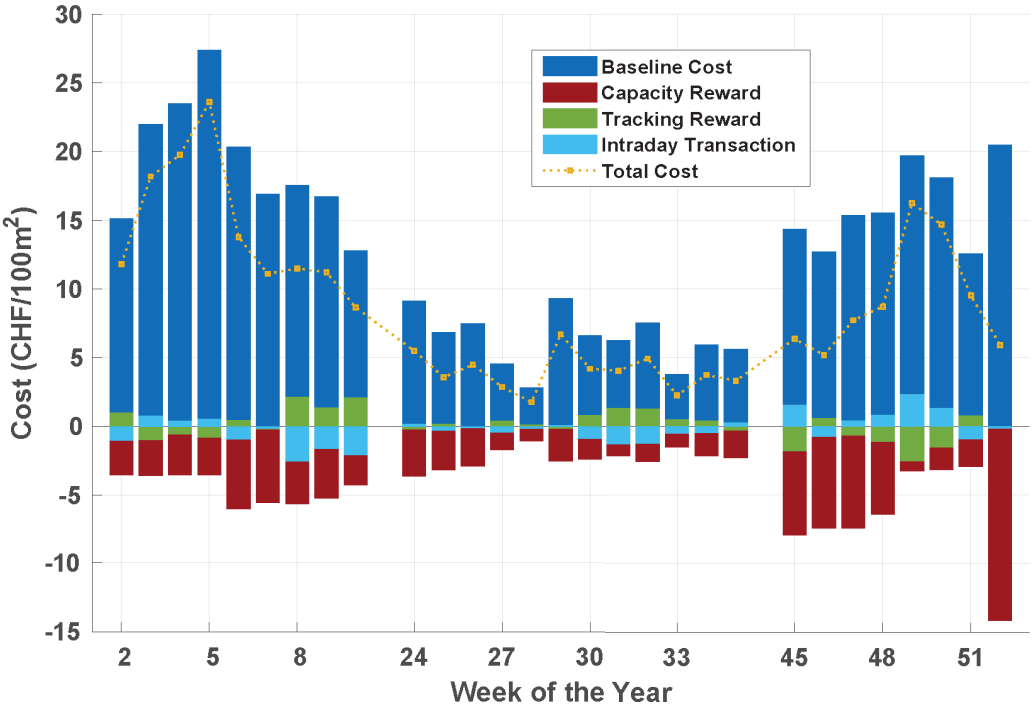

Figure 6.7 – Cost components for AGC tracking - Intraday with additional storage.

Impact of AGC tracking on occupant comfort

The occupant comfort is increased at a reduced cost (which is counter-intuitive). This is mainly due to the extra energy consumed to increase the baseline to provide (upwards and downwards) flexibility. In other words, the minimum price MPC aims at maintaining the temperature trajectories close to the constraints, while the zone temperatures are excited within the comfort limits when the building is participating in AGC tracking service, resulting in improved comfort.

The Figure. 6.8 is generated by gradually tightening the comfort constraints toward the ideal zone temperature, and re-running the simulations for all cases (for week 4 and 29). Each of these simulations gives us a point on the price vs comfort axis, as shown in Figure. 6.8. For AGC tracking, the same comfort is achieved at a lower cost. The AGC tracking case with the presence of additional storage enables the building to attain best comfort at least price when it also participates in the intraday market. Similar trend is observed for summer and winter weeks.

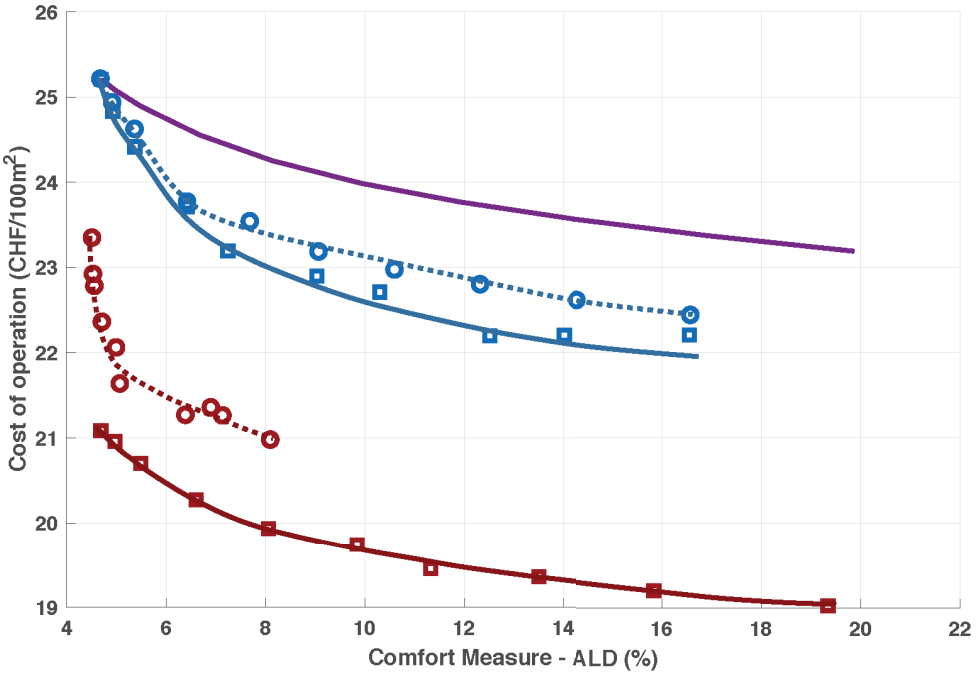

(a) Winter (Week 4)

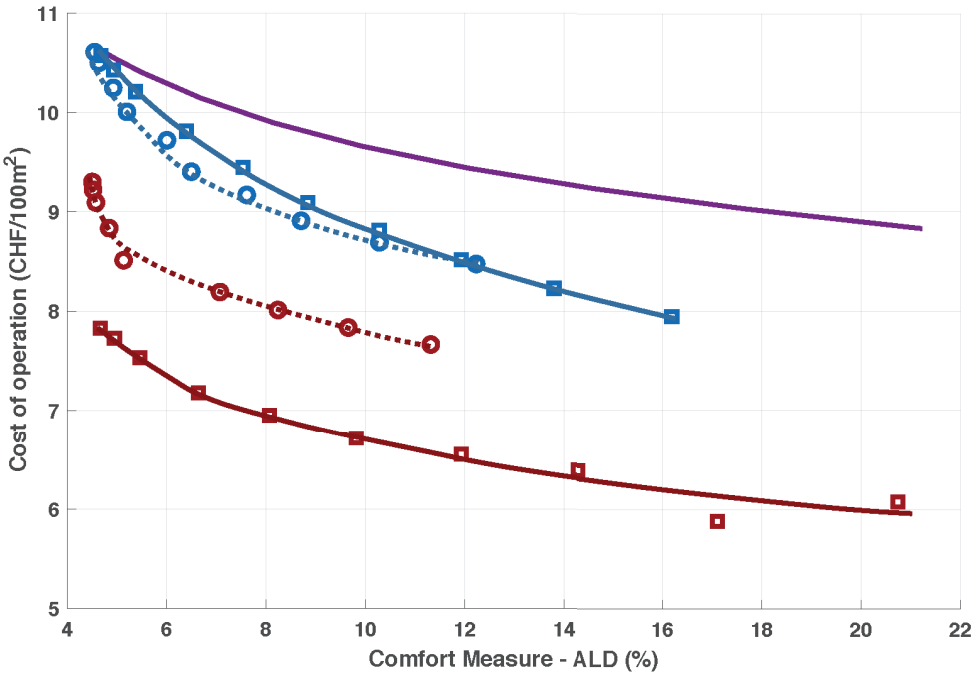

(b) Summer (Week 29)

Figure 6.8 – Cost of operation vs comfort: Solid purple: No AGC tracking without additional storage. Solid line: AGC Tracking - Intraday case, Dotted line: AGC tracking - No Intraday. Red: Additional thermal storage, Blue: No additional thermal storage.

Sensitivity to price of electricity

The economic benefits are sensitive to the electricity price. For a high electricity price, it might not be worth consuming extra energy to increase the baseline for providing the AGC tracking capacity. As outlined in Section 6.2, the electricity price is the sum of the spot electricity price, the distribution charges, and taxes. The distribution charges vary within Switzerland depending on the physical location of the load. The analysis presented so far is for Lausanne with a distribution price of approximately 100 CHF/MWh.

The impact of varying the distribution price between (40 CHF/MWh and 160 CHF/MWh) the range seen across Switzerland is studied. Results are depicted in Figure 6.9. The percentage reduction in operating cost increases with a decrease in the distribution charge. Furthermore, for the case of AGC tracking - No intraday and without additional storage, it is not worth providing the tracking service to the grid for a distribution price above 140 CHF/MWh. However, participation in the intraday market still makes AGC tracking worthwhile for this case.

Office buildings in locations with lower distribution prices can benefit more from providing AS to the grid.

6.7 Conclusion

This chapter presented the financial analysis of a typical office building providing ancillary service in Switzerland. The different markets, costs, and rewards involved in the provision of ancillary services were presented. The control methodology presented in Chapter 5 was adapted to account for all the costs, rewards, and the particular building HVAC considered in this study. The financial analysis was carried out using all the real data for the year 2014 with the following main outcomes:

- On average, providing secondary frequency control service to the grid results in savings for the building which are further increased by participating in the intraday market. The building without extra storage in its HVAC system saves on average 8.3% without and 11.1% with intraday market participation.
- Availability of thermal storage in the building HVAC system increases this financial benefit. For the building with thermal storage, the average savings in operational costs increase to 13%, while participating in the intraday energy market increase it to 29.5%.
- The provision of ancillary services to the grid increased the occupant comfort at a reduced price which is counter-intuitive. This is because the extra energy consumed to provide flexibility also improved occupant comfort.

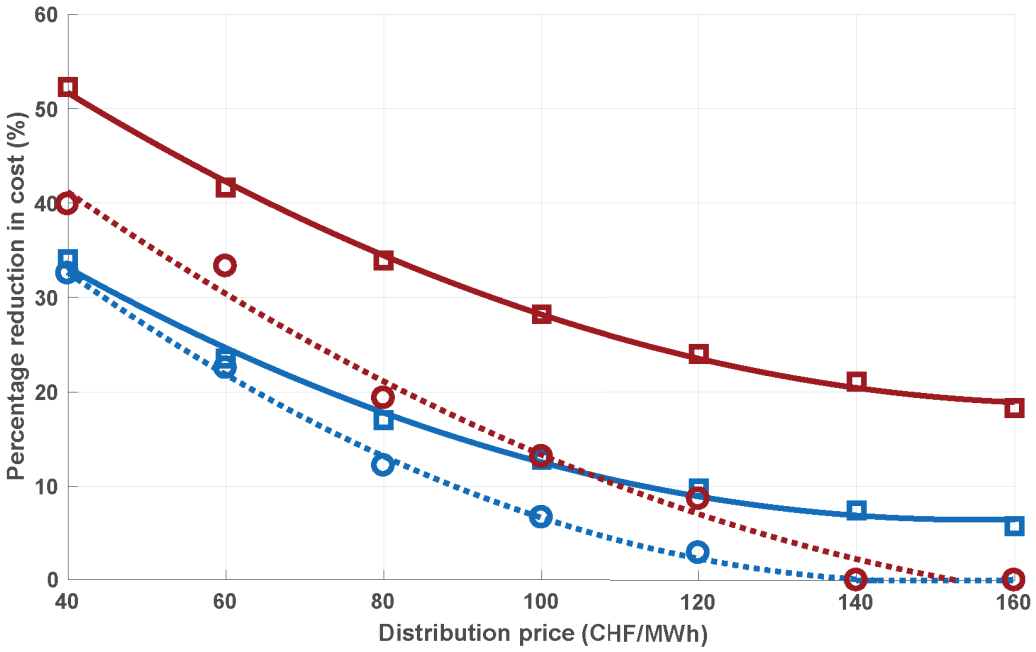

(a) Winter (Week 7)

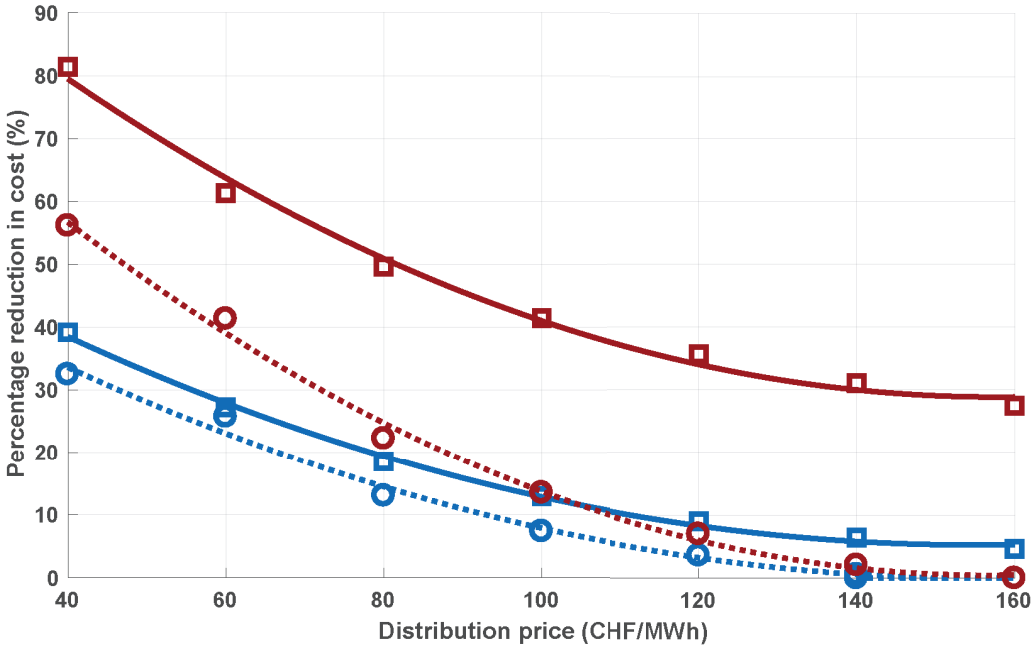

(b) Summer (Week 25)

Figure 6.9 – Percentage reduction in operating cost vs the distribution price of electricity: Solid lines: AGC Tracking - Intraday case, Dotted lines: AGC tracking - No Intraday case. Red: Additional thermal storage, Blue: No additional thermal storage.

- The economic benefit is sensitive to the electricity price. Since, electricity prices are slightly different (due to different distribution charges) at different locations in Switzerland, the financial benefit varies with the physical location of the building within Switzerland.

7 Ancillary Services Provision: Experiments

7.1 Introduction

As discussed in Section 5.2, most experimental works focus on the technical feasibility of simple strategies to implement power tracking in commercial HVAC systems. This work represents the first report of experimental results for frequency regulation, based on real recorded AGC signals, using a commercial building over a realistic time range, and the first work that applies a formal method to compute an optimal bid for AGC provision on a real system.

The experimental results in this Chapter are based on the experimental platform LADR (Laboratoire d'Automatique Demand Response), developed in collaboration with three other PhD students (Tomasz Gorecki, Luca Fabietti, and Altug Bitlislioglu) in the lab. The purpose of the platform is to validate the control methods and techniques developed in the lab, and to experimentally demonstrate the demand response capabilities of office buildings. Various different types of experiments were performed using LADR, and their results have been reported in [10], [14], and [112]. This Chapter focuses on the parts where I contributed the most, and specifically on the experimental validation of buildings providing secondary frequency control service using the stochastic control methods described in Chapter 5.

7.1.1 Contributions of this chapter

This chapter answers the question of the technical feasibility of office buildings providing frequency regulation services.

The design of a controller based on the control method described in Chapter 5 is presented for provision of the secondary frequency control service to the grid. An additional layer of fast controller is added to the closed loop AGC tracking control algorithm described in Section 5.6.3. The fast controller makes it possible to track the AGC signal at a faster

rate than the frequency of the closed loop MPC controller. The experimental platform developed in the lab for the validation of control algorithms is discussed.

Experiments are performed following the rules imposed by the current regulation of the electricity market in Switzerland. The effectiveness of the proposed controller is tested in experiments, for the provision of ancillary services, both with and without the building participating in the intraday market.

The performance of the presented control methodology is also compared to an alternative approximate solution method developed in the lab.

7.1.2 Structure of this Chapter

The particular control problem considered in the experiments is presented in Section 7.2. The experimental setup developed in the lab for the demonstration of the developed control algorithms is presented in Section 7.3. The simulation and experimental results of the proposed control scheme, without participating in the intrady market, and their comparison with an alternate solution method is presented in Section 7.4. The experimental results with intraday market participation are presented in Section 7.5, followed by a discussion on the additional elements required to support the real-time fast tracking of the AGC in Section 7.6. Finally, the conclusions are drawn in Section 7.7.

Notation: Bold letters denote sequence of vectors over time, the length of which is clear from context, e.g., $\mathbf{e} = [e_0^T, e_1^T, ..., e_{N-1}^T]^T$.

7.2 Control Problem

This section presents the particular control problem considered in the experiments. The formulation is based on the control scheme presented in Chapter 5. As discussed in Chapter 5, there are two phases (offline, and online) for a building providing secondary frequency control service to the grid. During the offline phase, at the beginning of the regulation period, the building needs to bid the flexibility γ, and the baseline consumption $\bar{\mathbf{e}}$ over the regulation period. During the online phase, the building is required to track the received AGC, while satisfying the operational and comfort constraints.

7.2.1 Bidding Problem

The bidding problem for the offline phase is formulated as in (5.6). As detailed in Section 7.3, electrical heaters are used in the experiments, therefore the total electrical consumption of the building is equal to the sum of the thermal power input in each zone. As a result, the generic HVAC constraint in (5.6) ($\mathbf{e} = h(\mathbf{u})$) is replaced by $\mathbf{e} = \Gamma\mathbf{u}$, where $\mathbf{u}$ is the thermal

power input to the building as defined in (5.4), $\Gamma := I_N \otimes \mathbf{1}^T$, with I_N an identity matrix of size N, and $\otimes$ is the Kronecker product.

Cost Function

The building receives a payment proportional to the capacity bid, while it pays for buying the baseline. The balance between the two depends on the difference between the cost of power and the unit reward price for capacity as explained in Chapter 6.

In this work, the goal is to experimentally demonstrate the technical feasibility of buildings providing AGC tracking service to the grid, therefore the cost function is simplified, maximizing the offered flexibility, *i.e.* $J = -\gamma$. As shown in Chapter 6, most of the economic benefit in participating in ancillary services provision comes from the capacity bid, therefore this is a reasonable simplification.

Approximate Solution Method

The bidding problem is approximated using the method described in Section 5.5. The intraday trades are optimized using the control policy (5.8) as described in Section 5.5.1. With the intraday policy fixed, the bidding problem is approximated by a two-stage robust (instead of stochastic) optimization problem.

Remark 12. *The resulting two-stage robust problem is the same as the scenario based problem* (5.11)*, with the difference that the cost function ($J = -\gamma$) is deterministic and the generic HVAC constraint ($\mathbf{e}^j = h(\mathbf{u}^j)$) is replaced by $\mathbf{e}^j = \Gamma \mathbf{u}^j$. Note that with a deterministic cost function, problem* (5.11) *is no more an approximate solution of the stochastic programming problem* (5.10)*, but instead a two-stage robust approximation of the bidding problem* (5.6)*, with the assumption that the uncertainty $\mathbf{a}$ lies in the set Ξ_{ts}, where Ξ_{ts} is assumed to be defined by the convex hull of a finite number, N_s of historic AGC signals.*

The optimizer of the scenario based problem is the capacity γ^* and the baseline $\bar{\mathbf{e}}^*$ over the regulation period.

7.2.2 Closed Loop control

The purpose of the closed loop control is to compute the thermal power input u_t applied to the building at each time step, such that the AGC tracking and comfort requirements are satisfied. During the online phase, the building is controlled using the stochastic MPC controller (5.15) and the closed loop algorithm described in Section 5.6.3 which computes an optimal power input u_t^* at time step t.

Fast Controller

The AGC is received from the grid at a frequency higher than the frequency of the closed loop controller. Therefore, the power consumption of the building is required to be modified at a faster rate to track the AGC. For this, a fast controller is used to choose the control input to the electric heaters at a rate faster than the closed loop controller. The fast controller receives the control input u_t^* from the closed loop controller at time step t, and it computes the power input share going to zone j, $\nu_t^j = \frac{u_t^*}{|u_t^*|}$ where ν_t^j denote the share of total input to zone j between time step t and $t+1$. The control input between time step t and $t+1$ is computed using the current value of the AGC and the corresponding value of the residual tracking signal, i.e., $u^j = \nu_t^j(\bar{e} + \gamma r)$.

Note that the thermal system is a low-pass filter and as a result fast variation of the regulation signal does not affect the output of the system. Therefore, it is reasonable to have a closed loop MPC at a lower frequency without any consequences.

7.3 Experimental Setup

This section describes the experimental platform LADR (Laboratoire d'Automatique Demand Response), developed with three other PhD students (Tomasz Gorecki, Luca Fabietti, and Altug Bitlislioglu) in the lab. The purpose of the platform is to validate the control methods and techniques developed in the lab, and to experimentally demonstrate the demand response capabilities of office buildings.

The work on the experimental platform was started in Summer 2014 and first set of experiments were conducted in the Winter 2014-15. The experimental platform has been improved over the years, and various different types of demand response experiments have been conducted by different lab members in the Winter 2015-16, and 2016-17. I was actively involved in the experiments performed in the first two seasons (Winter 2014-15 and 2015-16). The research outcomes of the experiments performed using LADR have been reported in the publications [10], [14], and [112].

7.3.1 LADR

Offices in the lab have been equipped with wireless temperature sensors and five rooms have been equipped with custom-tunned electric radiators for fast actuation, as shown in Figure 7.1. Room SE in Figure 7.1 is occupied by six PhD students while all the other rooms have single occupancy. A communication platform is developed which handles the flow of data and allows to control the electric heaters in closed loop and to carry out experiments.

Figure 7.1 – Floor map of the offices used in LADR. The offices shaded in grey have been equipped with sensors and electric radiators and used for experiments. Red squares show the position of the heating units.

7.3.2 Heaters

Electric heaters were chosen as the actuators because they can be operated at very fast rates, are relatively easy to control, and have simple models. The maximum power rating of the heaters is 1900 Watts at 230 Volts, adding up to a total maximum installed power consumption capacity of 9500 Watts. The heaters were originally equipped with a thermostat and a manual switch to adjust the heating between three distinct levels. To carry out experiments and to be able to modulate the power consumption at a fast rate, the heaters were modified with additional hardware. A solid-state relay was installed to switch on or off the heaters at a high frequency. A microcomputer (BeagleBone Black) was installed on board to control the switching of the relay and to communicate with the AGC tracking controller. The power consumption was modulated using pulse-width modulation (PWM) at 4Hz. The on-board microcomputer receives the control input from the tracking controller and generates the appropriate PWM signal to achieve the desired power consumption level. Note, that since the heaters are resistive elements, the power consumption directly translates into a thermal power input to the room.

7.3.3 Setup

The schematic of the experimental setup is shown in Figure 7.2. The temperature measurement is obtained from the Aeotec Z-Wave Multisensor installed in each office. The sensors send the measurements to a server using the Z-wave wireless protocol. Weather data (outside temperature, solar radiation, etc.) is collected from a nearby weather station via Internet on the server. The server is also connected to a weather forecast service and receives the predictions. All the data from the server is uploaded to a data server (designed with the Python framework Django) over the local network.

The control algorithm (offline and online) runs in MATLAB on the server computer using the temperature measurements, weather forecast, and the received AGC. The computed control input is communicated to the on-board microcomputers of the electric heaters over the local Ethernet network. The on-board heater microcomputers runs python code to control the PWM switching frequency. All the heaters are centrally controlled by the controller running on the server.

The data communication between the controller, data server, and the heaters is handled using YARP [113] which is an open-source software supporting cross-platform data interchange. The advantage of using YARP is that it allows easy communication of data between different devices running different programming languages (the controller runs on MATLAB, while the heaters are controlled using Python).

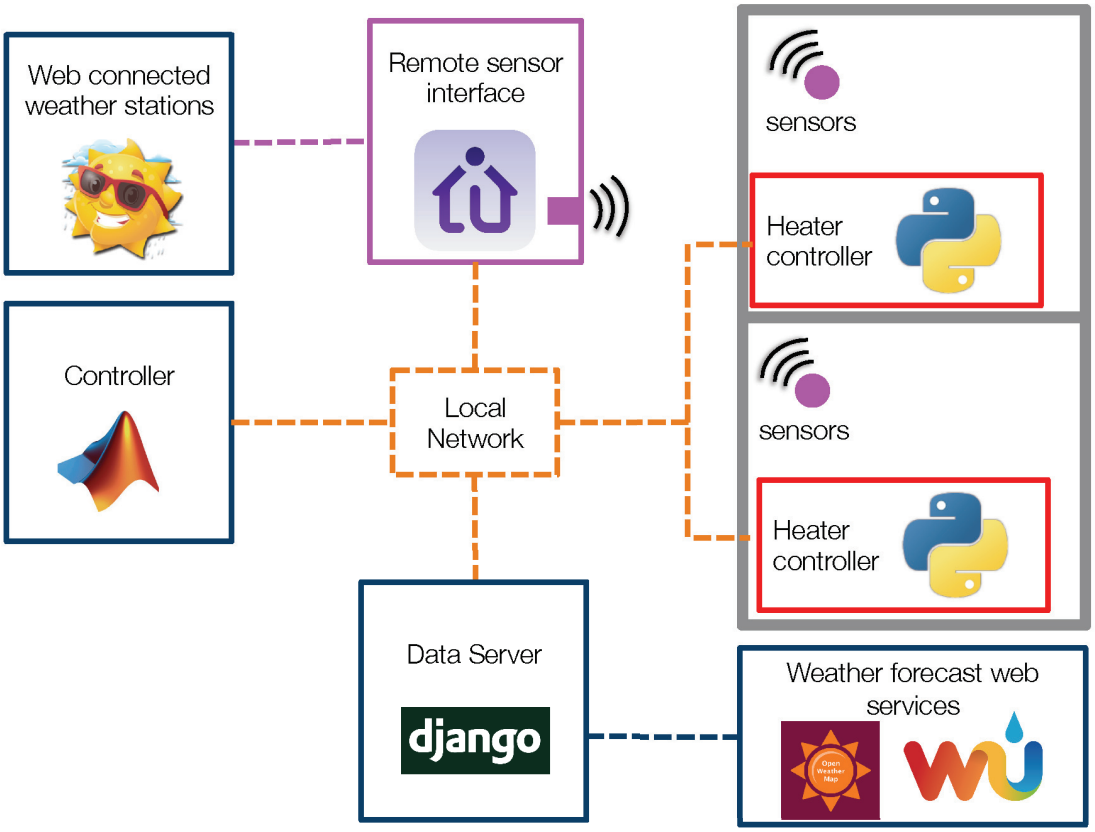

Figure 7.2 – Schematic of the experimental setup

7.3.4 Experiments 2014-15

During the first season of the LADR experiments (2014-15), the experiments were conducted in four offices accounting for a total area of 90 sq. meters. The rooms are characterized by a concrete heavyweight structure. The experiments were carried out overnight, when the offices were unoccupied and the impact of the outside weather was minimal (as the rooms were not impacted by solar radiation). The duration of each experiment was about 10 hours.

7.3.5 Experiments 2015-16

During the second season of the LADR experiments (2015-16), the experiments were conducted in five offices accounting for a total area of 115 sq. meters. The duration of each experiment was about 20 hours including the office hours when the offices were occupied. As shown in Figure 7.1 each office has a window and has varying exposures to the sun. As opposed to the first season, the disturbances (weather and occupancy) were also taken into account during the experiments.

7.3.6 Model Identification

The thermodynamic model of the offices is identified using standard black-box linear system identification. Each office was identified separately, since the thermal coupling between them is very week. The model of each room has one control input (thermal power input) and one output (room temperature), while it is also impacted by disturbances (outside temperature, and solar radiation).

Identification experiments were conducted and the data was collected. Each office was modeled with a second order Auto Regressive model with exogenous inputs (ARX) [114] with model parameters fitted using the experimental identification data. The disturbance inputs impacting the model were also considered as inputs during the identification procedure. The identified model has three inputs, thermal power input (control input), outside temperature (disturbance), and solar radiation (disturbance). The solar disturbance input for each office was different depending on its orientation.

The full model of the building is obtained by combining the individual models of the rooms and has five control inputs (heat input in each room), five outputs (temperatures), and two disturbance inputs (outside temperature, and solar radiation). The identified model is transformed into the standard state-space form as required in (5.4).

The identified models were validated and results showed that they capture the dynamics of the system adequately. For more details on the model identification and validation results, the readers are refereed to [10], and [14] for the results of first, and second experimental

season, respectively.

7.4 LADR AGC tracking without Intraday market participation

This section presents the simulation and experimental results of the LADR office building providing secondary frequency control service without participating in the intrday market, i.e. the residual tracking signal is equal to the AGC, and the intraday trades are zero. The efficacy of the control scheme described in Section 7.2 is demonstrated and its performance is compared with an alternative (multi-stage approximate) control method developed in the lab.

7.4.1 Multi-stage robust solution method

An alternate control method has been developed in the lab, approximating the solution of the bidding problem (5.6) using robust optimization methods. The key idea of the method is to retain the multi-stage structure of the bidding problem and to parameterize the two control policies in (5.6) using affine decision rules, i.e., the control decisions are an affine function of past disturbances (received AGC). The uncertainty **a** is assumed to be in a set Ξ_{ms} which is constructed using historic scenarios of the AGC signal. The resulting robust optimization problem can be transformed into a convex problem under certain technical assumptions (mostly convexity of the set Ξ_{ms}). The optimal solution of the problem results in a capacity bid and a baseline over the regulation period. The optimized control policies (affine decision rules) are used to compute the control input for closed loop operation. For more details on the multi-stage approximate control method, refer to [78], [10], and [79].

7.4.2 Simulation results

This section presents the simulation results demonstrating the effectiveness of the control scheme discussed in Section 7.2, and compares it to the multi-stage approximation described in Section 7.4.1.

Simulation setup

The identified model of the LADR offices is used for simulations. The sampling period is chosen equal to 15 minutes which provides a nice compromise between temporal resolution of the control and computational complexity of the problem formulation. The comfort range for temperature is chosen as 21 °C to 25 °C. The regulation period is assumed to be 10 hours. Perfect tracking of the unknown AGC signal is required, i.e., $m_e = 0$.

Both the approximate solution methods (two-stage robust described in Section 7.2, and

multi-stage robust described in Section 7.4.1) are used to solve to the bidding problem and compute the maximum power capacity that the building can support over the regulation period. The scenarios used to solve the bidding problem and to construct the uncertainty set for the multi-stage approximation method are obtained by breaking the yearly normalized AGC signal of 2013 into 876 ten hour samples. Solving the two bidding problems results in different values for the optimal bid $\gamma^\star$ and baseline $\bar{\mathbf{e}}^\star$.

To test the robustness, and quality of the solution, historical realizations of the AGC signal of 2014 are considered for validation. The AGC for 2014 is also broken into 876 ten hours test instances. Each ten-hours test AGC sample is multiplied by the optimal power capacity $\gamma^\star$ and added to the baseline $\bar{\mathbf{e}}^\star$ to obtain the total power signal to be tracked by the system. For the two-stage approximation, an open loop optimization problem is solved for each ten hour test sample to optimally distribute the power across the four zones while respecting the comfort constraints. Similarly, for the multi-stage approximation, the optimal affine control law is used to compute the open loop trajectories of the zones temperature. The result is depicted in Figure 7.3.

Analysis of results

As seen in Figure 7.3, there are a few differences between the two approaches both in terms of bid capacity and of thermal response of the system while providing AGC tracking.

The multi-stage approach is more conservative and results in a capacity bid of $\pm 1.85kW$ while the presented two-stage approach results in a capacity bid of $\pm 3.2kW$. This is visible in the bottom plots of Figure 7.3 where the AGC signals and their maximum amplitude are shown. The computed capacity represents 25% and 43% of the maximum available power, respectively.

The resulting temperature trajectories in the four zones of the building for all the considered AGC test samples are shown in the top plots of Figure 7.3. For the multi-stage approach, the zone temperatures stay more closely around 23 °C which represents the most robust state to be in to absorb both positive and negative realizations of the AGC. For the two stage approach, temperatures are closer to the constraints and violate the constraint slightly for a few AGC test samples.

7.4.3 Experimental Results

This section presents the experimental results testing the effectiveness of the control scheme discussed in Section 7.2, and compares it to the multi-stage approximation described in Section 7.4.1. The results are based on the overnight experiments performed during the first LADR experimental season (winter 2014-15). Experiments have been conducted over

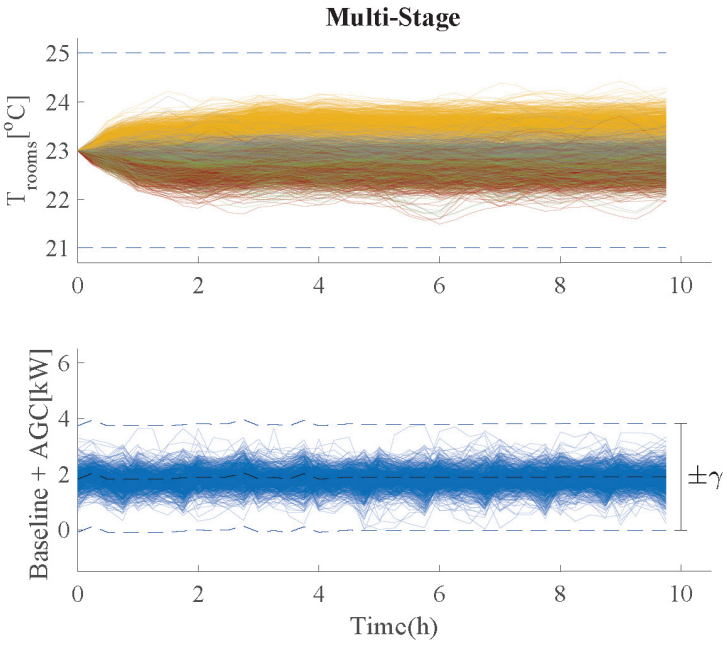

(a) Multi-Stage

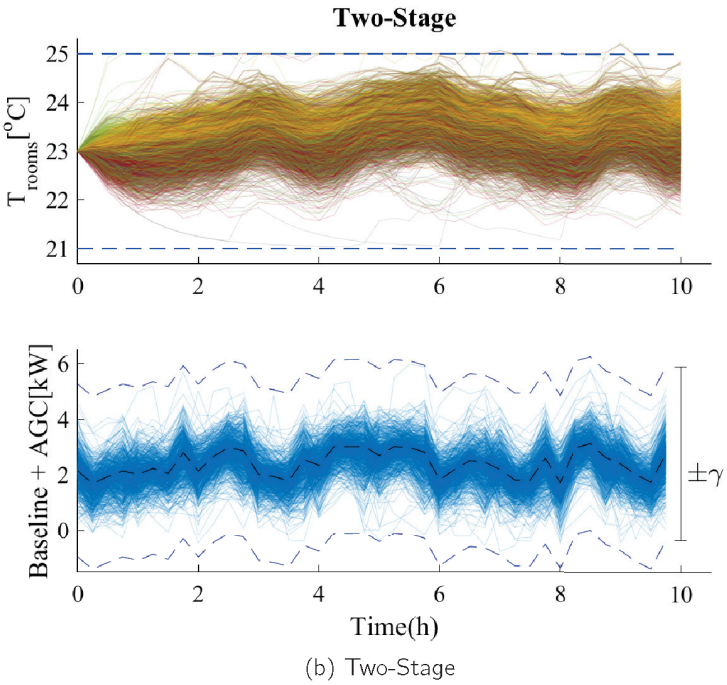

(b) Two-Stage

Figure 7.3 – Open-loop predictions for the multi-stage and two-stage controller for real AGC signals from 2014. The obtained capacity and baseline obtained off-line on data of 2013 are used to compare the two approaches applying 876 different signals extracted from the data set of 2014. Upper: Temperature in each of the 4 zones (different colors) during activation period. Lower: AGC signals superimposed on the computed baseline (black dashed line) and capacity bid bounds.

periods of 10 hours from 8 pm to 6 am on different days in February and March 2015. During the experiments, the outside conditions were relatively consistent with outdoor temperature ranging from 4 to 10^{o}C.

For the computation of the bid, it was assumed that the zones temperature at the beginning of the experiment is 23^{o}C to allow a meaningful comparison between different days, and with the simulation results. Therefore, the temperature was regulated to this value before each experiment. Since the same model and initial condition was used in simulation and in the experiment, the result of the bidding problem were the same, as detailed in Section 7.4.2, with optimal bids that correspond to 25 and 43 % of the installed capacity, respectively.

Different realizations of the AGC signal were used for testing in the experiments. After the commitment of the bid and baseline, the closed loop controller computes the control inputs, which determines how energy is split across the rooms, with a time step of 15 minutes. In practice, the frequency of update of the AGC signal is faster than 15 minutes, and the fast controller described in Section 7.2.2 is used to apply the control actions at a faster rate. A rate of one minute was used in the experiments. A Kalman filter is used to estimate the state of the system.

After computing optimal bids solving respectively the bidding problem described in Section 7.2.1 and the multi-stage robust problem described in Section 7.4.1, four closed loop experiments were run, applying two different AGC signals. Results are reported in Figures 7.4, and 7.5, for the first and the second AGC signal, respectively. For each experiment, four subplots are shown. The first one shows the evolution of the temperature in the four rooms, the second depicts the baseline and the total power consumption in the four rooms and how it is split between the rooms. It can also be observed there how the energy dispatch in the four rooms is re-adjusted in closed loop every 15 minutes. The third plot shows the scaled AGC signal that needs to be tracked and the fourth plot shows the integral of the AGC signal over time, which represents the energy stored in the system as a result of the tracking.

In the case of the two-stage method, the computed bid is higher and, therefore, results in larger tracking requirements which drive the temperature closer to the comfort limits. This confirms the results obtained in simulations. Small constraint violations are observed in the case of the two-stage method. This is expected since already in the case of perfect predictions and no model mismatch in simulations, the two-stage method displays an "agressive" behaviour and runs very close to the constraints. The magnitude of those violations is however below 0.5^{o}C.

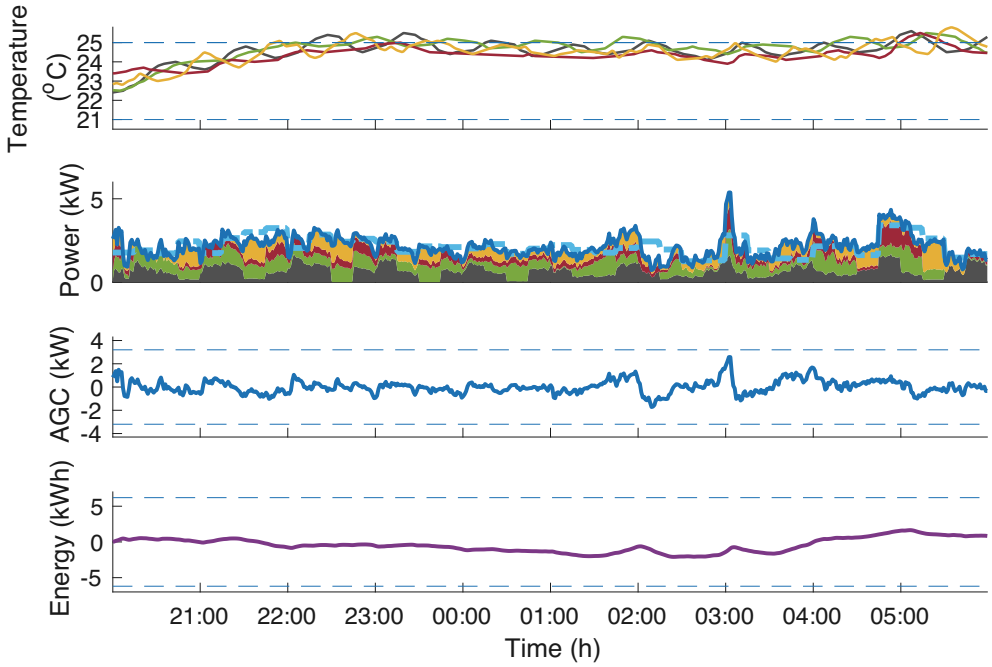

(a) Two-stage

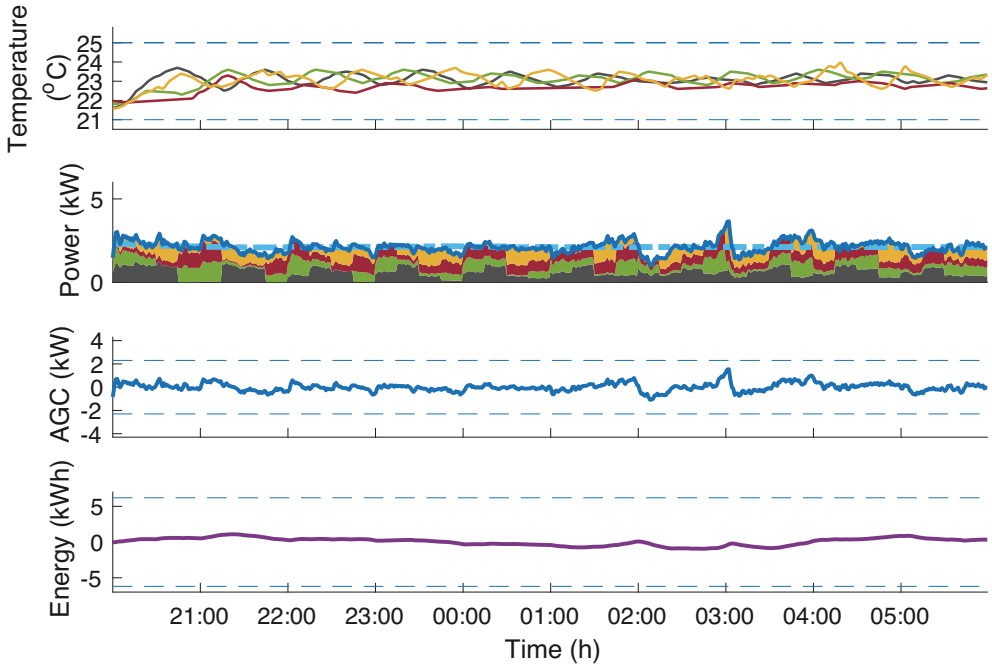

(b) Multi-stage

Figure 7.4 – Two experiments of AGC tracking. 1^{st} selected AGC signal extracted from real data of 2013, and is used to test and compare the two controllers. Upper: Temperature variation for different zones. Each color corresponds to the measured temperature in each zone. Middle Up: Baseline and power distribution among zones. Middle Down: AGC signal variation and capacity bid. Lower: Integral of the AGC.

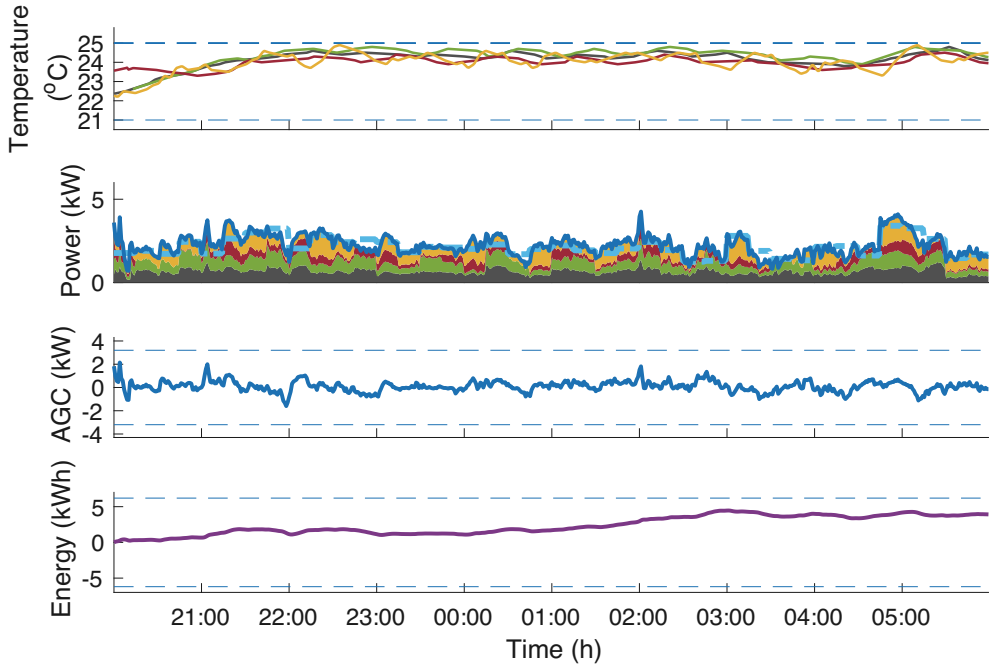

(a) Two-stage

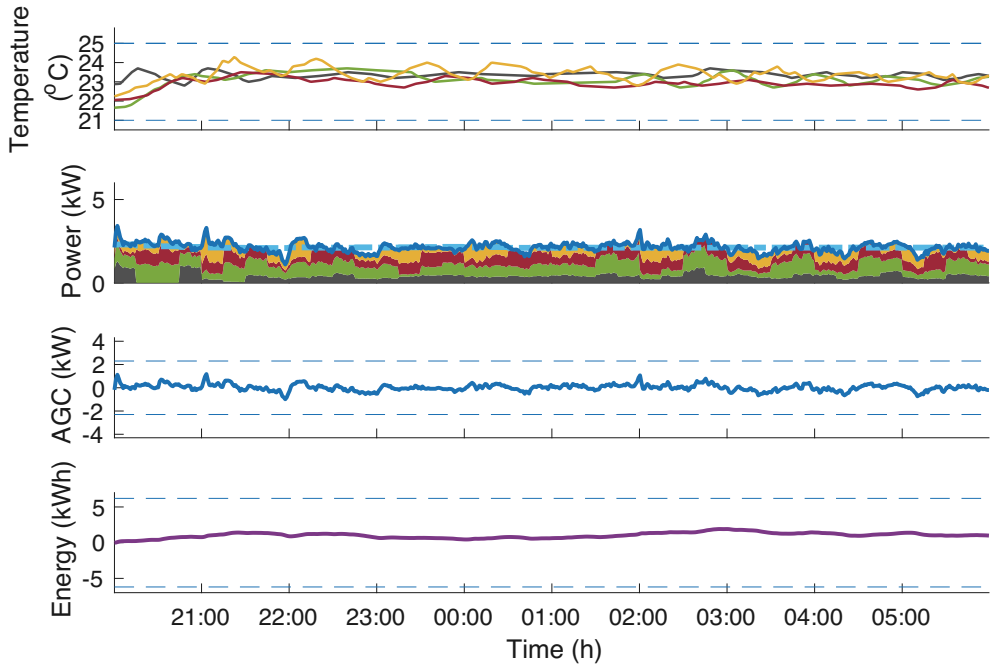

(b) Multi-stage

Figure 7.5 – Two experiments of AGC tracking. 2^{nd} selected AGC signal extracted from real data of 2013, and is used to test and compare the two controllers. Upper: Temperature variation for different zones. Each color corresponds to the measured temperature in each zone. Middle Up: Baseline and power distribution among zones. Middle Down: AGC signal variation and capacity bid. Lower: Integral of the AGC.

7.5 LADR AGC tracking with Intraday market participation

This section presents the experimental results of the LADR office building providing secondary frequency control service while also participating in the intrday market. The performance of the control scheme described in Section 7.2 is validated in experiments and the technical feasibility of a building providing secondary frequency control service, while also participating in the intraday market is tested.

7.5.1 Experimental Results

The results are based on the experiments performed during the second LADR experimental season (winter 2015-16). Experiments have been conducted over periods of 20 to 24 hours on different days in January and February 2016.

At the beginning of the regulation period, the bidding problem described in Section 7.2.1 is solved to compute the optimal baseline and capacity over the horizon. The scenarios of the residual tracking signal required to solve the bidding problem are generated using the intraday control policy described in Section 5.5.1, and the procedure explained in Section 5.6. A forecast of outside temperature and solar radiation over the regulation period is obtained from the weather server, and is used to solve the bidding problem.

During the online phase, different realizations of the AGC signal were used. The closed loop algorithm together with the fast controller described in Section 7.2.2 was used to compute the control inputs for each zone of the building. The intraday transactions were optimized using the control policy (5.8) using the procedure outlined in Section 5.6.3.

The experimental results for two of the days are shown in Figure 7.6, and 7.7. The offered capacity with four controlled zones on the first day was 3.4kW (45% of the installed capacity), and with three controlled zones on the second day was 2.85kW (50% of the installed capacity). There are four sub-plots in Figure 7.6, and 7.7. The top plot shows the day-ahead baseline obtained by solving the bidding problem in red, and the effective baseline in black. The effective baseline is the the sum of the day-ahead baseline and the modifications made by trading in the intraday market. The total power consumption is shown in blue, and the different colors show the distribution of total power in different zones. The difference between the total power (blue line) and the effective baseline (black line) is the received AGC (since tracking error is zero) and is shown in middle-down plot in these figures. The temperatures in different zones during the day are shown in the middle-up plot in these figures and it can be seen that it is between the comfort bounds (between 21 and 25^oC). The intraday trades are shown in the bottom plot in these figures.

As discussed in Section 6.5, the intraday trades help by reducing the energy content of the effective regulation signal that the building ends up tracking. As a result, it can be

seen in Figure 7.6, and 7.7 that the zone temperatures stay close to the maximum comfort temperature (23^oC) most of the time, improving the overall occupant comfort. This observation is consistent with the analysis in Section 6.6.3, and the conclusions of the experimental study [14].

Remark 13. *As expected, the offered capacities are higher when participating in the intrday market which is consistent with the results of the experimental study [14]. However, note that the experimental results (in terms of offered capacity) with and without intrday market participation (described in Section 7.4 and 7.5) are not very comparable because they were performed in two different years, with different controlled rooms, and for different horizons. The experiments with intrday participation considered a longer regulation period and the building zones were also subjected to un-modeled disturbances (due to occupancy and weather forecast errors).*

The experimental results demonstrate the efficacy of the control scheme proposed in Chapter 5. The results show that the proposed controller allows to successfully track the AGC signal and to provide flexibility to the grid, while achieving the primary objective of maintaining occupant comfort. The success of the experiments despite uncertainties in weather prediction and occupancy demonstrate the robustness of the proposed control approach.

7.6 Supporting element for real-time tracking

The AGC signal is transmitted with a sampling frequency of 1Hz, therefore the building providing secondary frequency control service to the grid is required to modify its consumption at a rate of 1Hz to track the AGC. One of the reasons of choosing electric heaters for the LADR setup was that they can be controlled at a fast rate. However, most commercial HVAC systems cannot be controlled at such a fast rate, therefore, the building needs a supporting element / resource that can track the fast part of the AGC signal.

It is proposed to couple the building with a fast storage element, e.g., an electric battery. The capacity required to track the AGC signal will still be provided by the virtual storage of the building using the proposed control method. The electric battery plays the role of capturing the small fast frequency variations of the signal (since the building operates at 15 minutes time step) which carry little energy themselves. Thus, the battery is used just to cover the difference between the 15 minutes average AGC signal (tracked by the building) and the fast AGC signal received every second.

The fast (1 Hz) AGC signal and the 15 minutes (average) AGC signal for a specific day are shown in Figure 7.8. The building tracks the 15 minutes average signal, while the battery tracks the difference between the 1Hz fast signal and the 15 minutes average signal as shown in Figure 7.8. This residual signal is zero-mean every 15 minutes by construction.

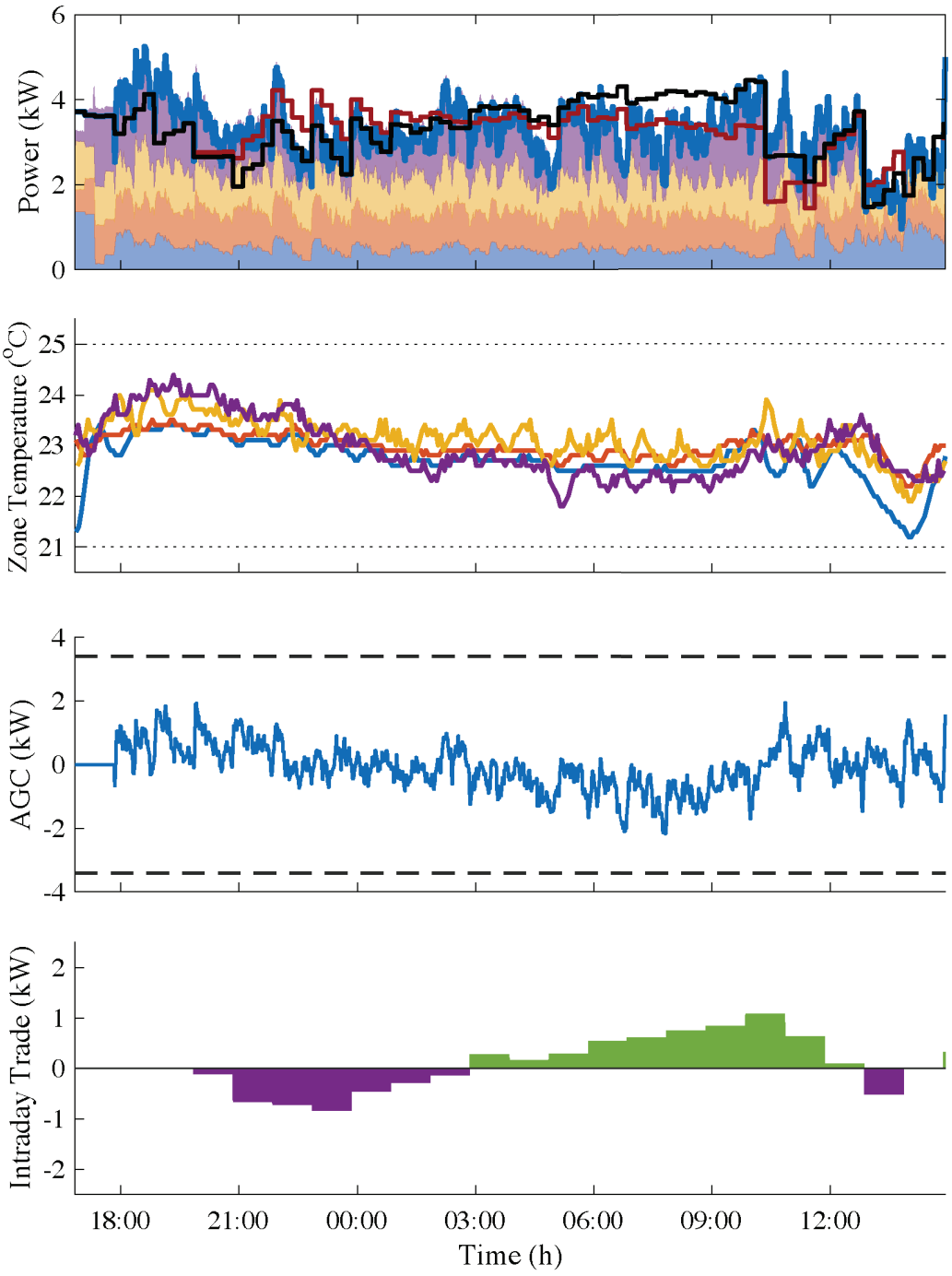

Figure 7.6 – Experiment of AGC tracking with Intraday participation - day 1. top: total power (blue), effective baseline (black), day-ahead baseline (red) and power distribution among zones, middle-up: zone temperatures - different colors correspond to temperatures measured in different zones, middle down: AGC, bottom: intraday trades.

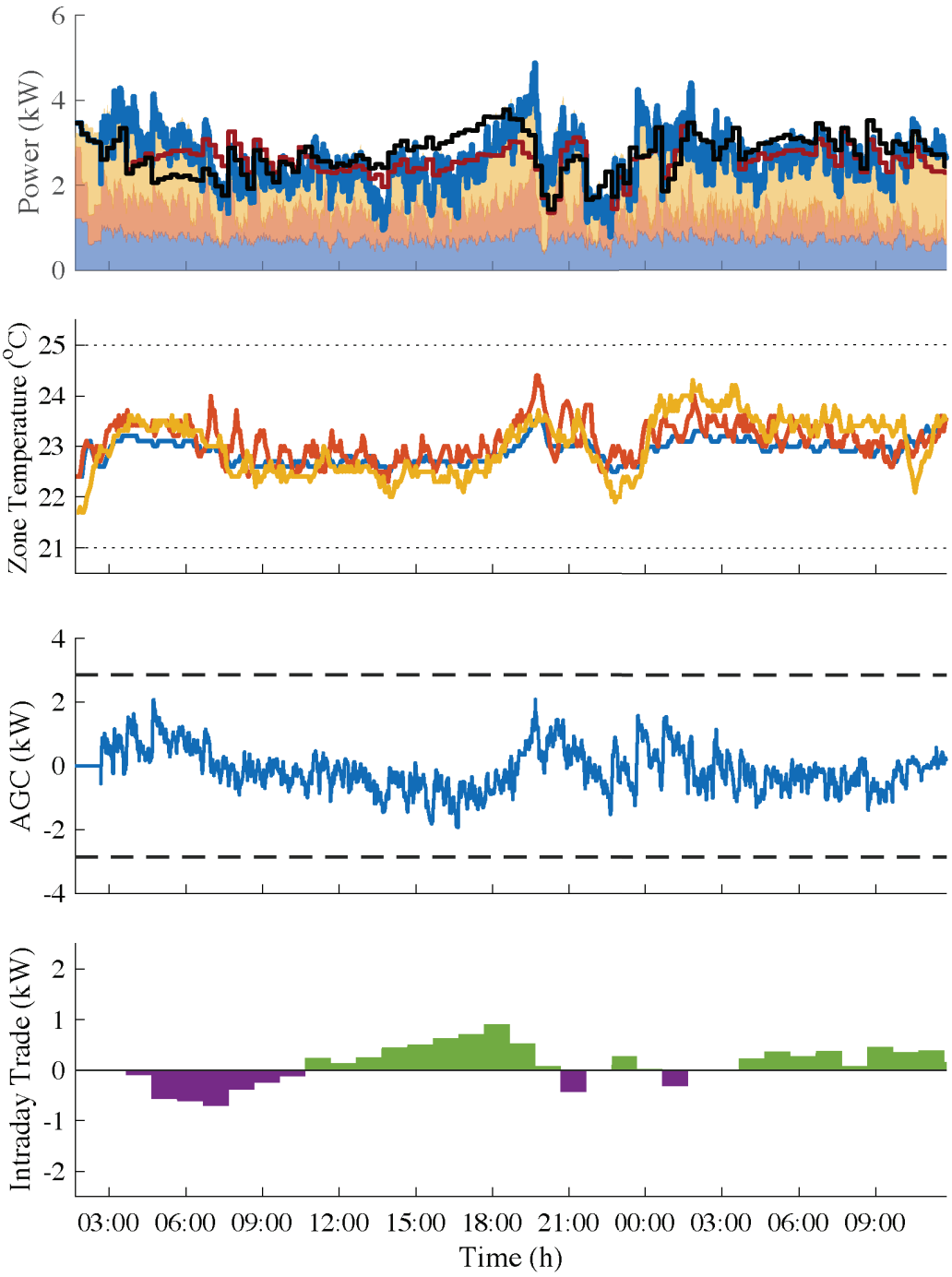

Figure 7.7 – Experiment of AGC tracking with Intraday participation - day 2. top: total power (blue), effective baseline (black), day-ahead baseline (red) and power distribution among zones, middle-up: zone temperatures - different colors correspond to temperatures measured in different zones, middle down: AGC, bottom: intraday trades.

The energy required to track such a power signal is its cumulative sum (shown in Figure 7.8 bottom).

The size of the required associated battery is estimated using historical AGC signal data. The worst-case scenario (in terms of cumulative sum and power peak) of the residual fast signal gives an estimate for the size of the required battery. The result suggest that only a small supporting electric battery with power limit of $\pm$1kW, and a capacity of 0.04kWh is required for every $\pm$1kW of capacity provided by the building. This is a very small number, compared to the capacity offered, due to the fact that the building serves the bulk of the energy-carrying part of the signal.

7.7 Conclusion

This chapter experimentally demonstrated the provision of regulation services using an occupied office building. The control scheme including a fast controller was presented, for the provision of regulation services, following the existing rules of the Swiss Market. The LADR experimental setup developed in the lab was described.

Experiments were performed over extended periods of time (10 to 24 hours) in occupied offices. The control method presented in Chapter 5 was experimentally validated. The building was able to provide flexibility to the grid by optimizing and fixing its baseline and capacity at the beginning of the regulation period, and tracking successfully the received AGC signal, while maintaining occupant comfort and operational constraints. The efficacy of the intraday control policy presented in Section 5.5.1 was also validated. The success of the experiments despite uncertainties in weather prediction and occupancy demonstrate the robustness of the proposed control approach.

The proposed control approach was also compared, both in simulations and experiments, to an alternative control method based on robust optimization methods, developed in the lab. The results showed that the proposed control method works well in practice and is less conservative compared to the alternative approach.

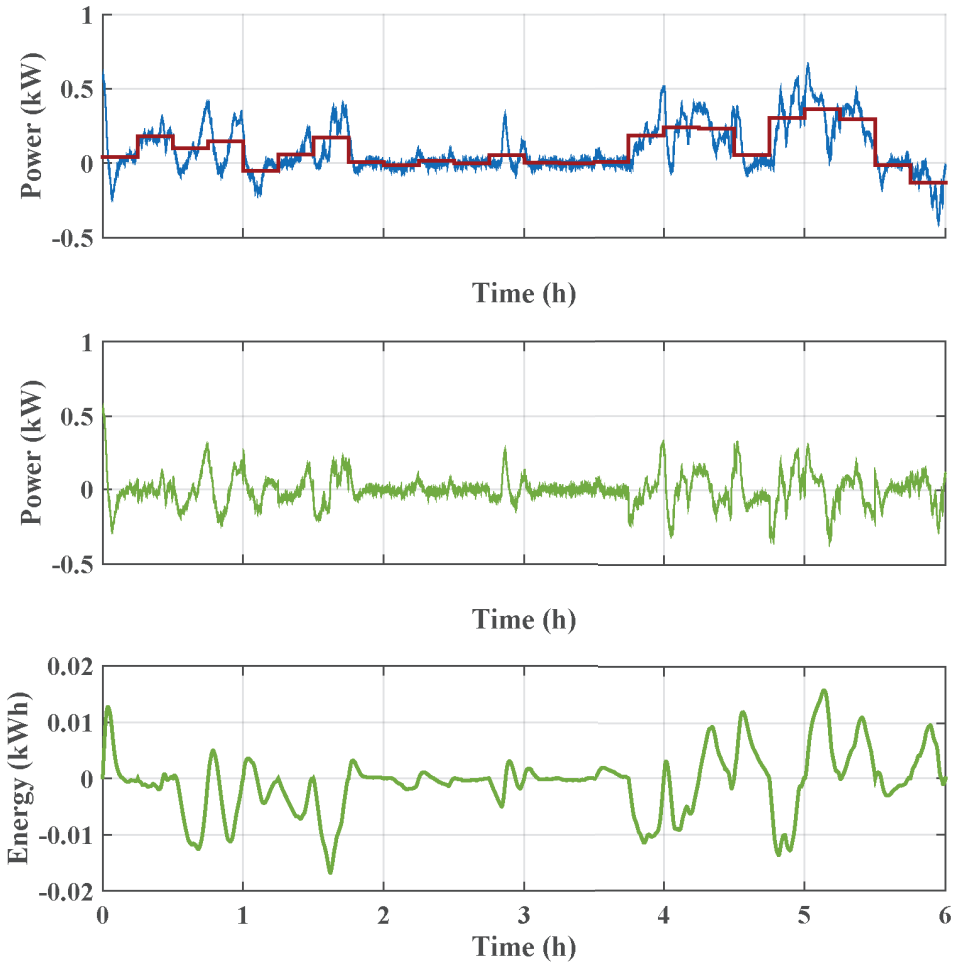

Figure 7.8 – AGC Signal. Upper: 15 minutes averaged AGC signal (red), 1s. AGC signal (blue). Middle: Difference between 1s. AGC signal and 15 minutes averaged AGC signal. Lower: Energy (Cumulative sum) of the difference between 1s. and 15 minutes averaged AGC signals.

Part III Hierarchical Control

8 Hierarchical Control of Building HVAC System for Ancillary Services Provision

8.1 Introduction

As discussed in Section 5.2, recent developments in the control of buildings for the provision of ancillary services neglect the complex dynamics of realistic HVAC systems which are common in most large offices and commercial buildings.

The existing model-based methods developed to characterize a building's flexibility [92], [93], [78], assume simplifying HVAC systems with a constant overall coefficient of performance (COP) of the heating / cooling equipment. These simplifying assumptions are often reasonable if the HVAC system is operated within certain region of operation. However, with these simplifying assumptions the HVAC system may not be operated at its optimum performance for providing flexibility to the grid. Moreover, the actual control of the complex HVAC equipment is often neglected in the existing literature, and only thermal and electrical power is directly considered in the flexibility controllers. This restricts the applicability of the control methods to simplistic HVAC systems, e.g., electric heaters etc.

Some of the analytic and heuristic based methods to estimate a building's flexibility consider realistic HVAC systems both in simulations [98], [99], [90] and experiments [102], [92], [103]. However, these control methods lack systematic approach and are difficult to generalize. The proposed methods do not consider the control of the full HVAC system, but are based on indirectly varying the speed of the main fan of the air-based HVAC systems for providing flexibility. It is shown that under certain conditions, small variations in fan speeds has minimal affect on occupant comfort.

Full control of complex realistic HVAC systems using optimization based methods has been studied in the past. MPC has been successfully applied for the control of building HVAC systems, both in simulations and experiments [37], [47], with the objective of minimizing energy use, but not for providing secondary frequency control services.

8.1.1 Contributions of this chapter

This chapter presents a hierarchical control scheme for the control of a typical building HVAC system for providing secondary frequency control service to the grid.

The proposed scheme separates the control of the building zones and the HVAC system. The problem is decoupled into three layers - local zone controllers, thermal flexibility controller, and electrical flexibility controller. The local building controllers are at the lowest level and track the temperature setpoints received from the thermal flexibility controller. The thermal flexibility controller maximizes the flexibility in the thermal consumption of the building zones, and abstracts out all the information required at the higher control layer. At the highest level, the electrical flexibility controller uses the thermal flexibility and controls the HVAC system to provide flexibility to the grid.

The two flexibility control layers are based on robust optimization methods. The thermal flexibility problem is formulated as a convex robust optimization problem and is approximated using linear decision rule policy, while the electrical flexibility problem is formulated as a non-convex robust optimization problem and is approximated using two-stage robust programming.

A control-oriented model of a typical HVAC system is developed, and simulations are carried out to demonstrate the efficacy of the proposed approach.

8.1.2 Structure of this chapter

The rest of the chapter is structured as follows. The problem of ancillary service provision is recalled briefly in Section 8.2. The concept of the proposed hierarchical control is introduced in Section 8.3. Section 8.4 presents the considered building thermodynamics model, and the developed control-oriented model of a typical HVAC system. The three levels of the hierarchical control scheme are detailed in Section 8.5. Simulation results are presented in Section 8.6, and conclusions are drawn in Section 8.7.

Notation: Bold letters denote sequence of vectors over time, the length of which is clear from context, e.g., $\mathbf{e} = [e_0^T, e_1^T, ..., e_{N-1}^T]^T$.

8.2 Ancillary Services

This section recalls the preliminaries of ancillary service provision by loads.

As discussed in Section 5.1.1, ancillary services are required by the grid to maintain safe operation and are procured from ancillary service providers (ASP's) - which can either be energy producers or consumers. The ASP's are paid in exchange for providing this service.

Ancillary services can be divided into various categories [88], [106], and frequency control is one of them. Frequency control is further divided into primary, secondary, and tertiary services based on the time scales, as described in Section 5.1.1. This chapter focuses on the control of building HVAC systems for the provision of secondary frequency control service, and is based on Swiss regulations.

As discussed in Chapter 5, the basic idea of secondary frequency control for loads is to modify the electric power consumption according to the requirements of the grid. In real-time operation the grid sends the regulation signal which indicates the desired change in consumption. The loads are required to increase or decrease their consumption proportional to the power capacity which the loads agree in advance. The reward of this service is a payment proportional to this capacity. The change in consumption is with respect to a pre-specified baseline power over the regulation period.

The control challenge is divided into two phases - bidding and online operation. The bidding phase is at the beginning of the regulation period and at this point the building needs to specify a baseline power and an offered capacity over the regulation period. During online operation the building is required to track the received regulation signal (in proportion to the declared capacity) with the difference of its consumption compared to the declared baseline.

8.3 Hierarchical Control Architecture

This section introduces the proposed hierarchical control architecture for providing secondary frequency control service to the grid. The objective of the control scheme is to maximize the flexibility of the building which can be provided as secondary frequency control service to the grid, while maintaining occupant comfort.

Remark 14. *Note that it is trivial to extend the proposed control method to optimize the exact economic objective using the cost function explained in Chapter 6, but since the focus is to demonstrate the control method, a relatively simple objective of maximizing the flexibility is considered in this Chapter.*

The proposed scheme separates the control of the building zones and the HVAC system. Similar separation also exist in the standard supervisory control architecture for building control [115], [116], where local controllers control the lower level equipment while the higher level supervisory controllers optimize the system efficiency and generates setpoints for the local controllers. The proposed control scheme has two phases - bidding/offline, and online. The offline, and online phase is illustrated in Figure 8.1, and 8.2, respectively, and the associated symbols are defined in Table 8.1. The proposed control has three levels - local building controllers, thermal flexibility controller, and electrical flexibility controller. The individual control layers are briefly explained next.

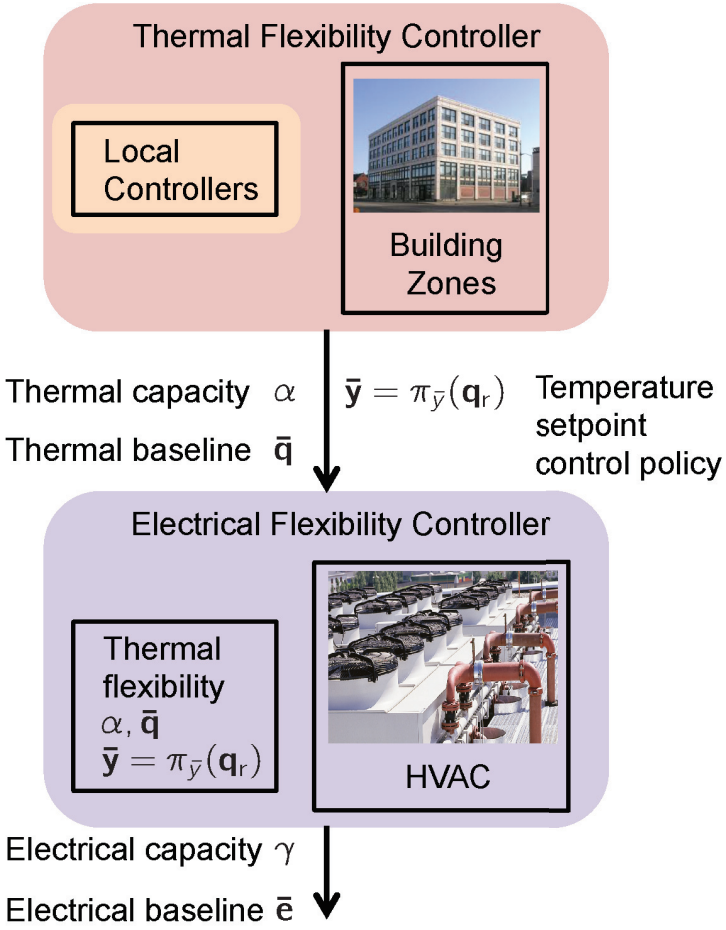

Figure 8.1 – Hierarchical Control Architecture: Bidding/Offline phase. See Table 8.1 for Symbol definition.

Symbol	Description
$\mathbf{a}$	Regulation (AGC) signal
γ	Electrical capacity
$\bar{\mathbf{e}}$	Electrical baseline power consumption
κ	HVAC control input
$\mathbf{q}_r$	Reference thermal power
α	Thermal capacity
$\bar{\mathbf{q}}$	Thermal baseline power consumption
$\bar{\mathbf{y}}$	Zone temperature setpoints
$\mathbf{q}$	Total thermal power transferred from the HVAC system to the building zones
u	Thermal power consumption of building zones
$\mathbf{y}$	Building zone temperatures

Table 8.1 – Hierarchical control architecture terminology.

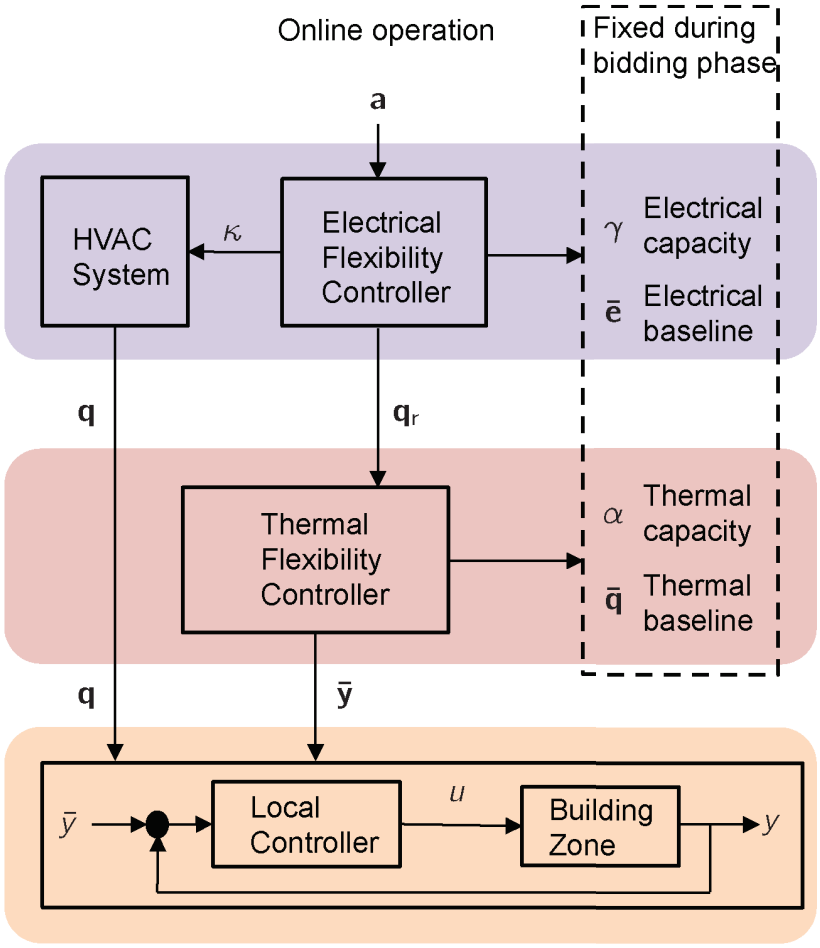

Figure 8.2 – Hierarchical Control Architecture: Online operation phase. See Table 8.1 for Symbol definition.

8.3.1 Local Controllers

The local building zone controllers are single-input-single-output (SISO) PI controllers for each controlled zone of the building, as show in Figure 8.2. The input of the controller is the temperature setpoint $\bar{y}$, and the output is the thermal power u which is required by the zone to achieve the setpoint. The total thermal power q required by all the zones come from the HVAC system, and is the sum of u's, as shown in Figure 8.2. A closed-loop dynamic model is obtained for the building zones with the local controllers in the loop. The input of this model is the temperature setpoint $\bar{y}$ in each zone, while the output is the total thermal power consumed q.

8.3.2 Thermal Flexibility Controller

The thermal flexibility controller uses the closed-loop dynamic model and characterize the available flexibility in the thermal consumption $\mathbf{q}$ of the building zones. This controller serves as an intermediate layer between the building thermodynamics and the HVAC system. It abstracts out all the information of the building zones required at the higher control level. The thermal flexibility controller has a bidding phase at the beginning of the regulation period and an online phase. During the bidding phase, it computes the baseline trajectory of thermal power over the regulation period $\bar{\mathbf{q}}$, and the thermal capacity α, which are fixed for the entire regulation period. The α and $\bar{\mathbf{q}}$ define the thermal flexibility of the building zones and are passed on to the electrical flexibility controller during the offline phase, as shown in Figure 8.1. The capacity α is a scaling of a reference thermal power trajectory $\mathbf{q}_\mathrm{r}$ (defined formally in Section 8.5.2). The total thermal power consumed by the zones is given by

$$\mathbf{q} = \bar{\mathbf{q}} + \alpha \mathbf{q}_r \tag{8.1}$$

Once $\bar{\mathbf{q}}$ and α are fixed, varying $\mathbf{q}_r$ during the on-line phase determines $\mathbf{q}$. The thermal flexibility controller also optimizes to compute a control policy of temperature setpoints as a function of reference thermal power, $\bar{\mathbf{y}} = \pi_{\bar{y}}(\mathbf{q}_\mathrm{r})$, such that the total thermal consumption is as defined by (8.1). This control policy is then used during the online phase to generate the temperature setpoints for the local zone controllers. As shown in Figure 8.2, the thermal flexibility controller receives a value of q_r from the higher control layer, and it generates $\bar{y}$ for the local zone controllers.

8.3.3 Electrical Flexibility Controller

The electrical flexibility controller uses the flexibility of the zones (defined by the thermal flexibility controller) and controls the HVAC system to maximize the electrical flexibility provided to the grid. It also has a bidding phase and an online operation mode. During the bidding phase, it receives the thermal flexibility characterization from the thermal flexibility

controller and computes an electrical baseline $\bar{\mathbf{e}}$, and capacity γ, as shown in Figure 8.1. The capacity γ is a scaling of the normalized AGC signal $\mathbf{a}$ received from the grid. During online operation, the controller tracks the scaled regulation signal with the difference of the chiller consumption and the baseline

$$\|\mathbf{e}_{\text{ch}} - \bar{\mathbf{e}} - \gamma\mathbf{a}\|_\infty \leq m_e \tag{8.2}$$

where $\mathbf{e}_{\text{ch}}$ is the electrical consumption of the chiller, and m_e is the allowed tracking error. It does so by utilizing the flexibility of the thermal zones and the HVAC system by choosing a suitable reference thermal power $\mathbf{q}_{\text{r}}$ and a corresponding feasible HVAC input κ.

Details of the control methodology are given in Section 8.5.

Remark 15. *Note that one of the advantages of the proposed scheme is the separation between the control of the building zones and the HVAC system. The building thermodynamics are usually linear, and therefore, the thermal flexibility problem can be formulated as a convex optimization problem. On the other hand, the HVAC system dynamics are often non-linear resulting in a non-convex optimization problem to characterize electrical flexibility. The advantage of the proposed scheme is that the number of the building zones affect only the size of the convex problem. The size of the resulting non-convex optimization problem stays the same. Therefore, the method scales better with the increase in the number of the building zones than if the problem was formulated as a single non-convex problem.*

8.4 Modeling

This section presents the building thermodynamics and the HVAC system models.

8.4.1 Building Thermodynamics

The building thermodynamics model is constructed from a high fidelity EnergyPlus model using the MATLAB toolbox OpenBuild [8], described in Chapter 3. The toolbox extracts all the relevant data from the EnergyPlus model and constructs a linear continuous-time state-space model of building thermodynamics. The continuous-time model is reduced using a standard Hankel-Norm based model reduction method and is discretized to obtain a model of the following form

$$\begin{aligned} \bar{x}_{i+1} &= \bar{A}\bar{x}_i + \bar{B}_u u_i + \bar{B}_d d_i \\ y_i &= \bar{C}\bar{x}_i \end{aligned} \tag{8.3}$$

where $\bar{x}_i \in \mathbb{R}^n$ is the state, $u_i \in \mathbb{R}^m$ is the thermal power input to each zone of the building, $d_i \in \mathbb{R}^p$ is the disturbance input (weather, and internal gains), and $y_i \in \mathbb{R}^q$ is the temperature in each zone at time step i.

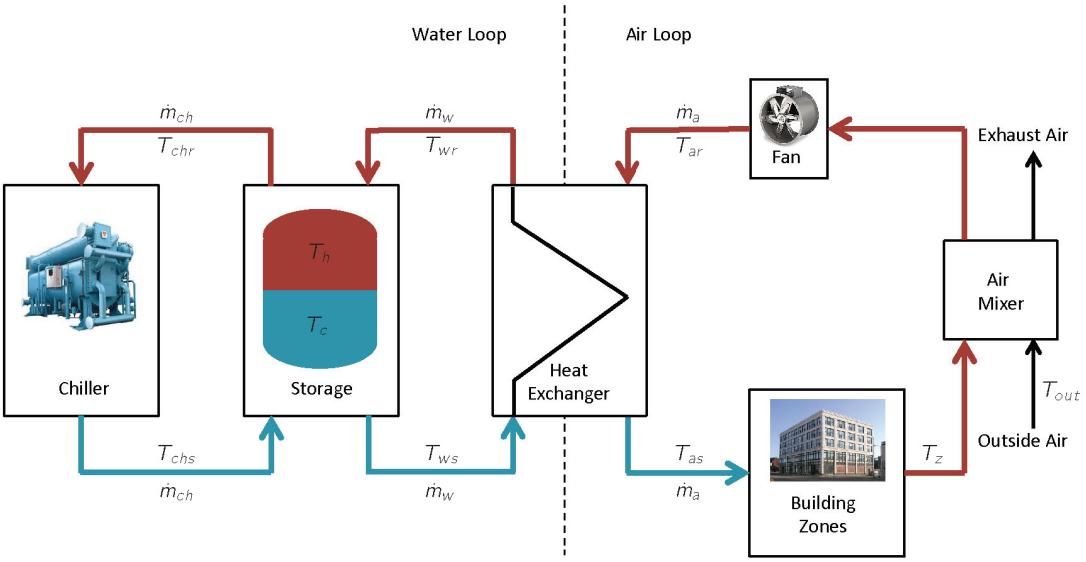

Figure 8.3 – HVAC Schematic

8.4.2 Heating Ventilation and Air-Conditioning System

Various different types of HVAC systems exist in different office buildings. The differences are usually based on the building size, geographical location, construction type, etc. However, forced air based HVAC systems are common in most modern large office buildings, and therefore, are considered here. The components of a typical air based HVAC system are presented and a control-oriented model is developed. The HVAC components in any particular building may differ but the fundamentals are similar, and the presented hierarchical control strategy can therefore be extended to any particular case. Note that without loss of generality, the description in this Section is for the operation of the HVAC system in the cooling (summer) season. Similar methodology can be used to obtain a similar model for the heating (winter) season.

The schematic of the HVAC system and the thermal storage considered in this paper is shown in Figure 8.3. The system consists of a water loop and an air loop. In Figure 8.3, blue arrows show the flow direction of the chilled water (or air), while red arrows show the flow direction of the warm water (or air). The chiller is the most electric energy consuming component in the HVAC system and produces the thermal energy to cool the water in the water loop. Chilled water is stored in the stratified thermal energy storage tank, from which it goes to the heat exchanger. In the heat exchanger, the thermal energy is transferred from the water loop to the air loop. The warm water coming out of the heat exchanger is stored back in the tank before it goes back to the chiller. In the air loop, the air coming from the building zones is mixed with outside fresh air, and is passed through the heat exchanger where it is cooled and is used to regulate the zone temperatures.

The goal is to develop a model that can be used as a prediction model in optimization based control schemes. The following simplifying assumptions are made:

Assumption 1. *Lower level HVAC controllers operate the chiller, pumps and fans to achieve the desired supply temperatures and mass-flow rates in the water, and air loops. The lower-level controllers are assumed to be fast enough and no tracking errors are considered. Therefore, steady-state dynamics are considered and all transients are neglected.*

Assumption 2. *The water supply pipes in the water loop and the air ducts in the air loop are loss-less and their dynamics are neglected.*

Assumption 3. *The water in the storage tank is subject to minor mixing and is modeled as a stratified system with layers of warm water at the top and cold water at the bottom. The water layers are lumped together into warm and cold water at temperatures T_h and T_c, respectively.*

Remark 16. *The Assumption 1 is reasonable because the sampling time of the lower level HVAC controllers is usually faster than the optimal control layer. The losses in the water pipes and air ducts are usually very small and therefore Assumption 2 is reasonable to reduce the modelling complexity. Note that similar simplifying modelling assumptions have been used in literature [47], [117], [118] and Assumption 3 has also been experimentally tested to be reasonable [37], [47].*

A simplified yet descriptive mathematical model of the HVAC system components is presented next.

Chiller

The chiller consumes electricity and produces the thermal energy required to cool the building. The thermal power produced by the chiller is given by

$$\mathbf{q}_{\text{ch}} = c_{water}\dot{\mathbf{m}}_{\text{ch}}^{T}(\mathbf{T}_{\text{chr}} - \mathbf{T}_{\text{chs}}) \tag{8.4}$$

where $\dot{m}_{ch}$ is the mass flow rate of the water passing through the chiller, c_{water} is the specific heat capacity of water, T_{chr} is the temperature of warm water returning to the chiller from the thermal storage, and T_{chs} is the temperature of the cold water supplied by the chiller. The electrical consumption of the chiller at time step i is given by

$$e_{ch,i} = \frac{q_{ch,i}}{COP_i} \tag{8.5}$$

where COP_i is the coefficient of performance of the chiller at time step i, and is defined as the ratio of the thermal power produced to the electrical power consumed. The COP is also a function of the outside temperature T_{out}, and the chiller supply temperature T_{chs},

and is given as

$$COP_i = \eta \frac{T_{chs,i}}{T_{out,i} - T_{chs,i}} \tag{8.6}$$

where η is the efficiency of the chiller.

Heat Exchanger

Thermal energy is transferred from the water loop to air loop in the heat exchanger. The thermal energy in warm air coming into the heat exchanger is transferred to chilled water, producing cold air, and warm water at the exit of the heat exchanger. Thermal power gained by the water is given as

$$\mathbf{q}_{\mathrm{w}} = c_{water} \dot{\mathbf{m}}_{\mathrm{w}}^{T} (\mathbf{T}_{\mathrm{wr}} - \mathbf{T}_{\mathrm{ws}}) \tag{8.7}$$

where $\dot{m}_w$ is the mass flow rate of the water passing through the heat exchanger, T_{ws} is the temperature of the chilled water supplied to heat exchanger, and T_{wr} is the temperature of the warm water returning from the heat exchanger to storage. Thermal power lost by air in the heat exchanger is given as

$$\mathbf{q}_{\mathrm{a}} = c_{air} \dot{\mathbf{m}}_{\mathrm{a}}^{T} (\mathbf{T}_{\mathrm{ar}} - \mathbf{T}_{\mathrm{as}}) \tag{8.8}$$

where $\dot{m}_a$ is the mass flow rate of the air passing through the heat exchanger, c_{air} is the specific heat capacity of the air, T_{ar} is the temperature of the air returning (coming from air mixer) to the heat exchanger, and T_{as} is the temperature of the chilled air supplied to the zones.

By the law of conservation of energy, the thermal power gained by the water is equal to the power lost by air. Power exchanged in the heat exchanger is also a function of the temperature difference between the water and the air, and is approximated by

$$\mathbf{q}_{\mathrm{HE}} = \mu^{T} (\mathbf{T}_{\mathrm{as}} - \mathbf{T}_{\mathrm{wr}}) \tag{8.9}$$

where μ is the average heat exchange coefficient of the heat exchanger.

Fan

The mass flow rate of the air $\dot{m}_a$ passing through the heat exchanger is regulated by the electric fan in the air loop. The electricity consumption of the fan is smaller than the chiller and is neglected.

Air Mixer

To maintain indoor air quality and carbon dioxide levels, the return air from the building zones is mixed with outside fresh air before being used for cooling the zones. Air mixer mixes a fixed ratio β of fresh air in the volume of air passing through it. The same amount of air is also sent out as exhaust as the mass flow rate at the inlet and outlet of the mixer is the same. As a result, the temperature of the return air coming in to the heat exchanger T_{ar} is a convex combination of the temperature of the building zone and the outside air, and is given as

$$\mathbf{T}_{\text{ar}} = \beta \mathbf{T}_{\text{out}} + (1 - \beta)\mathbf{T}_{\text{z}} \tag{8.10}$$

where T_z is the average temperature of all the building zones.

Building Zones

The local zone controllers distribute the total mass flow rate of chilled air $\dot{m}_a$ to meet the thermal requirement of each zone. The total thermal power required by the building zones to meet the temperature setpoints is approximated by

$$\mathbf{q} = c_{air}\dot{\mathbf{m}}_{\text{a}}(\mathbf{T}_{\text{z}} - \mathbf{T}_{\text{as}}) \tag{8.11}$$

Storage

According to Assumption 3, two layers of water are assumed in the storage - cold water at temperature T_c, and warm water at temperature T_h. The storage is a part of a closed hydraulic loop which means that the total mass flow rate of water entering and exiting is equal. Therefore, the total height h of the water in the storage is constant, and is equal to the sum of the heights of the cold (h_c) and warm (h_h) layer

$$h = h_c + h_h \tag{8.12}$$

Storage dynamics are defined by three states, the height h_c and temperature T_c of the cold water, and the temperature T_h of the warm water and are governed by the laws of conservation of mass and energy.

The increase in height of the cold water is a function of the mass flow rate of the chilled water entering the storage and is given by

$$\Delta h_{c,i} = \lambda \dot{m}_{ch,i} \tag{8.13}$$

where λ is a constant of storage parameters which convert the mass flow rate to the storage

height and is defined as

$$\lambda = \frac{\delta t}{\rho \pi r^2} \tag{8.14}$$

where δt is the discretization time step in seconds, ρ is the density of water, and r is the radius of the storage tank. Similarly, the increase in height of the warm water is given by

$$\Delta h_{h,i} = \lambda \dot{m}_{w,i} \tag{8.15}$$

The height of the cold water is updated at each time step by the net difference in the mass flow rate of the chilled water entering ($\dot{m}_{ch}$) and exiting ($\dot{m}_{w}$) the storage and is given by

$$h_{c,i+1} = h_{c,i} + \Delta h_{c,i} - \Delta h_{h,i} \tag{8.16}$$

It is assumed that the cold, and the warm water exiting the storage is at the temperature of the cold and the warm water layers, T_c, and T_h, respectively. It is also assumed that the cold water entering the storage is at a temperature T_{chs}, and it mixes uniformly with the rest of the cold water at a temperature T_c. With these assumptions, the temperature T_c is updated at each time step according to the law of conservation of energy, and is given by

$$T_{c,i+1} = \frac{(h_{c,i} - \Delta h_{h,i}) T_{c,i} + \Delta h_{c,i} T_{chs,i}}{h_{c,i+1}} \tag{8.17}$$

and similarly, the warm water temperature is updated as

$$T_{h,i+1} = \frac{(h_{h,i} - \Delta h_{c,i}) T_{h,i} + \Delta h_{h,i} T_{wr,i}}{h_{h,i+1}} \tag{8.18}$$

8.4.3 Feasible Set of HVAC control inputs

The states of the HVAC system are defined by

$$\theta := [\mathbf{h}_\mathrm{c}{}^T, \mathbf{T}_\mathrm{c}{}^T, \mathbf{T}_\mathrm{h}{}^T]^T$$

and the control inputs by

$$\kappa := [\dot{\mathbf{m}}_\mathrm{ch}^T, \dot{\mathbf{m}}_\mathrm{w}^T, \dot{\mathbf{m}}_\mathrm{a}^T, \mathbf{T}_\mathrm{chs}{}^T]^T$$

The set of feasible control inputs and the total thermal power consumed by the building zones is defined as the set of all the trajectories of the HVAC control inputs and building

power over the horizon, such that the operational constraints are respected, and is given as

$$\mathcal{H}(\theta, \mathbf{T}_\mathsf{z}) = \left\{ \kappa, \mathbf{q} \;\middle|\; \begin{array}{l} (8.4), (8.5), (8.6), (8.7), (8.8), (8.9), \\ (8.10), (8.11), (8.12), (8.16), (8.17), (8.18) \\ \mathbf{q}_\mathsf{HE} = \mathbf{q}_\mathsf{w} = \mathbf{q}_\mathsf{a} \\ \mathbf{T}_\mathsf{ws} = \mathbf{T}_\mathsf{c}, \qquad \mathbf{T}_\mathsf{chr} = \mathbf{T}_\mathsf{h} \\ \mathbf{T}_\mathsf{chs} \in \mathcal{T}_{chs}, \mathbf{T}_\mathsf{as} \in \mathcal{T}_{as} \\ \dot{\mathbf{m}}_\mathsf{w} \in \mathcal{M}_w, \dot{\mathbf{m}}_\mathsf{a} \in \mathcal{M}_a, \dot{\mathbf{m}}_\mathsf{ch} \in \mathcal{M}_{ch} \\ \mathbf{e}_\mathsf{ch} \geq 0 \\ \theta_0 = \theta, \qquad \forall i = 0, ..., N-1. \end{array} \right\} \tag{8.19}$$

where N is the horizon length, $\mathcal{T}_{chs}, \mathcal{T}_{as}$ are the sets defining the operational constraints on supply temperatures, and $\mathcal{M}_w, \mathcal{M}_a, \mathcal{M}_{ch}$ are the sets defining the physical constraints on the mass flow rates. Note that the set $\mathcal{H}$ is a function of the HVAC initial state θ_0 and the average temperature of the building zones $\mathbf{T}_\mathsf{z}$ over the horizon.

8.5 Control Scheme

This section presents the proposed control scheme.

8.5.1 Local Controllers

The objective of the local building controller is to track the temperature setpoint $\bar{y}$ in each zone, given by the user, or in this case by a higher level controller. The local controller considered here is a single-input-single-output (SISO) PI controller for each zone, and can be written as

$$\begin{aligned} u_i &= K_p(y_i - \bar{y}_i) + K_i(y_i - \bar{y}_i) + x_{PI,i} \\ x_{PI,i+1} &= K_i(y_i - \bar{y}_i) + x_{PI,i} \end{aligned} \tag{8.20}$$

where $K_p \in \mathbb{R}^m \times \mathbb{R}^q$ is the diagonal matrix representing the proportional gain, $K_i \in \mathbb{R}^m \times \mathbb{R}^q$ is the diagonal matrix representing the integral gain, and $x_{PI} \in \mathbb{R}^m$ is the additional state for the integral controller.

Closed-loop Dynamics

Using the thermodynamic model (8.3), and the feedback from the local controller (8.20), it is straight forward to write the closed-loop dynamics

$$\begin{aligned} x_{i+1} &= Ax_i + B_u\bar{y}_i + B_d d_i \\ q_i &= Cx_i + D\bar{y}_i \end{aligned} \tag{8.21}$$

using the augmented state $x_i = \begin{bmatrix} \bar{x}_i^T, & x_{PI,i}^T \end{bmatrix}^T$, where the input $\bar{y}_i \in \mathbb{R}^q$ is the temperature setpoint in each zone, and the output $q_i \in \mathbb{R}$ is the total thermal power consumed by the building at time step i. Note that $\bar{x}_i$ is the state of the thermodynamic model (8.3), and $x_{PI,i}$ is the additional state for the integral action.

Remark 17. *Note that the local controllers used in practice are usually SISO PI controllers designed individually for each zone as explained in [37]. One of the reasons it is reasonable to decouple the zone controllers is because usually the coupling between building zones is very weak. Note also that the presented hierarchical control scheme works also for different types of local controllers. The thermal and electrical flexibility controllers explained in Section 8.5.2, and 8.5.3 use only the description of the closed-loop model* (8.21) *where the inputs are the zone temperature setpoints and the output is the total thermal power required by the building zones. This model can also be obtained using system identification techniques [64], [68], [63] with any type of local controllers in the loop.*

Feasible Set of Local Control Inputs

The set of feasible setpoints and thermal power is defined as the set of all the trajectories of the setpoints to the local building controller and the corresponding total thermal power consumed by the building while the operational constraints are satisfied, and is given as

$$\mathcal{Q}(x, \mathbf{d}) = \left\{ \bar{\mathbf{y}}, \mathbf{q} \;\middle|\; \begin{array}{ll} x_{i+1} = Ax_i + B_u \bar{y}_i + B_d d_i & \\ q_i = Cx_i + D\bar{y}_i & \\ \bar{y}_i \in \mathcal{Y} & \\ x_0 = x, \qquad & \forall i = 0, ..., N-1. \end{array} \right\} \tag{8.22}$$

where the set $\mathcal{Y}$ defines the range of temperature setpoints according to comfort requirements. Note that the set $\mathcal{Q}$ is a function of the initial state x_0 of the closed loop system, and the weather disturbance $\mathbf{d}$ over the horizon.

8.5.2 Thermal Flexibility Controller

The goal of the thermal flexibility controller is to characterize the largest possible set of thermal power trajectories that can be tracked by the output of the closed loop system (8.21). The set Ξ_t defines the shape of the the thermal flexibility of the building. We are interested in the baseline thermal consumption $\bar{\mathbf{q}}$ over the horizon, and a scaling α of the set Ξ_t around the baseline, such that for any given reference thermal trajectory $\mathbf{q}_r$ in Ξ_t, a feasible setpoint input $\bar{\mathbf{y}}$ exists for the local controller that enables the thermal power consumption of the building $\mathbf{q}$ to track the sum of the baseline and the scaled reference thermal trajectory. This controller has two phases - bidding and on-line operation. During the bidding phase, the baseline thermal power $\bar{\mathbf{q}}$ and the scaling α of the set Ξ_t are optimized at the beginning of the regulation period, and its solution is passed on to the

electrical flexibility controller. During on-line phase, the electrical flexibility controller sends a reference thermal power q_r, which the thermal flexibility controller is required to track by generating an appropriate temperature setpoint for the local controllers.

Bidding Phase

The problem of thermal flexibility characterization is formulated as follows

$$\begin{array}{lll} \underset{\alpha,\bar{\mathbf{q}},\pi_{\bar{y}}}{\text{maximize}} & \alpha & \\ \text{s.t.} & (\bar{\mathbf{y}},\mathbf{q}) \in \mathcal{Q}(x,\mathbf{d}) & \\ & \bar{\mathbf{y}} = \pi_{\bar{y}}(\mathbf{q}_r) & \\ & \mathbf{q} = \bar{\mathbf{q}} + \alpha \mathbf{q}_r, \qquad & \forall \mathbf{q}_r \in \Xi_t \end{array} \tag{8.23}$$

where the decision variables are the thermal flexibility α, the baseline thermal power trajectory $\bar{\mathbf{q}}$, and the control policy $\pi_{\bar{y}}$, while the initial state of the system x, and the weather disturbance prediction over the horizon $\mathbf{d}$ are the problem data. The objective is to maximize the scaling α of the set Ξ_t.

During real-time operation, the reference signal $\mathbf{q}_r$ is revealed progressively and it is possible to adjust the control action $\bar{\mathbf{y}}$ accordingly, therefore the optimization is not over the control inputs but over the control policy $\bar{\mathbf{y}} = \pi_{\bar{y}}(\mathbf{q}_r)$. The constraints are required to be satisfied for all $\mathbf{q}_r$ in the set Ξ_t, therefore (8.23) is a multistage robust optimization problem. α and $\bar{\mathbf{q}}$ are the first stage variables while the rest are the subsequent stage variables.

Next, the uncertain set Ξ_t (defining the shape of the thermal flexibility), and a parameterization of the control policy $\pi_{\bar{y}}$ are defined which are needed to solve the robust optimization problem (8.23).

Thermal Uncertainty Set

The thermal uncertainty set Ξ_t defines the shape of the building's thermal flexibility and is defined as a N-dimensional box over the horizon, i.e., $\Xi_t := \left\{ \mathbf{q}_r \;\middle|\; -1 \leq \mathbf{q}_r \leq 1 \right\}$. The choice of the set Ξ_t defines the complexity of the resulting optimization problem. The box set is a good choice to allow the reference thermal trajectory to take any shape around the baseline. Furthermore, this relatively simple set also has computational advantages. See [79] for a discussion on handling similar optimization problems with more complicated sets. The thermal flexibility α is the scaling of the set Ξ_t.

Control Policy

The robust optimization problem (8.23) is an infinite dimensional problem because of the control policy $\pi_{\bar{y}}$, and thus is intractable in its exact form. Therefore, a tractable parameterization of the control policy is required to restrict the problem to the finite dimensional space. The following linear decision rule policy [119] is used, which has widely been used in literature and has nice computational properties

$$\bar{y}_i = \sum_{j=0}^{i} M_{i,j} q_{r,j} + v_i \tag{8.24}$$

and can be written in vectorized form as $\bar{\mathbf{y}} = \mathbf{M}\mathbf{q}_\mathrm{r} + \mathbf{v}$, where $M_{i,j}$ and v_i define the control policy, and are additional decision variables. The policy is required to be causal, i.e., the control action $\bar{y}_i$ can depend on the reference thermal power $q_{r,i}$ only up to time step i. This is achieved by imposing causality constraints on $\mathbf{M}$, i.e., $M_{i,j} = 0$ for $j > i$.

Robust Solution

With the set Ξ_t and the control policy defined, the robust optimization problem (8.23) can be formulated as a linear program using duality techniques discussed in [120], [121], [79] and summarized in Appendix C. The result of problem (8.23) is an optimal thermal flexibility α^*, baseline thermal power $\bar{\mathbf{q}}^*$, and the policy of temperature setpoints ($\bar{y} = \mathbf{M}^*\mathbf{q}_\mathrm{r} + \mathbf{v}^*$) for the local building controllers to track a scaled version of any reference thermal power trajectory $\mathbf{q}_\mathrm{r}$ in the set Ξ_t.

On-line Operation

During the on-line operation phase, the thermal flexibility controller generates the temperature setpoints for the local controllers, such that the total thermal power consumption of the building $\mathbf{q}$ is equal to the sum of the baseline $\bar{\mathbf{q}}^*$ and the scaled version of the reference thermal trajectory $\mathbf{q}_\mathrm{r}$ received from the electrical flexibility controller. This can be achieved either by using the control policy ($\mathbf{M}^*$ and $\mathbf{v}^*$) optimized during the bidding phase, or by re-optimizing the control policy by re-solving, at each time step, problem (8.23) with fixed γ^*, $\bar{\mathbf{q}}^*$, and Ξ_t.

8.5.3 Electrical Flexibility Controller

The goal of the electrical flexibility controller is to operate the building HVAC system to maximize the electrical flexibility that can be provided to the grid, while maintaining occupant comfort and operational constraints. It uses the thermal flexibility of the storage, and the building (defined in Section 8.5.2). This controller has two phases - bidding,

and on-line operation. During the bidding phase, a problem is solved every day at the beginning of the regulation period. The controller bids a capacity γ and the electrical baseline consumption $\bar{\mathbf{e}}$ over the regulation period. During on-line operation, the controller tracks, within some error bounds, the regulation signal received from the grid.

Bidding Phase

The electrical flexibility bidding problem is formulated as

$$\begin{array}{ll} \underset{\gamma,\bar{\mathbf{e}},\pi_\kappa,\pi_{q_r}}{\text{maximize}} & \gamma \\ \text{s.t.} & (\pi_\kappa(\mathbf{a}),\mathbf{q}) \in \mathcal{H}(\theta,\mathbf{T}_z) \\ & \mathbf{q} = \bar{\mathbf{q}}^* + \alpha^* \pi_{q_r}(\mathbf{a}) \\ & \pi_{q_r}(\mathbf{a}) \in \Xi_t \\ & \|\mathbf{e}_{\text{ch}} - \bar{\mathbf{e}} - \gamma\mathbf{a}\|_\infty \leq m_e, \qquad \forall \mathbf{a} \in \Xi_e \end{array} \tag{8.25}$$

where the decision variables are the electrical flexibility γ, the baseline $\bar{\mathbf{e}}$, the control policy π_{q_r} defining the reference thermal power, and the control policy π_κ defining the HVAC control input. m_e is the maximum allowed error for tracking the regulation signal and is a constant, while $\mathbf{a}$ is the normalized AGC signal received progressively from the grid and is unknown at the time of decision. The objective is to maximize the electrical flexibility γ. The constraints include the HVAC operational constraints, thermal flexibility constraint, feasibility of reference thermal power constraint, and the regulation signal tracking constraint. The thermal flexibility is defined by α^*, $\bar{\mathbf{q}}^*$, and Ξ_t and is fixed for this problem (as provided by the thermal flexibility controller).

During on-line operation, the regulation signal is revealed progressively and it is possible to adjust the control action κ, and $\mathbf{q}_\text{r}$ accordingly, therefore the optimization is not over the control inputs but over the control policy $\kappa = \pi_\kappa(\mathbf{a})$, and $\mathbf{q}_\text{r} = \pi_{q_r}(\mathbf{a})$, respectively. The regulation signal is assumed to lie in the set Ξ_e therefore, (8.25) is a multi-stage robust non-convex optimization problem. The first stage variables are the electrical flexibility γ, and the baseline $\bar{\mathbf{e}}$, while the rest are the subsequent stage decision variables.

Next, an approximation of the average building zones temperature $\mathbf{T}_z$ is defined which is needed to solve the electrical flexibility bidding problem.

Average building zones temperature

Building zones temperature is used by the local building controllers for temperature regulation, and is not available at the level of the electrical flexibility controller. Therefore, it is assumed that the zone temperatures are equal to the temperature setpoints given as input to the local controllers. With this assumption the average building zone temperature, at time step i, is given by $T_{z,i} = \frac{1}{p}\mathbf{1}^\top \bar{y}_i$, where $\mathbf{1}$ is a vector of ones of appropriate size and p is the total

number of zones. Using the linear decision rule policy defined in (8.24), the average zones temperature can be expressed in terms of q_r as

$$T_{z,i} = \frac{1}{p}\mathbf{1}^{\top}[\sum_{j=0}^{i} M_{i,j}q_{r,j} + v_i] \tag{8.26}$$

and can be written in the vectorized form as $\mathbf{T}_z = \Gamma(\mathbf{M}\mathbf{q}_r + \mathbf{v})$, where $\Gamma := \frac{1}{p}I_N \otimes \mathbf{1}^T$, with I_N an identity matrix of size N, and $\otimes$ is the Kronecker product.

Robust Solution

The electrical flexibility problem (8.25) is intractable in its exact form because of its non-convex multi-stage structure. To approximate (8.25), the multi-stage structure of the problem is reduced to two stages, and the causality requirements are relaxed. The first stage variables are the capacity γ, and the baseline $\bar{\mathbf{e}}$ which are decided before the realization of the uncertain parameter $\mathbf{a}$, while the rest are the second stage variables and can be adjusted after the realization of the uncertain parameter. The uncertainty set characterization required to solve the resulting two-stage robust optimization problem is presented next.

Uncertainty Set

The uncertainty set of the regulation signal is constructed as the convex hull of a finite number N_s of past observed regulation signals and is given as

$$\Xi_e = \left\{ \sum_{j=1}^{N_s} \lambda^j \mathbf{a}^j \mid \sum_j \lambda^j = 1, \lambda^j \geq 0 \right\} \tag{8.27}$$

where $\mathbf{a}^j$ are the previously observed AGC signal scenarios. The idea behind this data based uncertainty set is that if the controller is robust to past observed regulation signals, it should also perform well for an unknown, but similar, future regulation signal due to consistency of regulation signals over time.

Approximate Solution Method

The resulting two-stage robust optimization problem can be re-formulated into a tractable non-convex optimization problem using the definition of the average zone temperature

(8.26) and the set Ξ_e (8.27), and is given by

$$\begin{aligned} \underset{\gamma,\bar{\mathbf{e}}}{\text{maximize}} \quad & \gamma \\ \text{s.t.} \quad & (\kappa^j, \mathbf{q}^j) \in \mathcal{H}(\theta, \mathbf{T}_z{}^j) \\ & \mathbf{T}_z{}^j = \Gamma(\mathbf{M}^* \mathbf{q}_r{}^j + \mathbf{v}^*) \\ & \mathbf{q}^j = \bar{\mathbf{q}}^* + \alpha^* \mathbf{q}_r^j \\ & -1 \leq \mathbf{q}_r^j \leq 1 \\ & \|\mathbf{e}_{\text{ch}}^j - \bar{\mathbf{e}} - \gamma \mathbf{a}^j\|_\infty \leq m_e, \qquad \forall j = 1, ..., N_s \end{aligned} \tag{8.28}$$

where the superscript j defines the second stage decision variables corresponding to the j^{th} scenario of the regulation signal, and N_s is the total number of scenarios. The solution of (8.28) gives the optimal electrical flexibility γ^* and baseline $\bar{\mathbf{e}}^*$ over the regulation period.

On-Line Operation

The electrical flexibility bidding problem (8.28) is solved once at the start of the regulation period. This results in γ^*, and $\bar{\mathbf{e}}^*$ which are fixed for the complete regulation period. During on-line operation phase, the building receives the regulation signal at each time step from the grid and is required to track it within fixed error bounds. During on-line operation a slightly modified version of (8.28) is solved at each time step, where the flexibility γ^* and baseline $\bar{\mathbf{e}}^*$ are already fixed and the problem horizon is shrunk at each time step. The first time step of the input and the state trajectories are first stage variables, while variables for the rest of the horizon are still second stage decision variables. The objective is to find a feasible control input for the HVAC system κ and the reference thermal power q_r, at each time step, while tracking the received regulation signal. The reference thermal power is transmitted to the thermal flexibility controller at each time step, which generates the appropriate setpoints for the local controllers.

8.6 Simulations and Results

This section presents the simulation results to demonstrate the effectiveness of the proposed control strategy.

8.6.1 Simulation Setup

The simulations are performed with an ASHRAE standard five zone office building model taken from the reference database of the U.S. department of Energy [55]. The weather data and typical usage pattern of occupancy, electrical equipment, and lighting etc. are provided with the model and are assumed to be perfectly forecast in simulations. The AGC signal is considered unknown at the time of solving the bidding problem. The length of

Building	
Floor Area (m^2)	511
No. of Zones	5
Peak Occupancy (people/$100m^2$)	5.4
HVAC	
Chiller supply temperature T_{chs}	5 - 8 °C
Air supply temperature T_{as}	14 - 18 °C
Storage height	4 m
Chiller efficiency η	0.2
Fresh air mixing ratio β	0.2
Average heat exchanger coefficient μ	4 $kW/$ °C
Comfort	
Comfort temperature limits	20 - 24 °C
Optimum comfort temperature T_{ideal}	22 °C

Table 8.2 – Simulation Parameters

the regulation period is considered to be one day. The historic AGC signal of Switzerland generated by Swissgrid (Swiss grid operator) is used to construct the daily regulation signal scenarios needed to build set Ξ_e in (8.27). The number of scenarios N_s used are 60, and are limited by the computational complexity of the resulting optimization problem. However, the validation results suggest that the number is representative of the underlying probability distribution. The simulation parameters are given in Table 8.2.

8.6.2 Computations

The simulations are performed in MATLAB. The thermal flexibility control problem (8.23) is reformulated as a linear program (as described in Section 8.5.2) and is formulated using the parsing tool YALMIP [111] and solved using the GUROBI solver [122]. The electrical flexibility problem (8.28) is a non-convex optimization problem and is formulated using the optimization tool Casadi [123], and solved using the IPOPT solver [124]. The problem horizon is 24 hours with sampling time of 15 minutes.

8.6.3 Optimal Chiller and fan operation

Traditionally, the objective of the HVAC system control has been to operate the chiller at the maximum possible COP. This is the right thing to do when the objective is to minimize the total energy use or cost of operation. A closer look at the COP dynamics (8.6) reveal that the maximum COP can be achieved by maintaining a constant chiller supply temperature T_{chs} at the highest allowed level. This implies that the COP will be a function of the outside temperature only. Moreover, the electrical consumption of the fan in the air-loop is proportional to the mass flow rate of the air $\dot{m}_a$. It is easy to see from

(8.11) that if the air supply temperature T_{as} is fixed at its minimum possible limit, then minimum amount of $\dot{m}_a$ is required to supply a certain thermal power to the building zones, minimizing the electrical consumption of the fan. Intuitively, it is clear that fixing the supply temperatures (chiller T_{chs} and air T_{as}) is the economically optimal way of operating the HVAC system. It is also verified by solving the minimum energy optimization problem at the level of the electrical flexibility controller.

Therefore, in the following the problem is solved with fixed as well and varying supply (chiller and air) temperatures to investigate the results when the objective is to maximize the flexibility that can be offered to the grid.

8.6.4 Electrical Flexibility

Fixed supply temperatures

The thermal and electrical flexibility problems are solved with fixed supply temperatures ($T_{chs} = 8\,^{\circ}\text{C}$, $T_{as} = 14\,^{\circ}\text{C}$), and the results are depicted in Figure 8.4. The building has a flexibility of $\pm$2.5kW in its thermal power requirement. The thermal power supplied by the water loop to the air loop is higher than the zones requirement because of the extra thermal energy needed to maintain minimum fresh air requirements. The actual thermal flexibility in the water loop gets scaled up (non-linearly - depending on outside temperature), and is further augmented with the flexibility of the thermal storage. The resulting electrical flexibility provided by the building is $\pm$6.1kW.

The thermal and electrical baselines and the power trajectories corresponding to each regulation signal scenario are shown in Figure 8.4. The variation in the height of the cold water layer in the storage, and the temperature of the cold and warm layers are also shown. The temperature of cold water layer in the storage is constant at $8\,^{\circ}\text{C}$ because of the constant chiller supply temperature. It can be seen in Figure 8.4 that the chiller COP stays at its maximum allowed limit, while it varies with time because of the variation in the outside temperature.

Varying supply temperatures

The thermal and electrical flexibility problems are re-solved for the same day with supply temperatures allowed to vary in a range ($T_{chs} = 5 - 8\,^{\circ}\text{C}$, $T_{as} = 14 - 18\,^{\circ}\text{C}$), and the results are depicted in Figure8.5. The possibility of varying the chiller supply temperature T_{chs} means that the controller can choose the chiller COP within a certain range. This implies that the controller can spend more or less electrical power to produce a certain thermal power. This provides extra flexibility on top of the flexibility from the building thermodynamics and the storage. In this case the building provides the same thermal

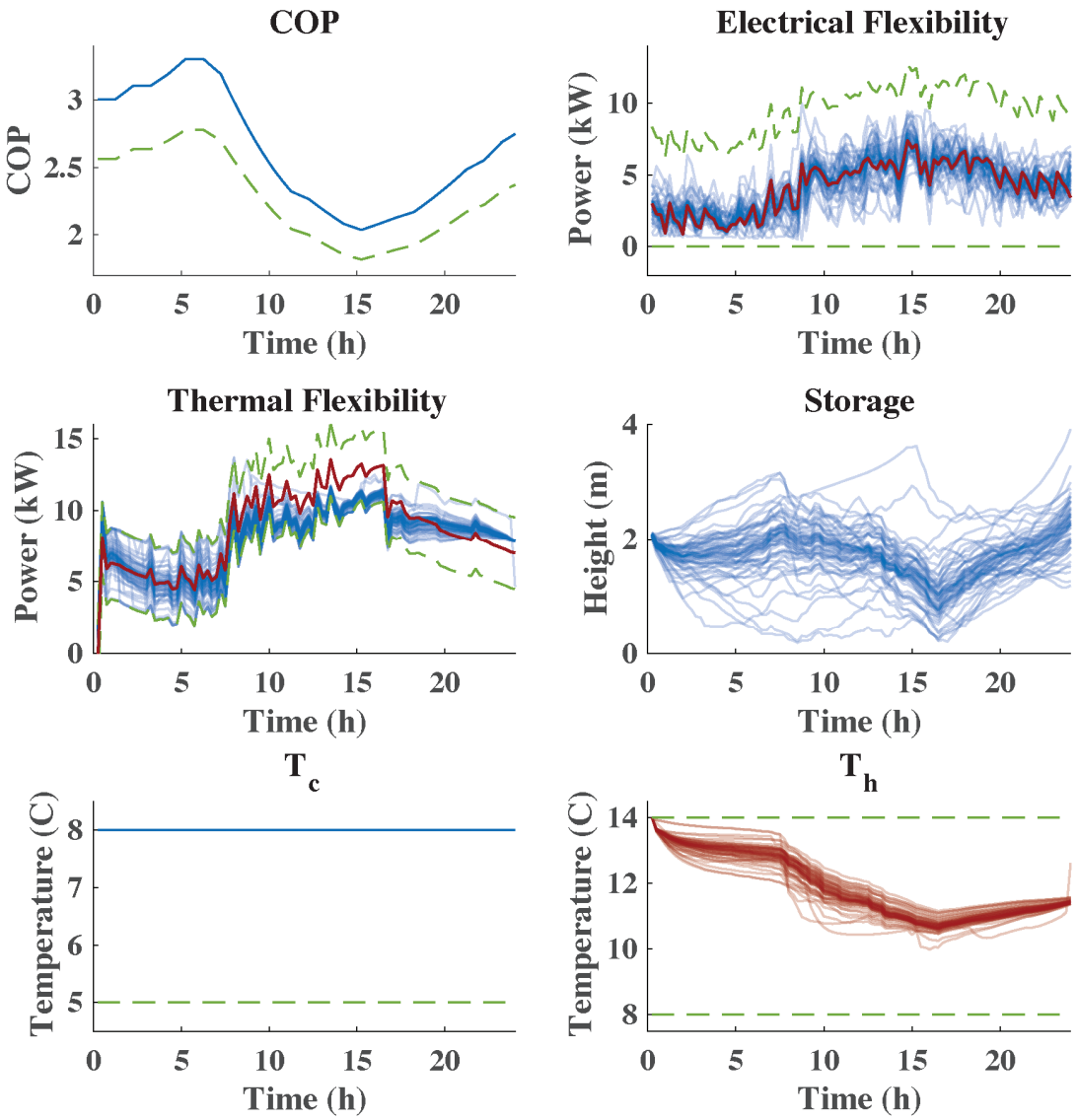

Figure 8.4 – Electrical Flexibility - Fixed supply temperatures. Top left: COP. Top right: Electrical power $\mathbf{e}_{ch}$ (blue), and baseline $\mathbf{e}_{b}$ (red). Middle left: Thermal power $\mathbf{q}$ (blue), and baseline $\mathbf{q}_{b}$ (red). Middle right: Height of cold layer in storage h_c. Bottom left: Temperature of cold layer in storage $\mathbf{T}_{c}$. Bottom right: Temperature of warm layer in storage $\mathbf{T}_{h}$ (dashed green lines denote operational constraints).

flexibility, while the electrical flexibility provided to the grid is increased to ±14.8kW. It can be seen in Figure 8.5 that there is a different trajectory of COP corresponding to each scenario of the regulation signal. Similarly, the height and temperature of the cold and warm storage layers have a different trajectory for each scenario.

The validation results for a specific day are shown in Figure 8.6. It can be seen in this figure that the zone temperatures for all the five zones are within the comfort limits, while the regulation signal is tracked. The received regulation signal, total electrical power consumption and the baseline power are also shown in Figure 8.6.

It should be noted that the extra flexibility achieved by exploiting the chiller COP depends on various factors including the range of outside temperature, required cooling capacity, etc. Therefore, the amount of extra flexibility might differ based on external factors. However, the result of the control scheme shows that when the objective is to maximize the flexibility, maintaining constant supply temperatures and operating the chiller at its maximum COP might not be the optimum behavior.

8.6.5 Occupant Comfort

The impact of providing flexibility on the occupant comfort is investigated and discussed in this section.

Comfort Measure

The ASHRAE 'Likelihood of Dissatisfied' (ALD) is used as a comfort measure [86]. ALD is a function of the absolute difference between the zone temperature and an ideal temperature. It is a standard measure, and is based on statistical data collected by ASHRAE. Comfort analysis is performed as a post-processing step, and an ALD value is computed for each time step in each zone. Average comfort per day is computed using the 'Long-term percentage of dissatisfied' (LPD), which is a function of ALD [86].

Flexibility vs Comfort

The simulation is repeated with different levels of comfort constraints around the ideal comfort temperature ($T_{ideal} = 22\,^{\circ}\mathrm{C}$), and each simulation gives a point on the flexibility vs comfort axis as shown in Figure 8.7. This figure can be interpreted as a Pareto curve where the desired direction is top-left (more flexibility with high comfort). The simulations are also repeated for the case of no thermal storage tank in the HVAC system for comparison. Results show that allowing the supply temperatures to vary provides more flexibility compared to when they are fixed (round markers above cross markers in Figure 8.7), and having the storage in HVAC system also allows to provide more flexibility compared to not having it

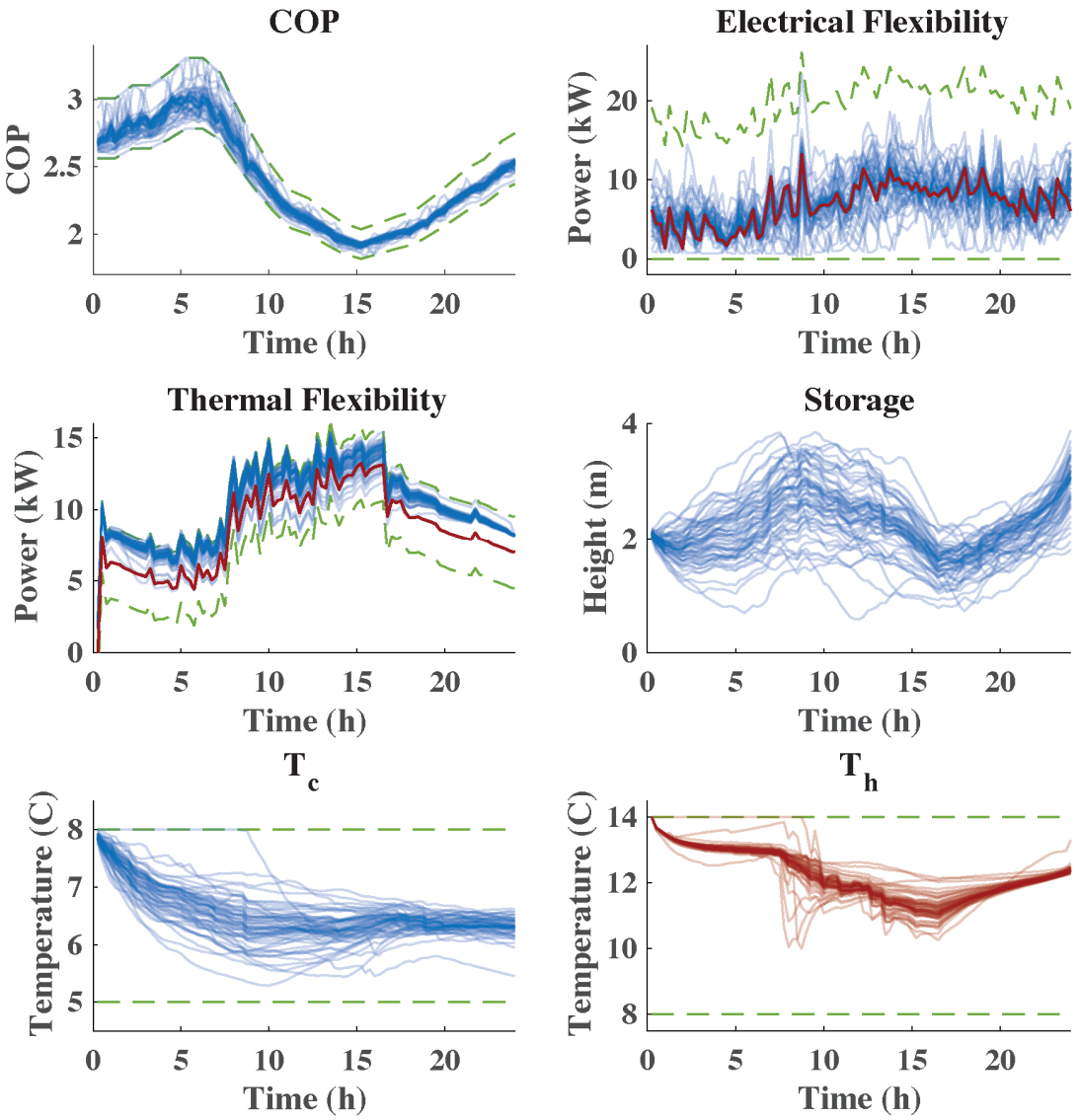

Figure 8.5 – Electrical Flexibility - Varying supply temperatures. Top left: COP. Top right: Electrical power $\mathbf{e}_{ch}$ (blue), and baseline $\mathbf{e}_b$ (red). Middle left: Thermal power $\mathbf{q}$ (blue), and baseline $\mathbf{q}_b$ (red). Middle right: Height of cold layer in storage h_c. Bottom left: Temperature of cold layer in storage $\mathbf{T}_c$. Bottom right: Temperature of warm layer in storage $\mathbf{T}_h$ (dashed green lines denote operational constraints).

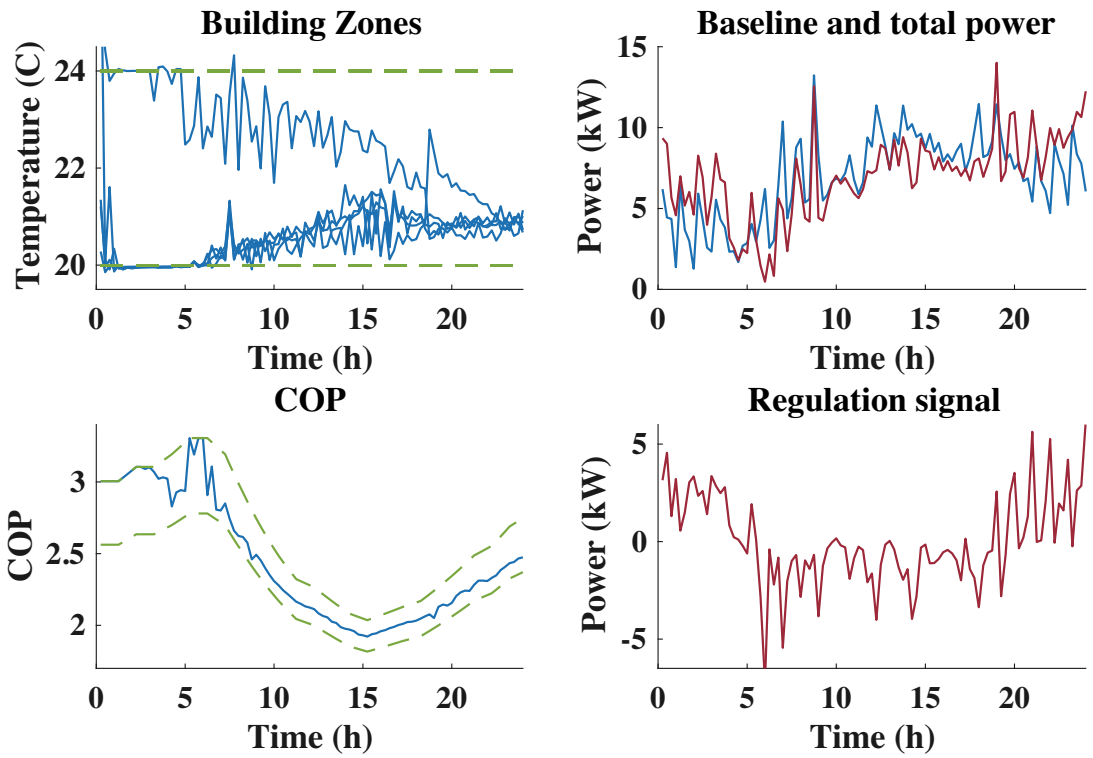

Figure 8.6 – Electrical Flexibility Validation - Varying supply temperatures. Top left: Zone temperatures. Top right: Electrical power $\mathbf{e}_{ch}$ (red), and baseline $\mathbf{e}_{b}$ (blue). Bottom left: COP. Bottom right: Regulation Signal $\mathbf{r}$ (dashed green lines denote operational constraints).

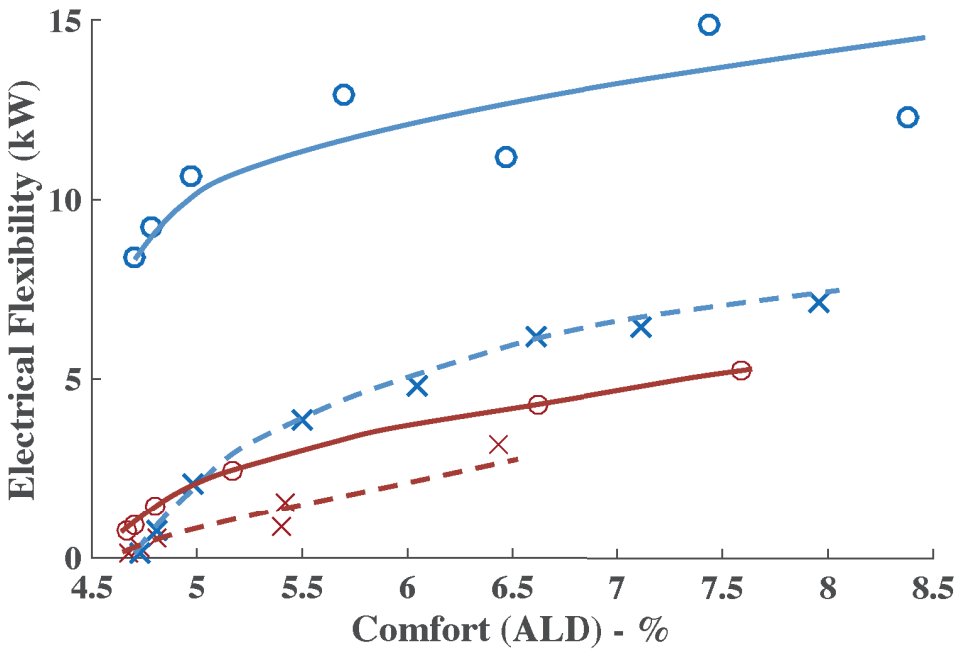

Figure 8.7 – Electrical flexibility γ vs comfort: Blue: With storage. Red: No storage. Solid line and round marker: Varying supply temperatures. Dashed line and cross marker: Fixed supply temperatures.

(blue markers above red markers in Figure 8.7). The result in Figure 8.7 is consistent with the discussion in Section 6.6.3, and shows that there is a trade-off between comfort and the provided flexibility.

Compared to minimum energy operation of the building, the flexibility providing controller improves the occupant comfort, as also seen in Section 6.6.3. The intuitive reason for this is that the extra energy consumed to maintain the baseline for up/down flexibility provision allows the zone temperatures to be in the middle of the comfort constraints most of the time as opposed to the minimum energy operation where the zone temperatures are kept close to the comfort limits. Moreover, tracking the regulation signal also excites the zone temperature within the limits, improving comfort.

8.7 Conclusion

This chapter presented a hierarchical control scheme for building HVAC systems to provide secondary frequency control service to the grid. A separation in the control of the building zones and the HVAC system was proposed using a three layer control architecture. The local building controllers tracked the temperature setpoints at the lowest level. The thermal

flexibility controller used robust optimization methods to maximize the flexibility in the thermal consumption of building zones, and provided it to the electrical flexibility controller. The electrical flexibility controller used the thermal flexibility and controlled the HVAC system using robust optimization methods to provided flexibility to the grid.

A control-oriented model of a typical HVAC system was developed and simulations were carried out to demonstrate the efficacy of the proposed control scheme. Simulation results showed that the full HVAC system can be controlled using the proposed scheme to provide flexibility to the grid. Results showed that exploiting the variable COP of the chiller might add extra flexibility on top of the flexibility from the building thermodynamics and storage. The occupant comfort was shown to increase compared to minimum energy operation, as a by-product of providing flexibility.

[redacted] Appendix

C Robust Solution

C.1 Dualizing a robust constraint

This section gives an overview of a standard tool in the literature [120], [121] to reformulate a robust constraint using duality. Let's consider the following robust constraint

$$(F\mathbf{P} + U)\mathbf{r} \leq c, \qquad \mathbf{r} \in \mathcal{R}$$

where F and U are the problem data, $\mathbf{P}$ is the optimization variable, and $\mathbf{r} \in \mathcal{R}$ is the uncertain parameter, while $\mathcal{R}$ is the polytopic uncertainty set defined as

$$\mathcal{R} = \{\mathbf{r} \in \mathbb{R}^N \mid R\mathbf{r} \leq h_r\}$$

It is well-known that this robust constraint can be formulated using a row-wise maximization, as follows

$$\max_{\mathbf{r}\in\mathcal{R}} \quad (F\mathbf{P} + U)\mathbf{r} \leq c$$

In the case where the uncertain set $\mathcal{R}$ is a polytope, the maximization problem is equal to the following dual problem

$$\begin{aligned} \min_{Z} \quad & Z^T h_r \\ \text{s.t.} \quad & R^T Z = (F\mathbf{P} + U)^T, \qquad Z \geq 0 \end{aligned}$$

where Z are the dual variables for each row of $(F\mathbf{P} + U)\mathbf{r}$. As a result the robust constraint can be replaced by the following constraints

$$Z^T h_r \leq c, \qquad F\mathbf{P} + U = Z^T R, \qquad Z \geq 0$$

where Z is the additional decision variable.

Similar tricks for more complicated constraints and uncertainty sets are discussed in [79]. This method is used to replace the robust constraints in the thermal flexibility problem (8.23) to formulate a tractable convex optimization problem, and the procedure is summarized next.

C.2 Reformulating the thermal flexibility problem

Using the the affine decision rule policy (8.24), the thermal flexibility problem (8.23) can be written as the following robust optimization problem

$$\begin{array}{ll} \underset{\alpha,\bar{\mathbf{q}},\mathrm{M},\mathrm{v}}{\text{maximize}} & \alpha \\ \text{s.t.} & (\bar{\mathbf{y}},\mathbf{q}) \in \mathcal{Q}(x,\mathbf{d}) \\ & \bar{\mathbf{y}} = \mathbf{M}\mathbf{q}_r + \mathbf{v} \\ & \mathbf{q} = \bar{\mathbf{q}} + \alpha\mathbf{q}_r, \qquad \forall \mathbf{q}_r \in \Xi_t \end{array} \tag{C.1}$$

where the matrix $\mathbf{M}$ is constrained to be lower-triangular for causality, and the uncertainty set Ξ_t is polytopic and can be written as

$$\Xi_t = \{\mathbf{q}_\mathrm{r} \in \mathbb{R}^N \mid S\mathbf{q}_\mathrm{r} \leq h\}$$

where $S \in \mathbb{R}^{ns\times N}$, and $h \in \mathbb{R}^{ns\times 1}$.

The state, input, weather disturbance, and output vectors in the definition of set $\mathcal{Q}$ (8.22) are stacked over the horizon as $\mathbf{x} = [x_1^T, x_2^T, ..., x_N^T]^T$, $\bar{\mathbf{y}} = [\bar{y}_0^T, \bar{y}_1^T, ..., \bar{y}_{N-1}^T]^T$, $\mathbf{d} = [d_0^T, d_1^T, ..., d_{N-1}^T]^T$, and $\mathbf{q} = [q_0^T, q_1^T, ..., q_{N-1}^T]^T$. Using appropriate stacked matrices $\mathbf{A} \in \mathbb{R}^{n_x N\times n_x}$, $\mathbf{B}_\mathrm{u} \in \mathbb{R}^{n_x N\times n_u N}$, $\mathbf{B}_\mathrm{d} \in \mathbb{R}^{n_x N\times n_d N}$, $\mathbf{C} \in \mathbb{R}^{n_y N\times n_x N}$, $\mathbf{D} \in \mathbb{R}^{n_y N\times n_u N}$, and $\mathbf{E} \in \mathbb{R}^{n_y N\times n_x}$, the dynamics of the closed loop system in set $\mathcal{Q}$ (8.22) can be written in the dense form, as a function of the initial state x_0, as follows

$$\begin{aligned} \mathbf{x} &= \mathbf{A}x_0 + \mathbf{B}_\mathrm{u}\bar{\mathbf{y}} + \mathbf{B}_\mathrm{d}\mathbf{d} \\ \mathbf{q} &= \mathbf{C}\mathbf{x} + \mathbf{D}\bar{\mathbf{y}} + \mathbf{E}x_0 \end{aligned} \tag{C.2}$$

where the stacked matrices are defined as

$$\mathbf{A} := \begin{bmatrix} A \\ A^2 \\ \vdots \\ A^N \end{bmatrix}, \qquad \mathbf{B}_\mathrm{u} := \begin{bmatrix} B_u & 0 & \cdots & \cdots & 0 \\ AB_u & B_u & 0 & \cdots & \vdots \\ A^2B_u & AB_u & \ddots & \ddots & \vdots \\ \vdots & \vdots & \ddots & \ddots & 0 \\ A^{N-1}B_u & A^{N-2}B_u & \cdots & AB_u & B_u \end{bmatrix}$$

$$\mathbf{B}_\mathrm{d} := \begin{bmatrix} B_d & 0 & \cdots & \cdots & 0 \\ AB_d & B_d & 0 & \cdots & \vdots \\ A^2B_d & AB_d & \ddots & \ddots & \vdots \\ \vdots & \vdots & \ddots & \ddots & 0 \\ A^{N-1}B_d & A^{N-2}B_d & \cdots & AB_d & B_d \end{bmatrix}, \qquad \mathbf{C} := \begin{bmatrix} 0 & \cdots & \cdots & 0 \\ C & 0 & \cdots & \vdots \\ 0 & \ddots & \ddots & \vdots \\ 0 & \cdots & C & 0 \end{bmatrix}$$

$$\mathbf{D} := I_N \otimes D, \qquad \mathbf{E} := \begin{bmatrix} C \\ 0 \\ \vdots \\ 0 \end{bmatrix}$$

Using (C.2), the constraints of the robust optimization problem (C.1), after appropriate substitutions, can be re-written as

$$\begin{aligned} \theta + \mathbf{G}\mathbf{v} - \bar{\mathbf{q}} + (\mathbf{G}\mathbf{M} - \mathbf{\Lambda})\mathbf{q}_r = 0 \\ y_{min} \leq \mathbf{M}\mathbf{q}_r + \mathbf{v} \leq y_{max}, \qquad \forall \mathbf{q}_r \in \Xi_t \end{aligned} \tag{C.3}$$

where $\theta = (\mathbf{CA} + \mathbf{E})x_0 + \mathbf{CB}_\mathrm{d}\mathbf{d}$, $\mathbf{G} = \mathbf{CB}_\mathrm{u} + \mathbf{D}$, and $\mathbf{\Lambda} = I_N \otimes \alpha$.

Dualizing the robust constraints (C.3) following the procedure explained in Section C.1, the robust optimization problem (C.1) can be formulated as the following linear program

$$\begin{aligned} \underset{\alpha,\bar{\mathbf{q}},\mathbf{M},\mathbf{v}}{\text{maximize}} \quad & \alpha \\ \text{s.t.} \quad & \theta + \mathbf{G}\mathbf{v} - \bar{\mathbf{q}} + \mathbf{Z}_1^T h \leq 0 \\ & \mathbf{G}\mathbf{M} - \mathbf{\Lambda} = \mathbf{Z}_1^T S \\ & \mathbf{Z}_1 \geq 0 \\ & -\theta - \mathbf{G}\mathbf{v} + \bar{\mathbf{q}} + \mathbf{Z}_2^T h \leq 0 \\ & -\mathbf{G}\mathbf{M} + \mathbf{\Lambda} = \mathbf{Z}_2^T S \\ & \mathbf{Z}_2 \geq 0 \\ & \mathbf{Z}_3^T h + \mathbf{v} \leq y_{max} \\ & \mathbf{M} = \mathbf{Z}_3^T S \\ & \mathbf{Z}_3 \geq 0 \\ & \mathbf{Z}_4^T h - \mathbf{v} \leq -y_{min} \\ & -\mathbf{M} = \mathbf{Z}_4^T S \\ & \mathbf{Z}_4 \geq 0 \end{aligned} \tag{C.4}$$

where $\mathbf{Z}_1 \in \mathbb{R}^{ns \times N}$, $\mathbf{Z}_2 \in \mathbb{R}^{ns \times N}$, $\mathbf{Z}_3 \in \mathbb{R}^{nuN \times N}$, $\mathbf{Z}_4 \in \mathbb{R}^{nuN \times N}$ are the dual variables (additional optimization variables), and y_{min} and y_{max} define the comfort set $\mathcal{Y}$.

The solution of the robust optimization problem gives the optimal baseline $\bar{\mathbf{q}}^*$, the scaling of the uncertainty set α^*, and the control law defined by $\mathbf{M}^*$ and $\mathbf{v}^*$.

9 Conclusion

This chapter summarizes the main conclusions of the thesis. This thesis addressed all the research questions raised in Chapter 1. The main conclusions are given below.

Part I - OpenBuild
This part answered the question of efficient modeling of building thermodynamics for optimization based control.

The open source MATLAB toolbox OpenBuild was developed to facilitate modeling, testing, and validation of building controllers. The toolbox enabled automatic extraction of linear state-space building thermodynamic models from EnergyPlus building models. The associated disturbance data (weather, internal gains, and occupancy) for the linear models was also extracted from EnergyPlus. The extracted models were validated using the original EnergyPlus models and the results showed that the linear models were reasonable in capturing the thermodynamics and predicting the thermal power requirement of the buildings. The toolbox also facilitates co-simulation between MATLAB and EnergyPlus. The toolbox gives access to a large number of validated standard building models of different types and the associated data to carry out realistic simulation studies.

Part II - Ancillary Services
This part answered the questions of characterizing buildings' flexibility, control of buildings to interact with different markets involved in the provision of ancillary services, and the economic and practical (technical) feasibility of buildings providing ancillary services.

The control problem of a building providing secondary frequency control service to the grid was presented in Chapter 5. The two phases (offline and online) of ancillary services provision were introduced. The bidding problem for the offline phase was formulated as a multi-stage uncertain optimization problem. An approximate solution method for the bidding problem based on a novel intraday control policy and two-stage stochastic programming was proposed. A closed loop algorithm based on a stochastic MPC controller was proposed

for the on-line phase. Simulation results showed that it is indeed possible for a building to act as a virtual storage and provide flexibility to the grid. The proposed controller showed satisfactory performance in simulations, and the building was able to track the received AGC, while satisfying the comfort requirements.

The financial analysis of a typical office building providing ancillary service in Switzerland was presented in Chapter 6. The different markets, costs, and rewards involved in the provision of ancillary services were presented. The control methodology presented in Chapter 5 was adapted to account for all the costs, rewards, and the particular building HVAC considered in the study. The financial analysis was carried out using all the real data for the year 2014 with the following main outcomes:

- On average, providing secondary frequency control service to the grid results in savings for the building which are further increased by participating in the intraday market. The building without extra storage in its HVAC system saves on average 8.3% without and 11.1% with intraday market participation.
- Availability of thermal storage in the building HVAC system increases this financial benefit. For the building with thermal storage, the average savings in operational costs increase to 13%, while participating in the intraday energy market increase it to 29.5%.
- The provision of ancillary services to the grid increased the occupant comfort at a reduced price which is counter-intuitive. This is because the extra energy consumed to provide flexibility also improved occupant comfort.
- The economic benefit is sensitive to the electricity price. Since, electricity prices are slightly different (due to different distribution charges) at different locations in Switzerland, the financial benefit varies with the physical location of the building within Switzerland.

The provision of regulation services using an occupied office building was experimentally demonstrated in Chapter 7. The control scheme presented in Chapter 5 was tested using the LADR experimental setup. The building was able to provide flexibility to the grid by optimizing and fixing its baseline and capacity at the beginning of the regulation period, and tracking successfully the received AGC signal, while maintaining occupant comfort and operational constraints. The success of the experiments despite uncertainties in weather prediction and occupancy demonstrated the robustness of the proposed control approach. The proposed control approach was also compared, both in simulations and experiments, to an alternative control method based on robust optimization methods, developed in the lab. The results showed that the proposed control method works well in practice and is less conservative compared to the alternative approach.

Part III - Hierarchical Control
This part answered the question of controlling the different components of a complex HVAC system for providing flexibility (ancillary service) to the grid.

A hierarchical control scheme for building HVAC systems to provide secondary frequency control service to the grid was presented in Chapter 8. A separation in the control of the building zones and the HVAC system was proposed using a three-layer control architecture. The local building controllers tracked the temperature setpoints at the lowest level. The thermal flexibility controller used robust optimization methods to maximize the flexibility in the thermal consumption of building zones, and provided it to the electrical flexibility controller. The electrical flexibility controller used the thermal flexibility and controlled the HVAC system using robust optimization methods to provide flexibility to the grid. A control-oriented model of a typical HVAC system was developed and simulations were carried out to demonstrate the efficacy of the proposed control scheme. Simulation results showed that the full HVAC system can be controlled using the proposed scheme to provide flexibility to the grid. Results showed that exploiting the variable COP of the chiller might add extra flexibility on top of the flexibility from the building thermodynamics and storage. The occupant comfort was shown to increase compared to minimum energy operation, as a by-product of providing flexibility.

Bibliography

[1] E. Commission, "Communication from the commission to the european parliament, the council, the european economic and social committee and the committee of the regions - a policy framework for climate and energy in the period from 2020 to 2030", European Commission, Tech. Rep., 2014.

[2] T. Hammons, "Integrating renewable energy sources into european grids", *International Journal of Electrical Power & Energy Systems*, vol. 30, no. 8, pp. 462–475, 2008.

[3] J. L. Sawin, F. Sverrisson, and W. Rickerson, "Renewables 2015 : Global Status Report", REN21, Tech. Rep., 2016.

[4] D. Callaway and I. Hiskens, "Achieving Controllability of Electric Loads", *Proceedings of the IEEE*, vol. 99, no. 1, pp. 184 –199, Jan. 2011, ISSN: 0018-9219. DOI: 10.1109/JPROC.2010.2081652.

[5] Z. Xu, D. S. Callaway, Z. Hu, and Y. Song, "Hierarchical coordination of heterogeneous flexible loads", *IEEE Transactions on Power Systems*, vol. 31, no. 6, pp. 4206–4216, 2016, ISSN: 0885-8950. DOI: 10.1109/TPWRS.2016.2516992.

[6] S. L. Andersson, A. K. Elofsson, M. D. Galus, L Göransson, S Karlsson, F Johnsson, and G Andersson, "Plug-in hybrid electric vehicles as regulating power providers: Case studies of Sweden and Germany", *Energy Policy*, vol. 38, no. 6, pp. 2751–2762, 2010, ISSN: 03014215. DOI: 10.1016/j.enpol.2010.01.006.

[7] P. J. Douglass, R. Garcia-Valle, P. Nyeng, J. Østergaard, and M. Togeby, "Smart Demand for Frequency Regulation: Experimental Results", *IEEE Transactions on Smart Grid*, vol. 4, no. 3, pp. 1713–1720, Sep. 2013, ISSN: 1949-3053. DOI: 10.1109/TSG.2013.2259510.

[8] T. Gorecki, F. Qureshi, and C. Jones, "Openbuild : an integrated simulation environment for building control", in *Control Applications (CCA), 2015 IEEE Conference on*, 2015, pp. 1522–1527. DOI: 10.1109/CCA.2015.7320826.

[9] F. A. Qureshi, I. Lymperopoulos, A. A. Khatir, and C. N. Jones, "Economic advantages of office buildings providing ancillary services with intraday participation", *IEEE Transactions on Smart Grid*, vol. PP, no. 99, pp. 1–1, 2016, ISSN: 1949-3053. DOI: 10.1109/TSG.2016.2632239.

[10] L. Fabietti, T. Gorecki, F. Qureshi, A. Bitlislioglu, I. Lymperopoulos, and C. Jones, "Experimental implementation of frequency regulation services using commercial buildings", *IEEE Transactions on Smart Grid*, vol. PP, no. 99, pp. 1–1, 2016, ISSN: 1949-3053. DOI: 10.1109/TSG.2016.2597002.

[11] F. Qureshi, T. Gorecki, and C. N. Jones, "Model Predictive Control for Market-Based Demand Response Participation", in *Proceedings of the 19th IFAC World congress*, vol. 47, Cape Town, South Africa, 2014, pp. 11 153–11 158.

[12] I. Lymperopoulos, F. A. Qureshi, T. Nghiem, A. A. Khatir, and C. N. Jones, "Providing Ancillary Service with Commercial Buildings: The Swiss Perspective", in *9th IFAC International Symposium on Advanced Control of Chemical Processes (ADCHEM)*, Whistler, BC, Canada, 2015.

[13] X. T. Nghiem, A. Bitlislioglu, T. T. Gorecki, F. A. Qureshi, and C. Jones, "OpenBuildNet Framework for Distributed Co-Simulation of Smart Energy Systems", in *Proceedings of the 14th International Conference on Control, Automation, Robotics and Vision*, 2016.

[14] T. T. Gorecki, L. Fabietti, F. A. Qureshi, and C. N. Jones, "Experimental Demonstration of Buildings Providing Frequency Regulation Services in the Swiss Market", *Energy and Buildings*, pp. –, 2017, ISSN: 0378-7788. DOI: http://dx.doi.org/10.1016/j.enbuild.2017.02.050.

[15] N. E. KLEPEIS, W. C. NELSON, W. R. OTT, J. P. ROBINSON, A. M. TSANG, P. SWITZER, J. V. BEHAR, S. C. HERN, and W. H. ENGELMANN, "The National Human Activity Pattern Survey (NHAPS): a resource for assessing exposure to environmental pollutants", en, *Journal of Exposure Science and Environmental Epidemiology*, vol. 11, no. 3, pp. 231–252, Jul. 2001, ISSN: 1053-4245. DOI: 10.1038/sj.jea.7500165.

[16] T. Kostiainen, I. Welling, M. Lahtinen, K. Salmi, E. Kähkönen, and J. Lampinen, "Modeling of Subjective Responses to Indoor Air Quality and Thermal Conditions in Office Buildings", *HVAC&R Research*, vol. 14, no. 6, pp. 905–923, Nov. 2008, ISSN: 1078-9669. DOI: 10.1080/10789669.2008.10391046.

[17] P. O. Fanger, "Thermal comfort. Analysis and applications in environmental engineering.", *Thermal comfort. Analysis and applications in environmental engineering.*, 1970.

[18] J. F. Nicol and M. A. Humphreys, "Adaptive thermal comfort and sustainable thermal standards for buildings", *Energy and Buildings*, Special Issue on Thermal Comfort Standards, vol. 34, no. 6, pp. 563–572, Jul. 2002, ISSN: 0378-7788. DOI: 10.1016/S0378-7788(02)00006-3.

[19] L. Pérez-Lombard, J. Ortiz, and C. Pout, "A review on buildings energy consumption information", *Energy and Buildings*, vol. 40, no. 3, pp. 394–398, 2008, ISSN: 0378-7788. DOI: 10.1016/j.enbuild.2007.03.007.

[20] WBCSD, "Transforming the Market: Energy efficiency in buildings", Tech. Rep., 2009.

[21] of the European Parliament, *Directive 2010/31/EU on Building Energy efficiency*, May 2010.

[22] X. Li and J. Wen, "Review of building energy modeling for control and operation", *Renewable and Sustainable Energy Reviews*, vol. 37, pp. 517–537, Sep. 2014, ISSN: 1364-0321. DOI: 10.1016/j.rser.2014.05.056.

[23] P. H. Shaikh, N. B. M. Nor, P. Nallagownden, I. Elamvazuthi, and T. Ibrahim, "A review on optimized control systems for building energy and comfort management of smart sustainable buildings", *Renewable and Sustainable Energy Reviews*, vol. 34, pp. 409–429, Jun. 2014, ISSN: 1364-0321. DOI: 10.1016/j.rser.2014.03.027.

[24] ASHRAE, "Supervisory Control Strategies and Optimization", in *2011 ASHRAE Handbook - HVAC Applications*, 2011.

[25] D. S. Naidu and C. G. Rieger, "Advanced control strategies for heating, ventilation, air-conditioning, and refrigeration systems—An overview: Part I: Hard control", *HVAC&R Research*, vol. 17, no. 1, pp. 2–21, 2011, ISSN: 1078-9669. DOI: 10.1080/10789669.2011.540942.

[26] J. E. Braun, "Reducing energy costs and peak electrical demand through optimal control of building thermal storage", *ASHRAE transactions*, vol. 96, no. 2, pp. 876–888, 1990.

[27] T. Nghiem and G. Pappas, "Receding-horizon supervisory control of green buildings", in *American Control Conference (ACC), 2011*, Jul. 2011, pp. 4416 –4421.

[28] J. Ma, S. Qin, B. Li, and T. Salsbury, "Economic model predictive control for building energy systems", in *Innovative Smart Grid Technologies (ISGT), 2011 IEEE PES*, Jan. 2011, pp. 1 –6. DOI: 10.1109/ISGT.2011.5759140.

[29] R Freire, G Oliveira, and N Mendes, "Predictive controllers for thermal comfort optimization and energy savings", *Energy and Buildings*, vol. 40, no. 7, pp. 1353–1365, 2008, ISSN: 03787788. DOI: 10.1016/j.enbuild.2007.12.007.

[30] F. Oldewurtel, A. Ulbig, A. Parisio, G. Andersson, and M. Morari, "Reducing peak electricity demand in building climate control using real-time pricing and model predictive control", in *2010 49th IEEE Conference on Decision and Control (CDC)*, Dec. 2010, pp. 1927 –1932. DOI: 10.1109/CDC.2010.5717458.

[31] J. Ma, J. Qin, T. Salsbury, and P. Xu, "Demand reduction in building energy systems based on economic model predictive control", *Chemical Engineering Science*, vol. 67, no. 1, pp. 92–100, Jan. 2012, ISSN: 0009-2509. DOI: 10.1016/j.ces.2011.07.052.

[32] R. Halvgaard, N. Poulsen, H. Madsen, and J. Jorgensen, "Economic Model Predictive Control for building climate control in a Smart Grid", in *Innovative Smart Grid Technologies (ISGT), 2012 IEEE PES*, Jan. 2012, pp. 1 –6. DOI: 10.1109/ISGT.2012.6175631.

[33] E. Vrettos, K. Lai, F. Oldewurtel, and G. Andersson, "Predictive Control of buildings for Demand Response with dynamic day-ahead and real-time prices", in *Control Conference (ECC), 2013 European*, Jul. 2013, pp. 2527–2534.

[34] J. Hu and P. Karava, "A state-space modeling approach and multi-level optimization algorithm for predictive control of multi-zone buildings with mixed-mode cooling", *Building and Environment*, vol. 80, pp. 259–273, Oct. 2014, ISSN: 0360-1323. DOI: 10.1016/j.buildenv.2014.05.003.

[35] H Spindler and L Norford, "Naturally ventilated and mixed-mode buildings - Part II: Optimal control", *Building and Environment*, vol. 44, no. 4, pp. 750–761, Apr. 2009, ISSN: 03601323. DOI: 10.1016/j.buildenv.2008.05.018.

[36] G. P. Henze, D. E. Kalz, S. Liu, and C. Felsmann, "Experimental Analysis of Model-Based Predictive Optimal Control for Active and Passive Building Thermal Storage Inventory", *HVAC&R Research*, vol. 11, no. 2, pp. 189–213, 2005, ISSN: 1078-9669. DOI: 10.1080/10789669.2005.10391134.

[37] Y. Ma, A. Kelman, A. Daly, and F. Borrelli, "Predictive Control for Energy Efficient Buildings with Thermal Storage: Modeling, Stimulation, and Experiments", *IEEE Control Systems*, vol. 32, no. 1, pp. 44 –64, Feb. 2012, ISSN: 1066-033X. DOI: 10.1109/MCS.2011.2172532.

[38] M. Houwing, R. Negenborn, and B. De Schutter, "Demand Response With Micro-CHP Systems", *Proceedings of the IEEE*, vol. 99, no. 1, pp. 200 –213, Jan. 2011, ISSN: 0018-9219. DOI: 10.1109/JPROC.2010.2053831.

[39] M. Kummert, P. Andre, and J. Nicolas, "Optimal heating control in a passive solar commercial building", *Solar Energy*, vol. 69, pp. 103–116, 2001.

[40] F. Oldewurtel, D. Sturzenegger, and M. Morari, "Importance of occupancy information for building climate control", *Applied Energy*, vol. 101, pp. 521–532, Jan. 2013, ISSN: 0306-2619. DOI: 10.1016/j.apenergy.2012.06.014.

[41] J. R. Dobbs and B. M. Hencey, "Model Predictive HVAC Control with Online Occupancy Model", *ArXiv:1403.4662 [cs]*, Mar. 2014.

[42] F. Oldewurtel, A. Parisio, C. N. Jones, D. Gyalistras, M. Gwerder, V. Stauch, B. Lehmann, and M. Morari, "Use of model predictive control and weather forecasts for energy efficient building climate control", *Energy and Buildings*, vol. 45, pp. 15–27, Feb. 2012, ISSN: 03787788. DOI: 10.1016/j.enbuild.2011.09.022.

[43] R. Gondhalekar, F. Oldewurtel, and C. N. Jones, "Least-restrictive robust periodic model predictive control applied to room temperature regulation", *Automatica*, vol. 49, no. 9, pp. 2760–2766, Sep. 2013, ISSN: 0005-1098. DOI: 10.1016/j.automatica.2013.05.009.

[44] X. Zhang, G. Schildbach, D. Sturzenegger, and M. Morari, "Scenario-based MPC for energy-efficient building climate control under weather and occupancy uncertainty", in *Control Conference (ECC), 2013 European*, Jul. 2013, pp. 1029–1034.

[45] P. May-Ostendorp, G. P. Henze, C. D. Corbin, B. Rajagopalan, and C. Felsmann, "Model-predictive control of mixed-mode buildings with rule extraction", *Building and Environment*, vol. 46, no. 2, pp. 428–437, Feb. 2011, ISSN: 03601323. DOI: 10.1016/j.buildenv.2010.08.004.

[46] G. P. Henze, A. R. Florita, M. J. Brandemuehl, C. Felsmann, and H. Cheng, "Advances in Near-Optimal Control of Passive Building Thermal Storage", *Journal of Solar Energy Engineering*, vol. 132, no. 2, p. 021 009, 2010, ISSN: 01996231. DOI: 10.1115/1.4001466.

[47] Y. Ma, F. Borrelli, B. Hencey, B. Coffey, S. Bengea, and P. Haves, "Model Predictive Control for the Operation of Building Cooling Systems", *IEEE Transactions on Control Systems Technology*, vol. 20, no. 3, pp. 796–803, May 2012, ISSN: 1063-6536. DOI: 10.1109/TCST.2011.2124461.

[48] S. Privara, Z. Vana, D. Gyalistras, J. Cigler, C. Sagerschnig, M. Morari, and L. Ferkl, "Modeling and identification of a large multi-zone office building", in *2011 IEEE International Conference on Control Applications (CCA)*, Sep. 2011, pp. 55 –60. DOI: 10.1109/CCA.2011.6044402.

[49] D. Kolokotsa, A. Pouliezos, G. Stavrakakis, and C. Lazos, "Predictive control techniques for energy and indoor environmental quality management in buildings", *Building and Environment*, vol. 44, no. 9, pp. 1850–1863, Sep. 2009, ISSN: 0360-1323. DOI: 10.1016/j.buildenv.2008.12.007.

[50] D. Sturzenegger, D. Gyalistras, M. Morari, and R. Smith, "Model Predictive Climate Control of a Swiss Office Building: Implementation, Results, and Cost-Benefit Analysis", *IEEE Transactions on Control Systems Technology*, vol. PP, no. 99, pp. 1–1, 2015, ISSN: 1063-6536. DOI: 10.1109/TCST.2015.2415411.

[51] M. Maasoumy and A. Sangiovanni-Vincentelli, "Smart connected buildings design automation: foundations and trends", *Foundations and Trends® in Electronic Design Automation*, vol. 10, no. 1-2, pp. 1–143, 2016, ISSN: 1551-3939. DOI: 10.1561/1000000043.

[52] D. B. Crawley, J. W. Hand, M. Kummert, and B. T. Griffith, "Contrasting the capabilities of building energy performance simulation programs", *Building and Environment*, vol. 43, no. 4, 661–673, 2008, ISSN: 03601323. DOI: 10.1016/j.buildenv.2006.10.027.

[53] D. B. Crawley, L. K. Lawrie, F. C. Winkelmann, W. F. Buhl, Y. J. Huang, C. O. Pedersen, R. K. Strand, R. J. Liesen, D. E. Fisher, M. J. Witte, and J. Glazer, "EnergyPlus: creating a new-generation building energy simulation program", *Energy and Buildings*, Special Issue: BUILDING SIMULATION'99, vol. 33, no. 4, pp. 319–331, Apr. 2001, ISSN: 0378-7788.

[54] R. Guglielmetti, D. Macumber, and N. Long, "OpenStudio: an open source integrated analysis platform", in *Proceedings of the 12th Conference of International Building Performance Simulation Association*, 2011.

[55] US Department of Energy: Office of Energy Efficiency and Renewable Energy, *Commercial Reference Buildings*. [Online]. Available: http://energy.gov/eere/buildings/commercial-reference-buildings.

[56] A. S. Anđelković, I. Mujan, and S. Dakić, "Experimental validation of a energyplus model: application of a multi-storey naturally ventilated double skin façade", *Energy and Buildings*, vol. 118, pp. 27 –36, 2016, ISSN: 0378-7788. DOI: http://dx.doi.org/10.1016/j.enbuild.2016.02.045.

[57] P. C. Tabares-Velasco, C. Christensen, and M. Bianchi, "Verification and validation of energyplus phase change material model for opaque wall assemblies", *Building and Environment*, vol. 54, pp. 186 –196, 2012, ISSN: 0360-1323. DOI: http://dx.doi.org/10.1016/j.buildenv.2012.02.019.

[58] N. M. Mateus, A. Pinto, and G. C. da Graça, "Validation of energyplus thermal simulation of a double skin naturally and mechanically ventilated test cell", *Energy and Buildings*, vol. 75, pp. 511 –522, 2014, ISSN: 0378-7788. DOI: http://dx.doi.org/10.1016/j.enbuild.2014.02.043.

[59] R. H. Henninger, M. J. Witte, and D. B. Crawley, "Analytical and comparative testing of EnergyPlus using IEA HVAC BESTEST E100–E200 test suite", *Energy and Buildings*, vol. 36, no. 8, pp. 855–863, Aug. 2004, ISSN: 0378-7788. DOI: 10.1016/j.enbuild.2004.01.025.

[60] W. Bernal, M. Behl, T. X. Nghiem, and R. Mangharam, "MLE + : A Tool for Integrated Design and Deployment of Energy Efficient Building Controls", in *Proceedings of the Fourth ACM Workshop on Embedded Sensing Systems for Energy-Efficiency in Buildings*, 2012, pp. 123–130.

[61] M. Wetter and P. Haves, "A Modular Building Controls Virtual Test Bed For The Integration Of Heterogeneous Systems", *IBPSA-USA Journal*, vol. 3, no. 1, pp. 69–76, 2008.

[62] E. Atam and L. Helsen, "Control-oriented thermal modeling of multizone buildings: methods and issues: intelligent control of a building system", *IEEE Control Systems*, vol. 36, no. 3, pp. 86–111, 2016, ISSN: 1066-033X. DOI: 10.1109/MCS.2016.2535913.

[63] S. Royer, S. Thil, T. Talbert, and M. Polit, "A procedure for modeling buildings and their thermal zones using co-simulation and system identification", *Energy and Buildings*, vol. 78, pp. 231 –237, 2014, ISSN: 0378-7788. DOI: http://dx.doi.org/10.1016/j.enbuild.2014.04.013.

[64] W. J. Cole, E. T. Hale, and T. F. Edgar, "Building energy model reduction for model predictive control using openstudio", in *2013 American Control Conference*, 2013, pp. 449–454. DOI: 10.1109/ACC.2013.6579878.

[65] I. Hazyuk, C. Ghiaus, and D. Penhouet, "Optimal temperature control of intermittently heated buildings using model predictive control: part i – building modeling", *Building and Environment*, vol. 51, pp. 379 –387, 2012, ISSN: 0360-1323. DOI: http://dx.doi.org/10.1016/j.buildenv.2011.11.009.

[66] J. E. Braun and N. Chaturvedi, "An inverse gray-box model for transient building load prediction", *HVAC&R Research*, vol. 8, no. 1, pp. 73–99, 2002. DOI: 10.1080/10789669.2002.10391290. eprint: http://www.tandfonline.com/doi/pdf/10.1080/10789669.2002.10391290.

[67] S. Bengea, V. Adetola, K. Kang, M. J. Liba, D. Vrabie, R. Bitmead, and S. Narayanan, "Parameter estimation of a building system model and impact of estimation error on closed-loop performance", in *2011 50th IEEE Conference on Decision and Control and European Control Conference*, 2011, pp. 5137–5143. DOI: 10.1109/CDC.2011.6161302.

[68] D. Zhou, Q. Hu, and C. J. Tomlin, "Model comparison of a data-driven and a physical model for simulating hvac systems", *ArXiv preprint arXiv:1603.05951*, 2016.

[69] D. Sturzenegger, D. Keusch, L. Muffato, D. Kunz, and R. Smith, "Frequency-domain identification of a ventilated room for mpc", in *IFAC World Congress on Automatic Control*, Cape Town, South Africa, Aug. 2014, pp. 593–598.

[70] Z. Váňa, J. Cigler, J. Široký, E. Žáčeková, and L. Ferkl, "Model-based energy efficient control applied to an office building", *Journal of Process Control*, vol. 24, no. 6, pp. 790 –797, 2014, Energy Efficient Buildings Special Issue, ISSN: 0959-1524. DOI: http://dx.doi.org/10.1016/j.jprocont.2014.01.016.

[71] D. Sturzenegger, D. Gyalistras, V. Semeraro, M. Morari, and R. S. Smith, "Brcm matlab toolbox: model generation for model predictive building control", in *American Control Conference (ACC), 2014*, IEEE, 2014, pp. 1063–1069.

[72] D. Sturzenegger, D. Gyalistras, M. Morari, and R. S. Smith, "Semi-automated modular modeling of buildings for model predictive control", in *Proceedings of the Fourth ACM Workshop on Embedded Sensing Systems for Energy-Efficiency in Buildings*, ser. BuildSys '12, New York, NY, USA: ACM, 2012, pp. 99–106, ISBN: 978-1-4503-1170-0. DOI: 10.1145/2422531.2422550.

[73] Y. Lin, T. Middelkoop, and P. Barooah, "Issues in identification of control-oriented thermal models of zones in multi-zone buildings", in *2012 IEEE 51st Annual Conference on Decision and Control (CDC)*, Dec. 2012, pp. 6932–6937. DOI: 10.1109/CDC.2012.6425958.

[74] U. DOE, *ENERGYPLUS Engineering Reference*. 2012.

[75] M. Wetter, "Co-Simulation of Building Energy and Control Systems with the Building Controls Virtual Test Bed", *Journal of Building Performance Simulation*, no. August, 2011.

[76] U. Maeder, F. Borrelli, and M. Morari, "Linear offset-free Model Predictive Control", *Automatica*, vol. 45, no. 10, pp. 2214–2222, Oct. 2009, ISSN: 0005-1098. DOI: 10.1016/j.automatica.2009.06.005.

[77] T. T. Gorecki and F. A. Qureshi, *OpenBuild Manual*. [Online]. Available: http://la.epfl.ch/files/content/sites/la/files/shared/common/Research/openbuild/Manual.pdf.

[78] T. T. Gorecki, A. Bitlislioğlu, G. Stathopoulos, and C. N. Jones, "Guaranteeing input tracking for constrained systems: theory and application to demand response", in *2015 American Control Conference (ACC)*, 2015, pp. 232–237. DOI: 10.1109/ACC.2015.7170741.

[79] A. Bitlislioglu, T. T. Gorecki, and C. N. Jones, "Robust tracking commitment", *IEEE Transactions on Automatic Control*, vol. PP, no. 99, pp. 1–1, 2017, ISSN: 0018-9286. DOI: 10.1109/TAC.2017.2663766.

[80] G. Stathopoulos, H. Shukla, A. Szucs, Y. Pu, and C. N. Jones, "Operator splitting methods in control", *Foundations and Trends® in Systems and Control*, vol. 3, no. 3, pp. 249–362, 2016, ISSN: 2325-6818. DOI: 10.1561/2600000008.

[81] L. GIULIONI, *Stochastic Model Predictive Control with application to distributed control systems*. Politecnico di Milano, 2015.

[82] M. P. Fanti, A. M. Mangini, M. Roccotelli, F. Iannone, and A. Rinaldi, "A natural ventilation control in buildings based on co-simulation architecture and particle swarm optimization", in *2016 IEEE International Conference on Systems, Man, and Cybernetics (SMC)*, 2016, pp. 002 621–002 626. DOI: 10.1109/SMC.2016.7844634.

[83] K. J. Kircher and K. M. Zhang, "Testing building controls with the bldg toolbox", in *2016 American Control Conference (ACC)*, 2016, pp. 1472–1477. DOI: 10.1109/ACC.2016.7525124.

[84] M. Schönemann, "Multiscale simulation modeling concept for battery production systems", in *Multiscale Simulation Approach for Battery Production Systems*. Cham: Springer International Publishing, 2017, pp. 59–129, ISBN: 978-3-319-49367-1. DOI: 10.1007/978-3-319-49367-1_4.

[85] DOE, "Auxiliary EnergyPlus Programs", Tech. Rep., 2013. [Online]. Available: https://energyplus.net/sites/default/files/pdfs_v8.3.0/AuxiliaryPrograms.pdf.

[86] S. Carlucci, *Thermal comfort assessment of buildings*. Springer, 2013.

[87] T. Borsche, A. Ulbig, M. Koller, and G. Andersson, "Power and energy capacity requirements of storages providing frequency control reserves", in *Power and Energy Society General Meeting (PES), 2013 IEEE*, 2013, pp. 1–5. DOI: 10.1109/PESMG.2013.6672843.

[88] Y. G. Rebours, S. Member, D. S. Kirschen, and M. Trotignon, "A survey of frequency and voltage control ancillary services — part i : technical features", *IEEE Transactions on Power Systems*, vol. 22, no. 1, pp. 350–357, 2007.

[89] S. Meyn, M. Negrete-Pincetic, G. Wang, A. Kowli, and E. Shafieepoorfard, "The value of volatile resources in electricity markets", *Proceedings of the IEEE Conference on Decision and Control*, pp. 1029–1036, 2010, ISSN: 01912216. DOI: 10.1109/CDC.2010.5717327.

[90] P. Zhao, G. P. Henze, S. Plamp, and V. J. Cushing, "Evaluation of commercial building HVAC systems as frequency regulation providers", *Energy and Buildings*, vol. 67, pp. 225–235, Dec. 2013, ISSN: 0378-7788. DOI: 10.1016/j.enbuild.2013.08.031.

[91] H. Hao, B. M. Sanandaji, K. Poolla, and T. L. Vincent, "Aggregate Flexibility of Thermostatically Controlled Loads", *IEEE Transactions on Power Systems*, vol. 30, no. 1, pp. 189–198, Jan. 2015, ISSN: 0885-8950. DOI: 10.1109/TPWRS.2014.2328865.

[92] M. Maasoumy, C. Rosenberg, A. Sangiovanni-Vincentelli, and D. S. Callaway, "Model predictive control approach to online computation of demand-side flexibility of commercial buildings hvac systems for supply following", in *Proceedings of the American Control Conference*, 2014, pp. 1082–1089, ISBN: 9781479932726. DOI: 10.1109/ACC.2014.6858874.

[93] E. Vrettos, F. Oldewurtel, G. Andersson, and F. Zhu, "Robust Provision of Frequency Reserves by Office Building Aggregations", in *Proceedings of the 19th IFAC World Congress*, Cape Town, South Africa, 2014.

[94] E. Vrettos and G. Andersson, "Scheduling and provision of secondary frequency reserves by aggregations of commercial buildings", *IEEE Transactions on Sustainable Energy*, vol. 7, no. 2, pp. 850–864, 2016, ISSN: 1949-3029. DOI: 10.1109/TSTE.2015.2497407.

[95] M. Balandat, F. Oldewurtel, M. Chen, and C. Tomlin, "Contract design for frequency regulation by aggregations of commercial buildings", in *2014 52nd Annual Allerton Conference on Communication, Control, and Computing (Allerton)*, Sep. 2014, pp. 38–45. DOI: 10.1109/ALLERTON.2014.7028433.

[96] E. Vrettos, F. Oldewurtel, and G. Andersson, "Robust energy-constrained frequency reserves from aggregations of commercial buildings", *IEEE Transactions on Power Systems*, vol. 31, no. 6, pp. 4272–4285, 2016, ISSN: 0885-8950. DOI: 10.1109/TPWRS.2015.2511541.

[97] X. Zhang, M. Kamgarpour, A. Georghiou, P. Goulart, and J. Lygeros, "Robust optimal control with adjustable uncertainty sets", *Automatica*, vol. 75, pp. 249 –259, 2017, ISSN: 0005-1098. DOI: http://dx.doi.org/10.1016/j.automatica.2016.09.016.

[98] H. Hao, A. Kowli, Y. Lin, P. Barooah, and S. Meyn, "Ancillary service for the grid via control of commercial building hvac systems", in *American Control Conference (ACC), 2013*, IEEE, 2013, pp. 467–472.

[99] H. Hindi, D. Greene, and C. Laventall, "Coordinating regulation and demand response in electric power grids using multirate model predictive control", *Innovative Smart Grid Technologies (ISGT), 2011 IEEE PES*, no. January, pp. 1–8, 2011. DOI: 10.1109/ISGT.2011.5759168.

[100] L. Zhao and W. Zhang, "A geometric approach to virtual battery modeling of thermostatically controlled loads", in *2016 American Control Conference (ACC)*, Jul. 2016, pp. 1452–1457. DOI: 10.1109/ACC.2016.7525121.

[101] D. Madjidian, M. Roozbehani, and M. A. Dahleh, "Battery Capacity of Deferrable Energy Demand", in *Proceedings of the IEEE Conference on Decision and Control*, arXiv: 1610.01973, 2016.

[102] M. Maasoumy, "Flexibility of commercial building hvac fan as ancillary service for smart grid", *IEEE Green Energy and Systems Conference (IGESC 2013)*, Nov. 2013.

[103] Y. Lin, P. Barooah, S. Meyn, and T. Middelkoop, "Experimental evaluation of frequency regulation from commercial building hvac system", *IEEE Transaction on Smart Grid*, vol. 6, no. no. 2, pp. 776–783, March 2015.

[104] L. Su and L. K. Norford, "Demonstration of hvac chiller control for power grid frequency regulation—part 1: controller development and experimental results", *Science and Technology for the Built Environment*, vol. 21, no. 8, pp. 1134–1142, 2015.

[105] E. Vrettos, E. C. Kara, J. MacDonald, G. Andersson, and D. S. Callaway, "Experimental Demonstration of Frequency Regulation by Commercial Buildings - Part II: Results and Performance Evaluation", *ArXiv:1605.05558 [math]*, May 2016, arXiv: 1605.05558.

[106] Y. G. Rebours, S. Member, D. S. Kirschen, and M. Trotignon, "A survey of frequency and voltage control ancillary services — part ii : economic features", *IEEE Transactions on Power Systems*, vol. 22, no. 1, pp. 358–366, 2007.

[107] A. Shapiro, D. Dentcheva, *et al.*, *Lectures on stochastic programming: modeling and theory*. SIAM, 2014, vol. 16.

[108] P. Pinson, H. Madsen, H. A. Nielsen, G. Papaefthymiou, and B. Klöckl, "From probabilistic forecasts to statistical scenarios of short-term wind power production", *Wind Energy*, vol. 12, no. 1, pp. 51–62, 2009, ISSN: 1099-1824. DOI: 10.1002/we.284.

[109] SwissGrid, *Basic Principles of Ancillary Services Products*. [Online]. Available: https://www.swissgrid.ch/dam/swissgrid/experts/ancillary_services/Dokumente/D160111_AS-Products_V9R1_en.pdf.

[110] EpexSpot, *European Power Exchange*. [Online]. Available: http://www.epexspot.com/en/.

[111] J. Lofberg, "Yalmip : a toolbox for modeling and optimization in matlab", in *Computer Aided Control Systems Design, 2004 IEEE International Symposium on*, 2004, pp. 284–289. DOI: 10.1109/CACSD.2004.1393890.

[112] L. Fabietti, T. T. Gorecki, E. Namor, F. Sossan, M. Paolone, and C. N. Jones, "Dispatching active distribution networks through electrochemical storage systems and demand side management", in *1st IEEE Conference on Control Technology and Applications*, Big Island, Hawaii, USA, 2017.

[113] G. Metta, P. Fitzpatrick, and L. Natale, "Yarp: yet another robot platform", *International Journal of Advanced Robotic Systems*, vol. 3, no. 1, p. 8, 2006.

[114] L. Ljung, "System identification", in *Signal Analysis and Prediction*, Springer, 1998, pp. 163–173.

[115] A. Dounis and C. Caraiscos, "Advanced control systems engineering for energy and comfort management in a building environment—a review", *Renewable and Sustainable Energy Reviews*, vol. 13, no. 6–7, pp. 1246 –1261, 2009, ISSN: 1364-0321. DOI: http://dx.doi.org/10.1016/j.rser.2008.09.015.

[116] S. Wang and Z. Ma, "Supervisory and optimal control of building hvac systems: a review", *HVAC&R Research*, vol. 14, no. 1, pp. 3–32, 2008. DOI: 10.1080/10789669.2008.10390991.

[117] N. Radhakrishnan, Y. Su, R. Su, and K. Poolla, "Token based scheduling for energy management in building {hvac} systems", *Applied Energy*, vol. 173, pp. 67 –79, 2016, ISSN: 0306-2619. DOI: http://dx.doi.org/10.1016/j.apenergy.2016.04.023.

[118] R. M. Vignali, F. Borghesan, L. Piroddi, M. Strelec, and M. Prandini, "Energy management of a building cooling system with thermal storage: an approximate dynamic programming solution", *IEEE Transactions on Automation Science and Engineering*, vol. PP, no. 99, pp. 1–15, 2017, ISSN: 1545-5955. DOI: 10.1109/TASE.2016.2635109.

[119] A. Ben-Tal, L. El Ghaoui, and A. Nemirovski, *Robust Optimization*, ser. Princeton Series in Applied Mathematics. Princeton University Press, 2009.

[120] P. J. Goulart, E. C. Kerrigan, and J. M. Maciejowski, "Optimization over state feedback policies for robust control with constraints", *Automatica*, vol. 42, no. 4, pp. 523 –533, 2006, ISSN: 0005-1098. DOI: http://doi.org/10.1016/j.automatica.2005.08.023.

[121] J. Löfberg, "Automatic robust convex programming", *Optimization Methods and Software*, vol. 27, no. 1, pp. 115–129, 2012. DOI: 10.1080/10556788.2010.517532.

[122] Gurobi, *Gurobi optimizer reference manual*, 2016. [Online]. Available: http://www.gurobi.com.

[123] J. Andersson, "A General-Purpose Software Framework for Dynamic Optimization", PhD thesis, Arenberg Doctoral School, KU Leuven, Department of Electrical Engineering (ESAT/SCD) and Optimization in Engineering Center, Kasteelpark Arenberg 10, 3001-Heverlee, Belgium, 2013.

[124] A. Wächter and L. T. Biegler, "On the implementation of an interior-point filter line-search algorithm for large-scale nonlinear programming", *Mathematical Programming*, vol. 106, no. 1, pp. 25–57, 2006, ISSN: 1436-4646. DOI: 10.1007/s10107-004-0559-y.

FARAN AHMED QURESHI

EPFL STI IGM LA3,
ME C2 396, Station 9, CH-1015, Lausanne, Switzerland
contactfaran@gmail.com

EDUCATION

2012 - PRESENT **Automatic Control Laboratory, EPFL, Switzerland**
Doctoral Assistant (Ph.D. Student)
- Research topic: Predictive control of buildings for demand response and ancillary services provision
- Supervisor: Prof. Colin Jones (colin.jones@epfl.ch)

2010 – 2012 **Eindhoven University of Technology (TU/e), The Netherlands**
Master of Science in Systems and Control
- Thesis title: Hardware constrained controller synthesis for high precision current amplifiers
- Supervisor: Prof. Mircea Lazar
- Average grade = 8.43/10 (Cum Laude)
- Recipient of full university scholarship for master studies at TU/e

2005 – 2009 **Ghulam Ishaq Khan Institute of Engineering Sciences and Technology, Pakistan**
Bachelor of Science in Electronic Engineering
- Thesis title: Directional sound receiver using microphone array
- CGPA = 3.89/4.00 (High Distinction)
- Ranked third in the graduating batch
- Awarded 2nd prize at the Final Year Design Project competition

WORK EXPERIENCE

2012 – PRESENT **Automatic Control Laboratory, EPFL, Switzerland**
Doctoral Assistant (Ph.D. Student)

2011 – 2012 **Prodrive Technologies B.V., Eindhoven, The Netherlands**
Graduation Project

2011 – 2011 **Delft Center for Systems and Control, Delft University of Technology, The Netherlands**
Internee

2009 – 2010 **Ericsson, Lahore, Pakistan**
Graduate Engineering Trainee

2008 – 2008 **Siemens, Lahore, Pakistan**
Internee

TECHNICAL SKILLS

Programming
- MATLAB/SIMULINK (Full professional proficiency)
- Python, C, VHDL (Basic knowledge)
- YARP
- MLE+ and EnergyPlus
- Scrum Agile framework

Mathematics
- Convex and non-convex optimization
- Optimization under uncertainty (stochastic and robust optimization)
- Control systems, optimization based control (model predictive control)
- Optimization software (CPLEX, GUROBI, IPOPT, YALMIP, CasADi)

LANGUAGES

English	Full professional proficiency
Urdu	Native language

PUBLICATIONS

- Faran A. Qureshi, and Colin N. Jones, “Hierarchical Control of Building HVAC system for Ancillary Services Provision“, submitted to Energy and Buildings, 2017.
- Faran A. Qureshi, Ioannis Lymperopoulos, Ali Ahmadi Khatir, and Colin Jones, “Economic Advantages of Office Buildings Providing Ancillary Services with Intraday Participation”, in IEEE Transactions on Smart Grid, 2016.
- Tomasz Gorecki, Luca Fabietti, Faran A. Qureshi, and Colin Jones, “Experimental Demonstration of Buildings Providing Frequency Regulation Services in the Swiss Market”, in Energy and Buildings, 2017.
- Luca Fabietti, Tomasz T. Gorecki, Faran A. Qureshi, Altug Bitlislioglu, Ioannis Lymperopoulos, and Colin Jones, “Experimental Implementation of Frequency Regulation Service using Commercial Building”, in IEEE Transactions on Smart Grid, 2016.
- Truong X. Nghiem, Altug Bitlislioglu, Tomasz Gorecki, Faran A. Qureshi, and Colin N. Jones, “OpenBuildNet framework for distributed co-simulation of smart energy systems”, in International Conference on Control, Automation, Robotics and Vision (ICARCV), 2016.
- Ioannis Lymperopoulos, Faran A. Qureshi, Truong Nghiem, Ali Ahmadi Khatir, and Colin N. Jones, “Providing Ancillary Service with Commercial Buildings: The Swiss Perspective”, in 9th IFAC Symposium on Advanced Control of Chemical Processes (ADCHEM), Whistler, Canada, June 2015.
- T. T. Gorecki, F. A. Qureshi, and C. N. Jones, “Openbuild: An Integrated Simulation Environment for Building Control”, in IEEE Conference on Control Applications (CCA), Sydney, Australia, Sept 2015.
- Faran A. Qureshi, Tomasz T. Gorecki, and Colin N. Jones, “Model Predictive Control for Market-based Demand Response Participation”, in 19th IFAC World Congress, Cape Town, South Africa, August 2014.
- Tomasz Gorecki, Faran Qureshi, Milan Korda, Luca Giulioni, and Colin N. Jones, “Stochastic MPC applied to buildings”, in ECMI conference on Mathematics in Industry, Taormina, Italy, July 2014.
- Faran A. Qureshi, Veaceslav Spinu, Korneel Wijnands, Mircea Lazar, “A Real-Time Control System Architecture for Industrial Power Amplifiers,” in American Control Conference (ACC), Washington D.C., USA, 2013.